

# The Geological Society Special Publications

## Multi-phase reactivations and inversions of Paleozoic-Mesozoic extensional basins during the Wilson Cycle: case studies from the North Sea (UK) and central Apennines (Italy)

--Manuscript Draft--

<b>Manuscript Number:</b>	GSLSpecPub17-232R1
<b>Article Type:</b>	Chapter
<b>Full Title:</b>	Multi-phase reactivations and inversions of Paleozoic-Mesozoic extensional basins during the Wilson Cycle: case studies from the North Sea (UK) and central Apennines (Italy)
<b>Short Title:</b>	Reactivation of Late Palaeozoic-Mesozoic extensional basins
<b>Corresponding Author:</b>	Vittorio Scisciani University of Chieti Chieti, Chieti Scalo (CH) ITALY
<b>Corresponding Author E-Mail:</b>	scisciani@unich.it
<b>Other Authors:</b>	Stefano Patruno Enrico Tavarnelli Fernando Calamita Paolo Pace David Iacopini
<b>Order of Authors (with Contributor Roles):</b>	Vittorio Scisciani (Conceptualization: Lead; Data curation: Equal; Writing – original draft: Lead; Writing – review & editing: Equal) Stefano Patruno (Conceptualization: Lead; Data curation: Equal; Formal analysis: Supporting; Writing – original draft: Equal) Enrico Tavarnelli (Data curation: Equal; Writing – review & editing: Supporting) Fernando Calamita (Conceptualization: Equal; Supervision: Lead) Paolo Pace (Data curation: Supporting; Writing – review & editing: Supporting) David Iacopini (Writing – review & editing: Supporting)
<b>Abstract:</b>	The Caledonian-Variscan orogens in Northern Europe and the Alpine-age Apennine range of Italy are classical examples of thrust belts that were developed at the expense of formerly rifted, passive continental margins and that experienced various degrees of post-orogenic collapse. Portions of these settings comprise the outer zones of orogenic belts and their adjoining foreland domains, where the effects of superposed deformations are mild-to-very mild, making it possible to recognise and separate structures produced at different times and to correctly establish their chronology and relationships. In this paper we integrate subsurface data (2- and 3D seismic reflection and well-logs), mainly from the North Sea, and structural field evidence, mainly from the Apennines, with the aim to reconstruct and refine the structural evolution of these two provinces that, in spite of their different ages and present-day structural framework, share repeated pulses of alternating extension and compression. The main outcome of this investigation is that in both scenarios, during repeated episodes of inversion that are a characteristic feature of the Wilson Cycle, inherited basement structures were effective in controlling stress localisation along faults affecting younger sedimentary cover rocks.
<b>Section/Category:</b>	Tectonic Evolution: 50 Years of the Wilson Cycle Concept
<b>Additional Information:</b>	
<b>Question</b>	<b>Response</b>
Are there any conflicting interests,	No

financial or otherwise?	
Samples used for data or illustrations in this article have been collected in a responsible manner	Confirmed

1 **Ref.:** Ms. No. GSLSpecPub17-232

2

3 **Volume:** Tectonic evolution: 50 years of the Wilson Cycle concept - Geological Society Special  
4 Publication

5

6 **Contribution type:** Original Research Paper

7

8 **New Title:** Multi-phase reactivations and inversions of Paleozoic-Mesozoic extensional basins during  
9 the Wilson Cycle: case studies from the North Sea (UK) and central Apennines (Italy)

10 **Previous Title:** Modes of reactivation of Late Paleozoic-Mesozoic extensional basins during the Wilson  
11 Cycle: case studies from the North Sea (UK) and central Apennines (Italy)

12

13 **Short title:** Reactivation of Late Palaeozoic-Mesozoic extensional basins

14

15 **Author list and affiliations:** Vittorio Scisciani <sup>(1)</sup>, Stefano Patruno <sup>(2)</sup>, Enrico Tavarnelli <sup>(3)</sup>, Fernando  
16 Calamita <sup>(1)</sup>, Paolo Pace<sup>(1,4)</sup>, and David Iacopini<sup>(5)</sup>

17 <sup>(1)</sup> Department of Engineering and Geology "G. d'Annunzio" - University of Chieti and Pescara (Italy)

18 <sup>(2)</sup> PGS Reservoir Limited, Weybridge, United Kingdom

19 <sup>(3)</sup> Department of Physics, Earth and Environment Sciences - University of Siena (Italy)

20 <sup>(4)</sup> G.E. Plan Consulting, Petroleum Geosciences, Via Ariosto 58, 44121 – Ferrara (Italy)

21 <sup>(5)</sup> Department of Geology and Petroleum Geology, School of Geosciences, University of Aberdeen,  
22 Scotland (United Kingdom)

23

24 **Corresponding Author:** [scisciani@unich.it](mailto:scisciani@unich.it)

25

26

27

28

29  
30  
31  
32  
33  
34  
35  
36  
37  
38  
39  
40  
41  
42  
43  
44  
45  
46  
47  
48  
49  
50  
51  
52  
53  
54  
55  
56  
57  
58  
59  
60  
61  
62  
63  
64  
65  
66

From: *Dr. Vittorio Scisciani,*  
*Dipartimento di Scienze della Terra,*  
*Università "G. D'Annunzio"*  
*Chieti-Pescara - Italy*

*To the attention of Woody Wilson, Ken McCaffrey, Tony Doré, Greg Houseman and Wiki Royden*  
*Guest Editors of the Volume: Tectonic evolution: 50 years of the Wilson Cycle concept*

Dear Woody, Ken, Tony, Greg and Wiki,

we are hereby forwarding the revised version of our manuscript titled "Multi-phase reactivations and inversions of Paleozoic-Mesozoic extensional basins during the Wilson Cycle: case studies from the North Sea (UK) and northern Apennines (Italy)" (the working title was: "Modes of reactivation of Late Paleozoic-Mesozoic extensional basins during the Wilson Cycle: case studies from the North Sea (UK) and central Apennines (Italy)").

This manuscript was submitted for publication on the Geological Society of London Special Publication titled "Tectonic evolution: 50 years of the Wilson Cycle concept".

The original version of the manuscript was carefully reviewed in the light of the referees (Thomas Phillips and Stuart Archer) and corresponding editor' (Woody Wilson) comments. Following their suggestions, the new version has been re-structured, reduced in length (from 215000 to less than 10,000 words) and made more fluent, simplifying redundant descriptions and details of the regional geology of the two study areas. The regional setting was simplified and an integrated description of the evolution of the two study area has been treated in the chapter entitled "Supra-regional evolution of Western Europe" (correlated with Figure 2 and the new Figure 3). Finally, the discussion was significantly shortened and rearranged in order to make the description of modes of structural reactivation and inversion patterns more homogeneous for the two areas; a new figure (Fig. 20) has been added to highlight the analogies in multiphase reactivation in the East Shetland Platform and Northern Apennines. In a specific paragraph of the discussion, the common controlling factors of multi-phase reactivations were emphasized.

We think that the new version of the manuscript has been significantly improved with respect to the previous form and we hope it is now fully suitable to contribute to the success of the outcoming volume of the GSL Special Publication.

67            We hope to hear back from your editorial decision soon, and we take this opportunity to thank  
68 you very much for your advice, and the reviewers for their constructive comments and suggestions.

69  
70            On behalf of all my co-authors, I send you my best wishes and remain  
71 Yours truly,

72  
73            Vittorio Scisciani

74  
75  
76  
77  
78

1 **Ref.:** Ms. No. GSLSpecPub17-232

2

3 **Volume:** Tectonic evolution: 50 years of the Wilson Cycle concept - Geological Society Special  
4 Publication

5

6 **Contribution type:** Original Research Paper

7

8 **Title:** Multi-phase reactivations and inversions of Paleozoic-Mesozoic extensional basins during the  
9 Wilson Cycle: case studies from the North Sea (UK) and central Apennines (Italy)

10

11 **Previous Working Title:** Modes of reactivation of Late Paleozoic-Mesozoic extensional basins during  
12 the Wilson Cycle: case studies from the North Sea (UK) and central Apennines (Italy) ""

13

14 **Short title:** Reactivation of Late Palaeozoic-Mesozoic extensional basins

15

16 **Author list and affiliations:** Vittorio Scisciani <sup>(1)</sup>, Stefano Patruno <sup>(2)</sup>, Enrico Tavarnelli <sup>(3)</sup>, Fernando  
17 Calamita <sup>(1)</sup>, Paolo Pace<sup>(1,4)</sup>, and David Iacopini<sup>(5)</sup>

18 <sup>(1)</sup> Department of Engineering and Geology "G. d'Annunzio" - University of Chieti and Pescara (Italy)

19 <sup>(2)</sup> PGS Reservoir Limited, Weybridge, United Kingdom

20 <sup>(3)</sup> Department of Physics, Earth and Environment Sciences - University of Siena (Italy)

21 <sup>(4)</sup> G.E. Plan Consulting, Petroleum Geosciences, Via Ariosto 58, 44121 – Ferrara (Italy)

22 <sup>(5)</sup> Department of Geology and Petroleum Geology, School of Geosciences, University of Aberdeen,  
23 Scotland (United Kingdom)

24

25 **Corresponding Author:** [scisciani@unich.it](mailto:scisciani@unich.it)

26

27

28

29

30 *Response to the reviewers' comments*

31

32 The manuscript has undergone to the revision in the lights of the scientific comments of the referees  
33 (Thomas Phillips and Stuart Archer) and the corresponding editor (Woody Wilson). Following their suggestions  
34 we restructured and shortened the manuscript, removing a great amount of details on the regional evolution  
35 of the two study areas and integrating the regional settings and the tectonic evolution in single common  
36 chapters (i.e., "Geological setting of the East Shetland Platform (ESP) and Northern Apennines (NA)" and  
37 "Supra-regional evolution of Western Europe"). Moreover, we added two new figures; the first (new Fig. 3 -  
38 including previous Figs. 4 and 13) is to help readers to follow the main plate and intra-plate Wilson cycles  
39 occurred during the evolution of the study areas and the second (Fig. 20) to make a comparison of the role  
40 played by the inherited structures during positive and negative reactivation in both the study areas.

41

42 Based on the general comments of the reviewers the following corrections have been carried out:

43 i) distinction between the work done in previous studies (included in the chapters #2 and #3) and our  
44 contribute (chapters #4-8);

45 ii) addition of a further figure (i.e., the new Fig. 20) to make more explicit the link between the inherited  
46 structures and the subsequent positive and negative reactivation in both the study areas and relative  
47 description in the text;

48 iii) enhanced integration between the study areas in the chapters #2 and #3;

49 iv) specific description and discussion of the influence of the inherited structures on the subsequent  
50 reactivation processes with comparison between the two study areas (third paragraph in the discussion).

51 v) tightening of the narrative and shorten of the the word count;

52 vi) improvement of the English language and grammar

53

54 As regards the general comments and concerns of the reviewer #1 (Thomas Phillips) and #2 (Stuart  
55 Archer), our responses (text in italic) are listed as follow:

56

57 Reviewer #1 comment: Throughout the manuscript the authors refer to "inherited structures emanating  
58 from basement" (Line 34), or "Caledonian basement grain structures" (Line74) – it is unclear what these  
59 structures are and what their geometry is. It is also difficult to see the relationship between the basement  
60 structures and the later faults, in particular on the figures, where the faults and inherited basement structures  
61 are not shown on the same fig.

62 *In all the seismic cross-section there are now annotations, and similarly this is now described at length in*  
63 *captions and in the main text. We highlight faults with different age of activity (and re-activations), ranging*

64 *from Caledonian thrusts and normal faults, Devonian normal faults, Variscan inversion, Permo-Triassic normal*  
65 *faults, Mid Cimmerian inversion, Late Jurassic normal faults, Alpine-age inversion etc.*

66

67 Reviewer #1 comment: The geological setting of the East Shetland Platform area, and of the wider North  
68 Sea is incredibly detailed. Some of the observations made in this section (i.e. lines 108-112) would benefit from  
69 being shown in a cross-section. However, it is often unclear how some of the information given in this section is  
70 relevant to the overall study. Some of this information could be streamlined in order to reduce the length of  
71 the study and to give more impact to the main results

72 *In the revised version of the manuscript the geological setting of the East Shetland Platform area was*  
73 *simplified and streamlined; the Lines 108-112 were deleted.*

74

75 Reviewer #1 comment: Currently, the descriptions of the main plate cycles, without any explicit  
76 reference to figures, reduce the impact of the overall results and observations later in the paper.

77 *This suggestion has been followed and the revised version includes the new Figure 3 with plate*  
78 *reconstructions that illustrate the main evolutionary stages of the two study areas.*

79

80 Reviewer #1 comment: Currently, some of the later results repeat points made in the geological setting. I  
81 would suggest streamlining the geological setting section to give more impact to the results later.

82 *In the revised version of the manuscript the geological setting of the East Shetland Platform area was*  
83 *simplified and streamlined.*

84

85 Reviewer #1 comment: Line 132-134 – The authors define a complete plate cycle as where oceanic  
86 spreading and continental collision has taken place, and an intra-plate cycle where extension and compression  
87 occur, without the requirement of oceanic crust. However, the authors then state that plate cycle (2), the  
88 Devonian-Variscan cycle (Line 200-241) is a plate-cycle, although no seafloor was generated during Devonian  
89 orogenic collapse. This should be referred to as an ‘intra-plate cycle.’

90 *In the revised version of the manuscript we re-defined the "classical/complete" and*  
91 *"foreland/incomplete" Wilson cycles occurred in the two study area during the Iapetus-Caledonian/Rheic-*  
92 *Variscan (lines 171- 180) and Permian-Present (lines 251-259) plate and intraplate cycles.*

93

94 Reviewer #1 comment: Some of the information when describing the different plate and intra-plate  
95 cycles appears to be extraneous with regards to the main aim of the paper, which is to identify reactivation  
96 within Wilson cycles. For example, much of the stratigraphic information (e.g. Lines 147-160) could be removed  
97 to streamline the paper without influencing the overall message.

98 *This part of the text in the previous version manuscript has been deleted.*

99

100 Reviewer #1 comment: Line 194-198 – more information needs to be given on the geometry of the  
101 lineaments if available?

102 Some of the implications of the observations stated in the results are unclear as to how they fit in with  
103 the overall paper

104 *This part of the text in the previous version manuscript has been deleted.*



105 Reviewer #1 comment: Line 473-479 – could you use potential field data, or older studies to shed some  
106 light onto the extent of the granite in this area?

107 *As far as we know the Bressay granite has not really been discussed in previous studies (e.g., Stephenson*  
108 *et al., 1999).*

109

110

111 Reviewer #1 comment: Line 498 – Where are the offshore continuations of the Great Glen fault and the  
112 axis of the Iapetus ocean? Although these structures are shown in Figure 3, these structures are not  
113 immediately clear relative to the main study area and are also not referenced in the text.

114 *A reconstruction of the basement units in the northern North Sea and surrounding areas has been included*  
115 *in Fig 4C where the offshore prosecution of the Great Glen fault and Iapetus oceanic units are illustrated.*

116

117

118 Reviewer #1 comment: Line 499-501 – more evidence is required to invoke inheritance for the  
119 similarities in strikes of these faults, and the links to the onshore Caledonide structures need to be shown. This  
120 is not shown in map view and therefore it is difficult to make the link between these pre-existing lines of  
121 weakness and the later faults. Evidence for the relationship between the lineaments and the later phases of  
122 activity is currently lacking. No figures are referred to throughout this section.

123 *The Tertiary positive inversion of the NNE-SSW Devonian master fault illustrated in Figures 10 and 11 has*  
124 *been described (e.g., lines 310-320); in addition, this Devonian normal fault is one of the extensional structures*  
125 *developed during the Devonian-age extensional collapse of the Caledonian Orogeny. In the text we argued that*  
126 *the attitude of the reactivated master faults, which shows a NNE-SSW strike, resembles the orientation of the*  
127 *main lineaments associated to the Caledonian Orogeny (e.g., lines 345-352).*

128

129 Reviewer #1 comment: More integration needs to be made at the beginning as to why both the North  
130 Sea and the Apennines are included in this study, and how they link together. Currently it seems that these  
131 form almost two separate papers that are stuck together. One suggestion could be to have a much shorter  
132 geological setting for both the North Sea and the Apennines at the beginning of the manuscript followed by  
133 two sections on the findings of this study. I feel that this would greatly improve the flow of the manuscript.....

134 *In the revised version of the manuscript we followed overall these suggestions.*

135

136 Reviewer #1 comment: The descriptions of the plate cycles within the Apennines (e.g. lines 529-571), are  
137 hard to follow without reference to figures that state where these structures and locations are relative to one  
138 another, particularly for people not familiar with the area. In addition, at this point it is also unclear how some  
139 of this information is related to the individual plate cycle, these descriptions should be simplified or at least  
140 located on a map.

141 *The description of the plate cycles within the Apennines has been rearranged in the chapter #3 ("Supra-*  
142 *regional evolution of Western Europe") and illustrated in the new Figure 3.*

143

144 Reviewer #1 comment: The section 'Field geology of the central Apennines' should potentially appear  
145 before the descriptions of the plate cycles, to serve as an introduction to the region.

146 *The section concerning the field geology of the Northern Apennines has been streamlined and the*  
147 *descriptions in the text are now limited to the results of fieldwork carried out to calibrate the seismic profile.*  
148

149 Reviewer #1 comment: Line 668-670 – this is setting up this part of the study, which should have been  
150 set up prior to the descriptions of the plate cycles in the Apennines. In places it appear that some sections of  
151 the manuscript do no link to the others. This section does not link to the overall aim of the paper

152 *The section concerning the field geology of the Northern Apennines has been streamlined and*  
153 *combined to the seismic interpretation; the descriptions in the text are now limited to the results of fieldwork*  
154 *carried out to calibrate stratigraphy and structures imaged in the seismic profile.*  
155

156 Reviewer #1 comments: The presence of the lineaments and inherited structures is not referred to  
157 throughout the text (eg. Line 729) even though this forms one of the main conclusions stated in the abstract.

158 Line 753 – very detailed descriptions of the seismic section and the imaged stratigraphy, but still unclear  
159 as to how this fits into the Wilson cycle story. Some good information occurs later (line 822 onwards, but some  
160 of the earlier information does not add to the main points.

161 Line 908-909 – The definition and identification of the structural grains can be made clearer

162 Line 921-937 – this seems partly repeated from earlier during the descriptions of the plate and intra-  
163 plate cycles.

164 *These parts of the manuscript were removed in the new version.*  
165

166 Reviewer #2 comment: One minor point of consistency is that the reviewers of this SP will need to  
167 decide early whether to use Wilson cycle or Wilson Cycle – the use of upper versus lower case C is  
168 inconsistently applied.

169 *The term Wilson Cycle has been used throughout the manuscript.*  
170

171 Reviewer #2 comment: I am unsure if the Mid Cimmerian Thermal doming event in the Central North Sea  
172 can be seen in the context of the Wilson cycle as it is neither part of an open closing nor ocean opening event.  
173 As we all know, the North Sea is a failed passive margin and the thermal dome probably represents the  
174 response to a transient plume event in an intra-plate setting.

175 *We treated the Mid Cimmerian event as a likely mantle plume erosion (Underhill & Prtington 1993)*  
176 *occurred in an intraplate setting.*  
177

178 Reviewer #2 comment: The two topics co-exist unsatisfactorily in the current manuscript rather than  
179 being weaved into an elegant compare and contrast type discussion.

180 *The discussion section has been reorganized and more analogies and comparisons between the complete*  
181 *and incomplete Wilson Cycles have been argue.*  
182

183 Reviewer #2 comment: One obvious problem with a section is Fig 17 where the quality of the seismic line  
184 does not (to my eye at least) allow the interpretation of all the detail below. If this is supported by outcrop  
185 observations then I suggest that you add an intermediate step – a cross section showing the outcrop control  
186 points and projecting the structural dip into the subsurface. In this way a basic line drawing might act as a  
187 stepping stone to the final interpretation.

188            *The new Fig. 16 includes a larger and better quality image of the seismic reflection profile. In particular in*  
189 *the new version, the two reflectors (corresponding to the base of siliciclastic turbidites and the Fucoidi Marls),*  
190 *that have been tied with a geological cross-section derived from fieldwork and have been used to control the*  
191 *subsurface interpretation, are now clearly imaged on the seismic profile.*  
192

193            In addition, the revised version of the manuscript takes into account of every specific point listed by the  
194 reviewers (points in the list and in the annotated version of the submitted manuscript of the reviewer #1 and  
195 #2, respectively)

# 1 **Multi-phase reactivations and inversions of Paleozoic-Mesozoic extensional basins during the** 2 **Wilson Cycle: case studies from the North Sea (UK) and central Apennines (Italy)**

## 3 4 5 **Short abstract**

6 The Caledonian-Variscan orogens in Northern Europe and the Alpine-age Apennine range of  
7 Italy are classical examples of thrust belts that were developed at the expense of formerly rifted,  
8 passive continental margins and that experienced various degrees of post-orogenic collapse. Portions  
9 of these settings comprise the outer zones of orogenic belts and their adjoining foreland domains,  
10 where the effects of superposed deformations are mild-to-very mild, making it possible to recognise  
11 and separate structures produced at different times and to correctly establish their chronology and  
12 relationships. In this paper we integrate subsurface data (2- and 3D seismic reflection and well-logs),  
13 mainly from the North Sea, and structural field evidence, mainly from the Apennines, with the aim to  
14 reconstruct and refine the structural evolution of these two provinces that, in spite of their different  
15 ages and present-day structural framework, share repeated pulses of alternating extension and  
16 compression. The main outcome of this investigation is that in both scenarios, during repeated  
17 episodes of inversion that are a characteristic feature of the Wilson Cycle, inherited basement  
18 structures were effective in controlling stress localisation along faults affecting younger sedimentary  
19 cover rocks.

## 20 21 **Introduction**

22 In orogenic belts the coexistence of deformed portions of oceanic crust and passive margin  
23 successions, in turn pulled-apart by subsequent continental breakup is often ascribed to the Wilson  
24 Cycle context (Wilson, 1966; Vauchez et al., 1997). Within these orogens formed by continental  
25 collision following the closure of ancient oceanic basins the pre-existing rifting discontinuities are  
26 commonly reactivated during subsequent compressional episodes in the context of positive inversion  
27 tectonics (e.g., Williams et al., 1989). Similarly, during post-collisional reworking of orogens a  
28 fundamental role has been recognised to be exerted by pre-existing anisotropies, such as reverse  
29 faults and compressive fabrics on younger extensional structures (Ring, 1994; Vauchez et al., 1997;  
30 Korme et al., 2004).

31 Although several separate examples of positive or negative inversion tectonics occurred in  
32 disparate times and across diverse structural settings (Harding, 1985; Cooper and Williams, 1989;  
33 Buchanan and Buchanan, 1995), few of these testify a complete Wilson Cycle from the initial rift  
34 phase to the final collisional and post-collisional stages.

35 In his seminal paper, Wilson (1966) first proposed the closure of a proto-Atlantic Ocean  
36 developed in early Paleozoic times followed by the assembly of the Gondwana supercontinent  
37 (known as Appalachian-Caledonian orogeny), its break-up, and re-opening of the Mesozoic-Cenozoic  
38 Atlantic Ocean. He also speculated that a similar but more recent event occurred along the present-

39 day Asian and circum-Mediterranean mountain belts following the total and partial closure of the  
40 Tethys Ocean.

41 Following the pioneering approach by Wilson, both the Caledonian orogen in Northern Europe  
42 and the Apennines fold-and-thrust belt of Italy were recognised as key areas to study the effects of  
43 the Wilson Cycle with repeated episodes of opening and closing of ocean and extensional basins along  
44 similar structural trends (e.g., Butler et al., 2006).

45 In the present work, we have selected two continental margins where regional geology, field  
46 structural evidence and subsurface data all point out to at least a complete Wilson Cycle (Figs. 1-3),  
47 with long-term preservation of structural grain and reactivation of pre-existing structures within both  
48 the suture zones and the foreland domains. The two study areas comprise the East Shetland Platform  
49 (ESP) in the UK North Sea (NS) and the south-eastern portion of the Northern Apennines (NA) of Italy,  
50 including the Umbria-Marche Apennine Ridge (UMAR) (Figs. 1, 4-5).

51 The results of our investigation indicate that the Wilson Cycle concept, useful for the description  
52 of the tectonic evolution of the NS and UMAR, may also be successfully applied in the study of other  
53 analogue foreland settings flanking the zones where multiple cyclical events that switch, from  
54 extension to compression and vice-versa, have occurred.

55  
56

#### 57 **Geological setting of the East Shetland Platform (ESP) and Northern Apennines (NA)**

58 The ESP is a large ( $\approx 62,000$  km<sup>2</sup>) Jurassic-Recent offshore platform in the UK North Sea (NS),  
59 bounded by the Orkney and Shetland Islands to the west, and by several Jurassic structural lows (e.g.,  
60 East Shetland Basin, Viking Graben, Outer Moray Firth, Witch Ground Graben) to the east and south  
61 (Figs. 1 and 4).

62 The outer half of the ESP hosts an expanded and weakly deformed Tertiary succession (1.0-2.0  
63 seconds two-way traveltime or TWT), usually resting on a thin horizontal veneer of Upper Cretaceous  
64 carbonate-rich Chalk Group sediments, which in turn overlies a highly tectonized 1.0-3.0 TWT seconds  
65 thick Devonian-age unit (Platt, 1995; Platt and Cartwright, 1998; Zanella and Coward, 2003; Patruno  
66 et al., in press). An angular unconformity separates the tilted and eroded Devonian unit and the sub-  
67 horizontal Cretaceous-Tertiary cover. Permo-Triassic intra-platform extensional basin fills are locally  
68 present (e.g., Richardson et al., 2005; Patruno and Reid, 2016; 2017). A series of widespread hiatuses  
69 and unconformities are partitioned by expanded seismic-stratigraphic units, directly linked to a  
70 succession of regional inversion tectonic events that have taken place in the last 850 million years  
71 (Patruno et al., in press; Figs. 2-3).

72 The Apennines of Italy is a prominent mountain range within the central Mediterranean region  
73 (Figs. 1 and 5). In particular, the NA are an arc-shaped east to north-east verging fold-and-thrust belt  
74 developed during Cenozoic times (Malinverno and Ryan, 1986; Carmignani and Kligfield, 1990). The  
75 NA continental margin forms a tectonic stack of thick-skinned thrust sheets with a tectonic pile  
76 including: i) fragments of ophiolites derived from the Mesozoic Ligurian Ocean and flysch units; ii) a

77 metamorphic core (Apuane Units) with basement imprinted by the previous Alpine and Variscan  
78 orogeny; iii) a foreland fold-and-thrust belt mainly composed of pre-Alpine Mesozoic-Palaeogene  
79 carbonates and syn-orogenic Miocene flysch and juxtaposed towards the E-NE onto the Adriatic  
80 foreland. Starting from the Miocene, the inner sector of the chain was also dissected by post-orogenic  
81 extension and magmatism (Carmignani and Kligfield, 1990; Carmignani et al., 1994; Calamita et al.,  
82 2000; Pizzi and Scisciani, 2000; D'Agostino et al., 2001).

83 These thrust sheets outcrop in the NA mountain belt and are buried underneath Pliocene-  
84 Quaternary syn-orogenic sediments in the Po Plain and Adriatic foreland. The highest topography  
85 zone of the NA (c. 3000 m) consists of two NW-SE trending carbonate mountain ridges (i.e., the  
86 Umbria-Marche and Lazio-Abruzzo ridges – UMAR and LAR, respectively) separated by the NNE-SSW  
87 trending Olevano-Antrodoco-Sibillini oblique thrust ramp (OAMS - Fig. 5). These ridges are composed  
88 by Triassic-Miocene syn-rift and passive-margin succession of the thinned Adriatic crust and their  
89 prominent structural elevation is testified by some of the oldest rocks (Late Triassic-Early Jurassic)  
90 exposures in the highest mountains of the entire Apennines belt (e.g., the Vettore Mt. and Corno  
91 Grande - Fig. 5).

#### 94 **Supra-regional evolution of Western Europe**

95 The geological evolution of the two study areas is here set within a framework of repeated  
96 mega-regional Wilson Cycles (with both complete and incomplete cycles), which are readily  
97 identifiable throughout Western Europe.

98 The ESP and NA study areas were subject to two very similar Proterozoic-Paleozoic plate cycles  
99 (albeit not completely overlapping and with different chronological duration), namely the *Iapetus-*  
100 *Caledonian Cycle* and the *Rheic-Variscan Cycle*. Following the Variscan Orogeny, both areas have been  
101 subject to cyclical reactivations and inversions of pre-existing structures. These reactivations took  
102 place in an intra-plate setting in the case of the NS (with at least two incomplete Meso-Cenozoic intra-  
103 plate extension-compression cycles), while in the NA a new “complete” orogeny-rifting-drifting-  
104 orogeny Wilson Cycle took place in Permian-Recent times (Figs 2-3).

#### 105 *Iapetus-Caledonian (ca. 850-405 Ma) and Rheic-Variscan (ca. 480-300 Ma) plate cycles*

106 In the Late NeoProterozoic and Cambrian, the paleogeography of Western Europe was  
107 dominated by the north-trending Iapetus Ocean, opened between the continental blocks of Laurentia,  
108 Baltica and Gondwana (Mac Niocaill et al., 1997- Fig. 3a). Since the Cambrian, Gondwana and Baltica  
109 had been in turns separated by the west-trending Tornquist seaway (Glennie and Underhill, 1998;  
110 Toghill, 2002).

111 In the Grampian Highlands of Scotland, set on the southern Laurentian continental margins, an  
112 early NeoProterozoic to Cambrian rifting event that preceded the opening of the Iapetus Ocean is  
113 recorded by up to 25 km of metamorphosed sedimentary rocks belonging to the “Dalradian  
114 Supergroup” (Strachan et al., 2002; Toghill, 2002; Stephenson et al., 2013). This succession has been

115 interpreted as a subsiding submarine shelf, evolving into a deeper basin and finally leading to ocean-  
116 floor spreading (Stephenson et al., 2013). The last stage is documented by the late NeoProterozoic  
117 submarine Tayvallich basalts outcropping in western Scotland (Stephenson and Gould, 1995;  
118 Macdonald and Fettes 2007; Fettes et al., 2011).

119 The Dalradian Supergroup is interposed between the Great Glen Fault to the north and the  
120 Highland Boundary Fault to the south (Ziegler, 1988; 1990; Glennie and Underhill, 1998; Coward et al.,  
121 1989; 2003). These deep-seated and long-lived northeast-trending tectonic lineaments, associated to  
122 the complete subduction and suturing of the Iapetus Ocean during the Caledonian Orogeny, can be  
123 expected to continue offshore towards the ESP area (Figs. 3a and 4d).

124 Avalonia was a small continental fragment which detached in the Early Ordovician from the  
125 northern Gondwanan margin by a new widening east-trending ocean, known as the Rheic Ocean (Fig.  
126 3a; Strachan, 2000; Nance et al., 2010, 2012). During Ordovician-Silurian times, the fast seafloor  
127 spreading of the Rheic Ocean led to the passive drifting of Avalonia northwards, and initiated the  
128 progressive three-plate convergence between Avalonia, Baltica and Laurentia in and around the  
129 present-day NS and Scottish-Norwegian regions (McKerrow et al., 2000a; Bluck, 2001; Mendum,  
130 2012; Coward et al., 2003; Nance et al., 2010; 2012 - Fig. 3a). The Iapetus and Tornquist oceans were  
131 eventually closed in Silurian times, leading to the Acadian-Grampian-Caledonian Orogeny (Trench and  
132 Torsvik, 1992; McKerrow et al., 2000a; Mendum, 2012) and to the final assemblage of a larger  
133 continent in the Early Devonian (Laurussia or Old Red Continent - Ziegler, 1988; 2012; Scotese and  
134 McKerrow, 1990; McKerrow et al., 2000b; Dalziel et al., 1994).

135 The assembly of the Caledonian Orogen was quickly followed, during Devonian times, by the  
136 extensional collapse of its thickened crust (e.g., McClay et al., 1986; Coward et al., 1989; Seranne,  
137 1992; Ziegler, 1992; Marshall and Hewett, 2003; Wilson et al., 2010 - Figs. 1 and 2). This post-orogenic  
138 extension produced many quickly-subsiding half-grabens throughout Laurussia, with accompanied  
139 lower Devonian volcanism and granitic intrusions identified both onshore Scotland and in the NS (e.g.,  
140 Utsira High, Halibut and Bressay granites). These fast-subsiding Devonian extensional basins hosted  
141 the deposition of thick continental clastic successions (Old Red Group - Glennie and Underhill, 1998).

142 The Devonian-Carboniferous extensional phase was eventually cut short, because the Late  
143 Carboniferous continental plates switched motion, leading to the subduction of the Rheic Ocean and  
144 the subsequent continental collision between Laurussia, Gondwana, and several intervening  
145 microplates (Variscan Orogeny), with the Early Permian assemblage of the Pangea mega-continent  
146 (Fig. 3b).

147 Remnants of the Caledonian Orogenic belt span northern Britain and Norway, with Lower  
148 Paleozoic crystalline rocks (or "Caledonian basement") thought to underlie the entirety of the  
149 present-day NS Basin (Abramovitz and Thybo, 2000; Scheck et al., 2002; Coward, 1990; Coward et al.,  
150 2003; Zanella and Coward, 2003; Bassett, 2003). On the contrary, the Variscan metamorphic core  
151 belts today straddle the ancient plate margin of Laurussia and Gondwana, from the eastern U.S. and  
152 Newfoundland to Morocco, Iberia, France, Germany and the Ural Mountains. In particular, the  
153 northern, approximately east-trending front of the Variscan orogenic belt spans south-western

154 England, Wales and Ireland (Fig. 3b; Leveridge and Hartley, 2006). In southern Europe, the Paleozoic  
155 basement of Sardinia along with the scattered outcrops in the NA, Western Alps and Calabria is the  
156 result of the Variscan continental collision between the northern Gondwanan margin and the  
157 Armorica micro-plate (Fig. 3b; Carmignani et al., 1994; Franceschelli et al., 2005; Giacomini et al.,  
158 2006; von Raumer and Stampfli, 2008; Rossi et al., 2009). As a consequence, the Variscan belt is  
159 expected to transect underneath the NA mountain belt (Vai, 2001; Doglioni and Flores, 1996).

160 Caledonian and Variscan orogenic belt “core complexes” are therefore present over the Greater  
161 NS area and part of central-southern Europe (including the NA), respectively. Conversely, the NS and  
162 much of southern Europe (including the NA) represented part of the foreland of the far-field Variscan  
163 and Caledonian orogenies, respectively. Nevertheless, large-scale Caledonian-age uplift/erosion and  
164 local folding (Sardic deformation) took place in Sardinia and Iberia (Fig. 2 - Carmignani et al., 1994;  
165 Romão et al., 2005). Similarly, episodes of Variscan-age intra-plate compression and uplift/erosion  
166 leading to the partial inversion of Devonian-Carboniferous sedimentary basins, have been identified in  
167 Britain and the NS (e.g., Fraser and Gawthorpe, 1990; Corfield et al., 1996; Thomson and Underhill,  
168 1993; Hay et al., 2005), including the ESP (Patruno et al., in press; Figs. 3 and 4). The end of the  
169 Variscan foreland compressional phase in the NS is marked by a regional peneplanation surface,  
170 usually referred to as “Base Permian Unconformity”.

171 In the NS and northern Britain, the Iapetus-Caledonian plate cycle therefore corresponds to a  
172 “classical/complete” Wilson Cycle (from likely pre-Iapetus compression to Iapetus extension and  
173 ocean spreading and back to Caledonian compression), while the Rheic-Variscan plate cycle can be  
174 described as a “foreland/incomplete Wilson Cycle” (from Caledonian orogeny to a Devonian extension  
175 which does not culminate in ocean spreading and back to foreland Variscan compression). The  
176 opposite is true for the NA and southern Europe. Here, the Iapetus-Caledonian cycle is a  
177 foreland/incomplete Wilson Cycle (no Iapetus-equivalent ocean formation in this region and far-field  
178 Caledonian compression), while the Rheic-Variscan plate cycle represents a classical/complete Wilson  
179 Cycle (from likely pre-Rheic compression to Rheic extension and ocean spreading and back to Variscan  
180 compression).

181  
182 *Permian-Present plate and intraplate cycles (ca. 280/260-0 Ma)*

183 Following the Variscan orogeny the NS and NA areas suffered multiple Permian-Jurassic rifting  
184 episodes, associated to the breakup of Pangea (Decourt et al., 1993; Stampfli and Borel, 2002). In  
185 southern Europe this extensional processes resulted in the opening of three distinct oceanic arms  
186 (Figs. 2-3c), including: i) the Permian-Triassic Ionian-East Mediterranean ocean (Finetti and Del Ben,  
187 2005); ii) the Middle Triassic North-Western Tethys (Hallstatt-Meliata and Vardar oceans; Kozur,  
188 1991); and iii) the latest Triassic-Middle Jurassic Alpine Tethys (including the Ligurian-Piedmont  
189 Ocean; Stampfli and Borel, 2002). The two oldest oceans formed the western termination of the Neo-  
190 Tethys whereas the last was an eastward ramification of the central Atlantic opening.

191 On the contrary, in the NS/ESP, the whole post-Variscan Permian-Recent evolution took place in  
192 an intra-plate setting (Figs. 2-3c-e). In the NS, the initial Permo-Triassic rifting is often related to the



193 reactivation and inversion of old Caledonide lines of weakness (Ziegler, 1988; 1990; 1992; Glennie and  
194 Underhill, 1998; Wilson et al., 2010; Patruno et al., in press). In general, two main Permo-Triassic  
195 phases of crustal thinning occurred (rift I and rift II in Fig. 2). In the NS/ESP these two syn-rift units  
196 correspond to expanded middle Permian clastics and volcanics (Rotliegend Group) and to lower  
197 Triassic clastics, often confined within syn-depositional half-grabens and grabens (Færseth and  
198 Råvnas, 1998; Stemmerik et al., 2000; Richardson et al., 2005; Patruno and Reid, 2017; Patruno and  
199 Lampart, 2018; Patruno et al., in press). These two units are separated by upper Permian evaporitic  
200 cycles of the Zechstein Group, which were deposited in largely post-rift thermal relaxation basins  
201 (Glennie et al., 2003; Ziegler, 1988; 1990; Ziegler et al., 2004; 2006; Peryt et al., 2010; Patruno et al.,  
202 in press). In the NA, there are extensional basins infilled by two distinct sedimentary cycles,  
203 respectively of Permian to Early Triassic and of Middle Triassic to Early Jurassic age – e.g., Martini et  
204 al., 1986; Ciarapica and Passeri, 2005; Fantoni and Franciosi, 2010).

205 After the Permo-Triassic phase, active rifting mainly occurred in Lower and Late Jurassic in the  
206 NA and NS/ESP, respectively (Figs. 2-3C).

207 In the NA, this rifting led, in the Early Jurassic, to the partial drowning of the widespread  
208 carbonate platforms in the NA (Ciarapica and Passeri, 2002; Scisciani and Esetime, 2017). During the  
209 Late Jurassic-Early Cretaceous, the NA Jurassic rifting evolved into the definitive oceanization of the  
210 Ligurian-Piedmont Ocean (Alpine Tethys in Fig. 3c – Stampfli and Borel, 2002; Bortolotti and Principi,  
211 2005).

212 Meanwhile, prior to the Late Jurassic rifting, in the NS Aalenian thermal doming caused a new  
213 phase of regional uplift/erosion (Fig. 2), linked to the development of a transient mantle-plume head  
214 and leading to the extrusion of the Rattray Series and the Forties Igneous Province in the Central NS  
215 (Ziegler, 1992; Underhill and Partington, 1993; 1994; Davies et al., 1999; Coward et al., 2003; Hendrie  
216 et al., 2003; Husmo et al., 2003). The erosional truncation associated to this uplifting event is known  
217 as Mid Cimmerian Unconformity (e.g., Patruno and Reid, 2016). Renewed active extension in the NS  
218 began with a diffuse Bajocian-Bathonian proto-rifting which evolved in the Late Jurassic-Ryazanian  
219 main and last rifting event of this region (Færseth and Ravnås, 1998; Glennie and Underhill, 1998;  
220 Nøttvedt et al., 2000; Ziegler, 1990; 1992; Steel, 1993; Coward et al., 2003; Fraser et al., 2003;  
221 Patruno et al., 2015a,b,c; Patruno, 2017; Turner et al., 2018). The areas to the footwall of the border  
222 faults of the three main rift-related regional lows (i.e., Viking Graben, Moray Firth and Central  
223 Graben), including the ESP, became relatively stable Jurassic-Recent platforms (Figs. 3c, 4-5). As with  
224 the Permo-Triassic extension, and unlike the Jurassic rifting-drifting in the NA, the Late Jurassic rifting  
225 in the NS was aborted before ocean floor formation.

226 A new switch in relative plate motion in the “Mid Cretaceous” triggered the progressive  
227 convergence between the Eurasian/Corsica-Sardinian and African-Adriatic continental margins, which  
228 lead to the closure of the interposed Penninic-Piedmont-Ligurian Ocean and the Eocene-Recent  
229 Alpine/Apennine continental collision (Malinverno and Ryan, 1986; Dewey et al., 1989; Carmignani  
230 and Kligfield, 1990; Calamita et al., 2007) (Figs. 2, 3d-e). The onset of this plate convergence was

231 possibly reflected by the abrupt lithostratigraphic transition in the NA from typical passive-margin  
232 pelagic limestones to Aptian-Albian marlstones (Patrino et al., 2015d; Unida and Patrino, 2016).

233 During this Eocene-Recent collisional stage (Fig. 3d,e), the NA consisted of an eastward to north-  
234 eastward migration of compressive fronts, coupled by foredeep development ahead of the advancing  
235 thrust-belt (Ricci Lucchi, 1986; Patacca and Scandone, 1989; Boccaletti et al., 1990).

236 These Neogene thrust structures have subsequently been affected by arrays of post-orogenic  
237 normal faults (Fig. 5), showing maximum fault-throws of 600-1500 meters and trending roughly  
238 parallel to the previous compressive structures (Calamita et al., 2000; Pizzi and Scisciani, 2000; Pizzi  
239 and Galadini, 2009). Several hangingwall-related intermontane basins infilled with thick Pliocene-  
240 Quaternary continental deposits (e.g., Galli et al., 2008) are associated to the occurrence of moderate  
241 magnitude ( $M \leq 7$ ) historical and instrumental earthquakes (e.g., Calamita et al., 2000).

242 In the NS/ESP, the propagation of weak and localized intra-plate Alpine-age compressions  
243 interrupted the Cretaceous-Tertiary regional thermal subsidence (Figs. 1, 3d and 4; Alberts and  
244 Underhill, 1991; Butler, 1998; Patrino et al., in press). Furthermore, a post-Paleocene easterly tilting  
245 affected the whole U.K. NS. As a consequence, on the western portion of the ESP, we observe  
246 Paleozoic sediments outcropping to the seafloor (Underhill, 1991; Hillis et al., 1994; Patrino et al., in  
247 press; BGS 250k Marine Bedrock Map), while in the eastern portion of the ESP, the Paleozoic is  
248 overburdened by 2000 m of Cenozoic clastic sediments.

249 In summary, in the post-Variscan, the two study area shows the following regional geology  
250 differences.

- 251 - The NA is constructed through a new “classical/complete” Wilson Cycle (from Variscan  
252 compression to Permian-Jurassic Western Tethys extension and ocean spreading and back  
253 to Cretaceous-Recent Alpine/Apenine orogenesis). Post-orogenic Plio-Quaternary  
254 extensional collapse may in fact be interpreted as the early onset of a new cycle.
- 255 - The NS/ESP region instead underwent through at least two “foreland/incomplete” Wilson  
256 Cycles in an intra-plate setting: (1) from Variscan compression to Permo-Triassic rifting, and  
257 back to Mid Cimmerian uplift; (2) from Mid Cimmerian uplift to Late Jurassic rifting,  
258 interrupted by Cretaceous-Palaeogene thermal subsidence, and then partly inverted by far-  
259 field Alpine inversion and, close to the coastlines, by Neogene regional uplift.

260

261

## 262 **Seismic interpretation of the ESP**

263 The analysis of recently-acquired 3D seismic surveys over the outer ESP, coupled with the  
264 available stratigraphic well information, revealed significant traces of repeated tectonic inversion  
265 events.

266 On the basis of well data alone (e.g., the regional well correlation panel shown in Fig. 6),  
267 discrete regional unconformities can be inferred, corresponding in age to the regional uplift and  
268 erosion events discussed in the previous chapter. These are the following:

- 269 1) Base Tertiary Unconformity - identified locally by an erosional top Chalk contact, and possibly  
270 related to mantle plume related epirogenetic uplift.
- 271 2) Intra-Cretaceous Unconformity - possibly related to early Alpine age uplift, with a direct  
272 contact between upper Chalk and Cromer Knoll groups.
- 273 3) Base Cretaceous Unconformity (or BCU) - situated at the base of the preserved Cromer Knoll  
274 Gp. and representing the end of rift unconformity.
- 275 4) Mid Cimmerian Unconformity (MCU or BJU = Base Jurassic Unconformity) - hiatus/truncation  
276 at the base of the preserved Jurassic package, highlighted by the direct contact between  
277 upper-middle Jurassic units (e.g., Pentland, Heather or Kimmeridge Clay formations) with  
278 lower Triassic or, on structural highs, even older units.
- 279 5) The top and base of the lower Permian Rotliegend Group, if preserved, corresponds to two  
280 discrete erosional surfaces associated with the Variscan Orogeny. However, these and possible  
281 deeper Caledonian unconformities are not well documented, as most wells have shallower  
282 TDs.

283 Each of these erosional surfaces is also visible across several seismic lines as time-equivalent  
284 angular unconformities. In particular, in Figure 7b a Devonian to lower Carboniferous package has  
285 been tilted and truncated by the Base Permian unconformity. A thin Zechstein to Triassic package is  
286 subject to a lower amount of tilt and is truncated by the BJU. Finally an upper Jurassic package shows  
287 an even lower amount of tilt and is truncated by the BCU. The stratal packages bounded by these  
288 unconformities are characterized by increased tectonic subsidence rates (Fig. 7c), particularly in  
289 relationship with the Devonian post-orogenic collapse event and the post-Variscan Permo-Triassic rift-  
290 related mini-basins (Figs. 7c-7d).

291 Discrete unconformity surfaces can be identified only in intra-platform depocentral areas  
292 characterized by maximum stratigraphic preservation of Carboniferous-Cretaceous units, which are  
293 normally absent elsewhere on the ESP (e.g., Piper Shelf in Figs. 6-7 and Crawford-Skipper Basin in Fig.  
294 8; Patruno and Reid, 2017; Patruno and Lampart, 2018; Patruno et al., in press). The unconformities  
295 instead merge together towards persistent structural highs (e.g., Kraken High, Fladen Ground Spur  
296 and Halibut Horst in Figs. 7-9). Intra-platform Carboniferous-Jurassic depocentres and persistent  
297 structural highs are also characterized by very different fault density (Fig. 9). Main age of fault activity  
298 ranges from Devonian, Permo-Carboniferous, Triassic and Jurassic-Cretaceous, and each fault age  
299 population shows a characteristic strike trend (Fig. 9; Patruno et al., in press). In particular, both east-  
300 trending well correlation panels and seismic lines across the Piper Shelf – Fladen Ground Spur areas  
301 (Figs. 6 and 7) reveal several sub-BCU extensional faults, with different timing of activity. Fault 6 in  
302 Figure 7a for example is associated to a partly inverted Rotliegend syn-rift wedge, whilst Fault 9  
303 relates to both upper Jurassic and Permo-Triassic syn-rift wedges (also see backstripped evolution  
304 along a similar transect in Patruno, 2017). The Rotliegend syn-rift wedge bounded by Fault 6 and the  
305 Jurassic-Early Paleocene reflectors lying on it are subject to late inversion, highlighted by a gentle  
306 anticlinal folding of these reflectors, against which later Palaeogene reflectors onlap (Fig. 7a). An Eo-  
307 Alpine and Mid Cimmerian inversion age was proposed for this structure by Patruno and Reid (2018).

308 This inverted sedimentary wedge corresponds to one of the Carboniferous-Permian mini-basins  
309 highlighted by the time-thickness map (Fig. 7d).

310 Further north, relatively minor Late Cretaceous and Paleocene compressional inversion phases  
311 are revealed by: (1) the gentle folding of the Carboniferous-Paleocene reflectors in the Crawford-  
312 Skipper Basin (Fig. 8; also see Patruno and Reid, 2017); (2) the larger-scale antiformal folding of the  
313 Fladen Ground Spur, with Late Cretaceous strata becoming progressively thinner towards the  
314 antiformal culmination of this area and Paleocene reflectors onlapping against it (Fig. 8); (3) the minor  
315 reverse reactivation event for a major Devonian master-fault on the Kraken High, with an associated  
316 fault-related anticline formed by the overlying Paleocene reflectors, forming the structural closure for  
317 the Kraken oil field. (Fig. 10). This half-graben is associated to an expanded (up to 2.0 seconds TWT)  
318 hangingwall Devonian succession, including possible syn-rift wedge geometries (Figs. 8, 10). This is  
319 just one of the several extensional structures developed during the Devonian-age extensional collapse  
320 of the Caledonian Orogeny.

321 A few km to the north of Kraken, a prominent Devonian syncline is related to the same syn-  
322 depositional master-fault (Fig. 11). Below the Devonian reflectors (Units 1-2 in Fig. 11), a distinctly  
323 opaque seismic stratigraphic unit is tentatively identified as metamorphic basement (Units 3-4). This  
324 unit is about 1.0 second (TWT) thick, and do not contains any visible reflectors. Below this seismically  
325 opaque "basement" a second more highly reflective strata (Unit 5) is observed overlying a third more  
326 opaque seismic package. Fazlikhani et al. (2017) showed that a very similar tripartite sub-division of  
327 the basement seismic facies can be observed throughout the rest of the northern NS.

328 The Devonian successions in this area range from thick shale and sandstone intercalations in the  
329 main syncline, to conglomerates and breccias away from it (e.g., wells A and B). The Early Devonian,  
330 characterized by granite wash grading to granite in Well C ("Bressay Granite") could either be an  
331 intrusion localized in a small area surrounding the well (e.g., Unit 3 in Fig. 11) or could be interpreted  
332 as an acoustically transparent "basement" (Unit 4). Unfortunately, the regional extent and thickness  
333 of the intrusions is unknown and unconstrained by further data (Stephenson et al., 1999)

334 The highly reflective Unit 5 underneath the seismically transparent basement is fortuitously  
335 penetrated by Well D, drilled across the ESP/Viking Graben border fault. According to the analysis of  
336 this well, this unit is composed of gneiss/schists rich in hornblend and biotite, with an Early Devonian  
337 radiometric metamorphic cooling (Bassett, 2003). As a consequence Unit 5 possibly represents a  
338 transition between different compositions of crystalline rocks, likely to give rise to a significant  
339 contrast in acoustic impedance (e.g., acidic granites over basic gneiss?).

340 We interpret Unit 5 as possible pre-Devonian Caledonides or shear zones (e.g., Seismic Facies 2  
341 of Fazlikhani et al., 2017) based on: (1) the lower Devonian metamorphic cooling age, and (2) the  
342 presence of likely north-westerly verging compressional compressive structures (at least in the south-  
343 eastern half of the line). In the north-western half of the line, the presence of likely extensional  
344 structures inside the same "Caledonide" package is counterintuitive. A possible explanation is that the  
345 north-western half of the line may represent a foreland area of the Caledonian Orogeny. The frontal  
346 Caledonian thrust was possibly situated in proximity of the previously mentioned Devonian master-

347 fault, which can be mapped laterally for several tens of km (thick red fault on Kraken High in Fig. 9).  
348 This Devonian master-fault and other deeper faults that cut Unit 5 all show a NNE-SSW strike  
349 resembling the main lineaments associated to the Caledonian Orogeny (e.g., the Great Glen Fault and  
350 its offshore continuation), and to the likely orientation of the axis of the Iapetus Ocean (Figs. 3a, 4 and  
351 9; Patruno et al., in press). This suggests a long-term preservation of the structural grain from the  
352 Caledonian compression to the Devonian extension up until the Alpine-age inversion (Figs. 9 and 12;  
353 Patruno et al., in press).

354

355

### 356 **Field geology of the NA**

357 In this section, seismic and outcrop data in the UMAR are tied, with the aim to reconstruct a  
358 balanced crustal geological cross-section of the outer NA. Moreover, due to the low resolution of  
359 vintage seismics, a detailed structural fieldwork has been carried out along some key regional-scale  
360 thrust zones, in order to define the field-scale geometric structural-stratigraphic relationships.

361 The UMAR comprises a series of east/north-east-verging folds, with 5-8 km wavelength, gentle  
362 backlimbs and near vertical-to-overturned forelimbs (Calamita et al., 2012). Thrust planes commonly  
363 truncate the east/north-eastern limbs of the folds (Fig. 13) with a shortening of c. 1-3 km achieved by  
364 each thrust and the related fold.

365 The eastern UMAR comprises four thrust-related anticlines, in which the more continuous  
366 corresponds to the Igno Mt.-Valnerina Anticline (Fig. 13). Some of these folds are displaced by NW-SE  
367 trending Quaternary normal faults, juxtaposing recent continental deposits in the hanging-wall to  
368 Jurassic-Miocene carbonates in the footwall, and responsible for recent destructive earthquakes  
369 (Calamita et al., 2000).

370 A detailed structural fieldwork has been carried out in the Igno Mt. Anticline area (Fig. 14). This  
371 anticline shows an overturned forelimb with Jurassic-Cretaceous strata overlaying gently SW-dipping  
372 Cretaceous-Miocene beds (Calamita et al., 1993). The anticline is cored by a Jurassic condensed  
373 pelagic succession, while the back-limb is affected by a set of WSW-dipping normal faults (Fig. 14).  
374 The presence of a thick and complete Mesozoic pelagic succession in the downthrown block indicates  
375 a Jurassic syn-sedimentary activity for these normal faults. A Miocene reactivation of these structures  
376 is suggested by Miocene channelized conglomerates cutting into their footwall. Clear Quaternary  
377 activity indicators (like fault scarps and triangular facets) are missing, suggesting a pre-thrusting  
378 foreland flexural-induced extension (cf., Scisciani et al., 2000b). The normal fault pre-thrusting activity  
379 and the thrust hangingwall ramp onto footwall ramp relationship observed in the field constrained  
380 the balanced geological cross-section for the Igno Mt.-Valnerina thrust, allowing estimating a  
381 shortening of about 1.7 km (Fig. 14b).

382 North-eastward to Igno Mt. the Camerino Basin has been interpreted as a Miocene normal  
383 fault-controlled basin, filled by Miocene turbidites (Scisciani et al., 2000b). This area was affected by  
384 the 2016 Visso-Norcia-Amatrice normal-faulting seismic sequence (Emergeo Working Group, 2016).

385 The eastern margin of the Camerino basin corresponds to the gently dipping back-limb of the Sibillini  
386 Mts. Anticline (Fig. 13). The regionally-extensive Sibillini Mts. thrust and thrust-related fold shows a  
387 curved geometry expressed by two segments, respectively trending NW-SE (northern sector) and  
388 NNE-SSW (Vettore Mt. apical central sector, with maximum shortening and structural elevation), that  
389 continue southward into the north-trending Olevano-AnTRODoco thrust (Fig. 13). At least the central  
390 part of the Sibillini Mts-Olevano-AnTRODoco thrust coincides with an inherited NNE-trending  
391 lineament (Ancona-Anzio line in Castellarin et al., 1982) separating the persistent Mesozoic Apulian  
392 (Lazio-Abruzzi) carbonate platform to the east from the time-equivalent Umbria-Marche pelagic basin  
393 to the west, and its arcuate shape has been commonly interpreted to be controlled by this structural  
394 inheritance (Alberti et al., 1996; Butler et al., 2006; Calamita et al., 2011; Pace et al., 2011; Scisciani  
395 and Esestime, 2017).

396 The best exposures of the main thrusts crop-out along the Fiastrone Valley (along the NW-  
397 trending thrust segment), located few kilometres southward to the trace of the seismic line (Figs. 13  
398 and 15), where the Jurassic-Cretaceous carbonate succession (including Lower Jurassic Calcare  
399 Massiccio Fm.) form a thrust-related anticline emplaced onto Paleogene strata. The steeply dipping-  
400 to-overtained forelimb describes a hanging-wall ramp superimposed onto a footwall flat.

401 A balanced cross-section reconstructed by the collected surface geological data indicates a  
402 shortening of c. 4.0 km (Fig. 15). A shortening of c. 2.0 km was estimated more to the north (Mazzoli  
403 et al., 2005), and close to the seismic line trace (Fig. 13) documenting a reduction of the orogenic  
404 contraction away from the apex of the salient (Vettore Mt. area).

405  
406

#### 407 **Subsurface geology of the outer NA**

408 In this work, we selected a recently released seismic reflection profile transecting the UMAR  
409 from the inner Umbria Valley to the outer Laga Basin, through the intervening Camerino and  
410 Colfiorito basins (Figs. 5, 13-16). Key reflectors were correlated through: (a) geological fieldwork in  
411 proximity of the seismic trace; and (b) direct ties between well-log stratigraphy and seismic by using  
412 check-shot or synthetic seismograms of deep wells drilled close to the seismic profile.

413 The reconstructed seismic stratigraphy is consistent with previous studies (Bally et al., 1986;  
414 Mirabella et al., 2008; Scisciani and Montefalcone, 2005; Scisciani et al., 2014), and consists of eight  
415 units with distinctive seismic facies and bounding reflectors (Fig. 16). Units 3-7 have been drilled in  
416 the Massicci Perugini ridge-Tiber Valley (about 10.0 km to the north-west of the seismic line) and  
417 show a good correlation along the profile. Conversely, in the eastern sector, the older intervals (Units  
418 6-8) are unconstrained due to the shallow penetration of exploration wells. Nevertheless, the results  
419 of combined gravimetric and magnetic modelling indicate homogenous characteristics of the deeper  
420 intervals along the entire seismic profile (Scisciani et al., 2014).

421 The seismic profile displays an overall westwards thinning of the Liassic-Miocene pre-orogenic  
422 succession, which is in agreement with the outcropping geology (Deiana and Piali, 1994; Scisciani et  
423 al., 2010).

424 The Pliocene-Quaternary continental deposits (Unit 1) are restricted to the hanging-wall of  
425 west-dipping normal faults in the Umbria Valley and Colfiorito Basin (Fig. 16), where they  
426 unconformably overlie the older and deformed units. The Miocene siliciclastic deposits (Unit 2)  
427 correspond to poorly reflective seismic facies with respect to the underlying Unit 3, and are confined  
428 to the Umbria Valley, Camerino Basin and Laga Basin - Fig 16).

429 The Marne a Fucoidi reflector at the base of Unit 3 (EK in Fig. 16) overlies a very reflective  
430 package which terminates downward into a reflection-free interval, corresponding to the massive and  
431 monotonous Liassic shallow-water carbonates (Calcare Massiccio Formation). The Marne a Fucoidi  
432 and Top Calcare Massiccio reflectors are therefore distinctive and can be confidentially traced  
433 regionally, illustrating the deep geometry of outcropping structures. The three large wavelength (5-10  
434 km) folds in the seismic section correspond to the Subasio Mt., Igno Mt.-Valnerina and Sibillini Mts.  
435 thrust-related anticlines. Clear reflector terminations against the thrust faults are visible in both  
436 hanging-wall and foot-wall blocks. The resulting hanging- and foot-wall ramp geometry let the thrusts  
437 achieve a limited amount of shortening: about 4.0 km for the principal and regional Sibillini Mts.  
438 thrust and lower for the others.

439 Underneath the core of the large-scale UMAR ridge, the Paleozoic-Triassic interval (Units 6-7) is  
440 significantly thicker (maximum TWT-thickness of 3.8 s) than in the areas underneath the Umbria  
441 Valley and the footwall of the Sibillini Mts. Thrust (about 1.2 and 1.8 s, respectively). These lateral  
442 thickness variations are also preserved after performing time-to-depth conversion of the seismic  
443 profile, suggesting that they are not artifacts.

444 In particular, Unit 7 has been correlated with the slightly metamorphosed Verrucano facies in  
445 adjacent wells (Scisciani and Estime, 2017). This unit shows a wedge-shaped geometry in the  
446 hangingwall of normal faults at depth (Fig. 16). Some of these faults show a variation of the offset  
447 with depth that is typical of positive inversion tectonics: faults have a normal offset at depth that  
448 changes to reverse up-dip (e.g., Williams et al., 1989), with a mild degree of inversion (*sensu* Cooper  
449 and Williams, 1989). The geometry of the lower part of Unit 6 (presumably corresponding to the Late  
450 Triassic evaporites) clearly depicts the vertical extrusion of the over-thickened Mesozoic syn-rift basin  
451 infill. The thick wedge of lower Unit 6 at depth corresponds at surface with the long-wavelength  
452 exhumed carbonate ridge and with the region of highest topographical elevation (Fig. 16).

453 At shallow depth in the seismic profile, several high-angle faults terminate against low-angle  
454 thrusts (e.g., SP1600-1800, 2080-2130, and 2150-2420 in Fig. 16). Some of these high-angle faults  
455 show a good correlation with outcropping Jurassic and Miocene normal faults that commonly occur in  
456 the core and back-limb of anticlines. This setting corresponds to short-cut geometries that are typical  
457 of positive inversion tectonics where a thrust fault truncates across the footwall of a pre-existing  
458 inverted normal fault (e.g., Figs. 15-16; Cooper and Williams, 1989; Coward, 1994).

459 The west-dipping Quaternary Colfiorito normal fault system merges downward into a previous  
460 Neogene thrust plane, as suggested by the continuity of the gently -dipping fault plane reflections at  
461 1.0-2.0 seconds (TWT) of depth (SP1400-1500 in Fig. 16). Conversely, the Quaternary Subasio Mt.  
462 normal fault system is likely associated with a décollement layer within the Triassic evaporites, as  
463 suggested by: (a) the fault down-throw apparently decreasing down-dip; and (b) the top phyllites  
464 reflector being only moderately offset (SP200-500 in Fig. 16).

465

#### 466 **Integrated fieldwork and seismic interpretation: positive and negative inversions in the NA**

467 The interpretation and time-to-depth conversion of the seismic line in Figure 16 has been used  
468 to constrain a regional balanced and restored geological cross-section across the outer sector of the  
469 NA (Fig. 17). The basement geometry is characterized by a structural depression located underneath  
470 the UMAR salient. The adjoining basement highs are placed beneath the Umbria Valley and Laga  
471 Basin. The inferred basement physiography highlights a large pre-existing basin filled with Triassic and  
472 probably late Paleozoic sediments. The resulting structural style appears strictly controlled by the  
473 inversion and vertical extrusion of this deep Paleozoic-Triassic extensional basin.

474 The UMAR separates two thick siliciclastic turbiditic wedges infilled during the Burdigalian-  
475 Serravalian (Marnoso-Areancea Fm.) and Messinian (Laga Formation) times. These wedges are 2000-  
476 5000 m thick (e.g., Boccaletti et al., 1990) and their present-day transversal extension is at least of 60  
477 km. In the interposed ridge, the siliciclastic turbidites are generally lacking or extremely reduced in  
478 thickness with the exception of few NNW-SSE trending confined basins delimited by normal faults  
479 (e.g., the Camerino Basin in Fig. 5 and 13; Scisciani et al., 2001). Analogous extensional basins infilled  
480 by siliciclastic foredeep sediments have been found both in the eastern (Belforte basin and Cingoli  
481 area) and western sector (Gubbio basin) of the UMAR (e.g., Scisciani et al., 2002; Mirabella et al., 2004  
482 - Figs. 5 and 13). The syn-sedimentary normal faults trend NNW-SSE to N-S, are both E- and W-dipping  
483 and show a range of throw from about 100 to 800m. Thick turbiditic successions are concentrated in  
484 the basin depocentres, with synsedimentary slumps, slide scars and coarse grained deposits sourced  
485 by steep paleo-scarps created by the synsedimentary normal faults. The evident increase in  
486 conglomerates and coarse grained sandstones close to the paleoscarps suggest the synsedimentary  
487 control exerted by the normal fault in the development of these confined basins (Ricci Lucchi, 1986).  
488 By contrast the structural highs are capped by thin and condensed sequences of hemipelagic shales or  
489 are deeply eroded. Detailed stratigraphic studies indicate that the extensional faults were active and  
490 controlled the deposition of Late Miocene foredeep turbidites included in the Marnosa-Arenacea  
491 (Burdigalian-Tortonian), Camerino sandstones (Tortonian-early Messinian) and Laga (early Messinian)  
492 Formations. Moreover, several of these normal faults frequently reactivated pre-existing extensional  
493 structures, including Jurassic and Cretaceous pre-orogenic faults. The Miocene normal faults are  
494 commonly deformed or truncated by subsequent folds and thrust faults developed during the  
495 Apennines compressive tectonics.



496 Prevailing thrust hangingwall ramp onto footwall ramp geometric relationships have been  
497 constrained through both fieldwork and seismic interpretation. The total shortening associated with  
498 the Neogene compressive deformation is about 7.7 km (i.e., c. 10% of the total section length), with  
499 each thrust and related fold realizing a maximum shortening of 4.0 km (e.g., for the Sibillini Mts.  
500 thrust).

501 The common occurrence in the anticline backlimbs of high-angle WSW-dipping normal faults  
502 truncated by Neogene thrusts propagated with a short-cut geometry highlights the key role played by  
503 positive inversion tectonics in the Apennines orogeny. Another relevant feature is the negative  
504 reactivation of low-angle thrust fault segments by recent active normal faults, including the WSW-  
505 dipping Colfiorito and Visso-Norcia normal fault systems (indicated with "X" and "Y" in Fig. 16,  
506 respectively). These fault systems were responsible for two strong recent seismic sequences with  
507 main-shocks of Mw 6.0 (1997 in Colfiorito) and Mw 6.5 (2016 in Visso-Norcia), respectively. The dense  
508 network of seismic stations installed during these recent earthquakes clearly imaged the deep active  
509 fault geometry (Barba and Basili, 2000; Chiaraluce et al., 2017). Two evident SSW-dipping areas with  
510 densely concentrated aftershock locations are consistent with the geometry of the normal fault  
511 systems reconstructed by both field data and seismic interpretation. All these methodologies suggest  
512 that the active normal faults negatively reactivate preceding thrust segments.

513

514

## 515 **Discussion**

516

### 517 *Structural reactivation and inversion patterns in the ESP*

518 A lateral transition between compressional belt, foredeep and mainly extensional foreland  
519 structural domains can be clearly interpreted for a young and relatively well-preserved orogeny like  
520 the Apennines (e.g., Finetti et al., 2005). Instead it is much more challenging to reconstruct the  
521 structural setting for older collisional belts such as the Caledonian Orogen where subsequent high-  
522 pressure metamorphic core complex formation and widespread phases of erosional truncation often  
523 obliterated the remnants of earlier structural configurations. However, as the offshore ESP was likely  
524 subject to a lower degree of metamorphic obliteration of the Caledonian belt configuration than in  
525 the onshore it was possible to observe and highlight the coexistence of Caledonian-age normal faults  
526 and compressional structures (Fig. 11). These offshore structures have been mapped in 3D, revealing  
527 an overall north-trending strike-orientation that is virtually undistinguishable from the Devonian-  
528 Jurassic structural grain of this area, and the hypothesized offshore trend of the Iapetus Suture (Fig.  
529 3a). It can therefore be inferred that these possible Caledonian-age extensional structures were  
530 formed in the palaeo-foreland of the evolving Caledonian orogen. Moreover, the Devonian normal  
531 master-fault that underlies the Kraken area might have coincided with the front of the Caledonian  
532 belt, as no trace of deep-seated compressional deformation is observed beyond it.

533 Irrespective of kinematic and age of activity, all mapped Caledonian, Devonian, Permo-Triassic  
534 and Jurassic-Cretaceous faults share similar trends (Fig. 9). Two areas can be identified in the outer

535 ESP, one with structural grain parallel to the north-trending Viking Graben, the other with conjugate  
536 fault trends mirroring the east-trending Witch Ground Graben. This long-term preservation of  
537 structural grains and the reconstructed polyphase history of tectonic inversion and reactivation of the  
538 same structural zones of weakness highlights the profound impact of structural inheritance in the  
539 NS/ESP (e.g., Fig. 12; Johnson and Dingwall, 1981; Bartholomew et al., 1993; Glennie and Underhill,  
540 1998).

541 During this polyphase post-Devonian inversion history, the multiple intra-plate compressional  
542 phases lead to the deposition of up to five main regional erosional unconformities: (1) Saalian  
543 (Variscan orogeny); (2) Mid Cimmerian (Mid North Sea Doming); (3) Late Cimmerian (BCU); (4) Intra-  
544 Cretaceous (Eo-Alpine); (5) Base Tertiary and Paleocene Alpine unconformities (Fig. 2). These events  
545 correspond to “peaks of absence” of the time-equivalent rocks from >75% of the ESP wells (Patruno  
546 et al., in press).

547 In particular, the Late Carboniferous Variscan compression lead to extensive foreland-type uplift  
548 and erosions (Figs. 6 and 7d), which were significant over certain portions of the ESP, such as the  
549 Fladen Ground Spur and Kraken High. These areas became permanently inverted into long-lasting  
550 positive features, with erosional processes which started sourcing sediments to the adjacent relative  
551 depocentres (Freer et al., 1996; Fig. 12). We suggest that, consistently with the main supra-regional  
552 Variscan kinematic (Fig. 3b), the local maximum compression vectors were oriented roughly north-  
553 south (Fig. 12b). A number of Devonian reflector folds (e.g., Figs. 7-8) were possibly due to Variscan  
554 intra-plate compressional stress propagation.

555 Although the Late Triassic to Aalenian hiatus has been recorded by nearly all the ESP wells  
556 (Patruno and Reid, 2017; Figs. 6 and 7d), evidence of significant Aalenian uplift is particularly strong in  
557 the vicinity of the South Viking Graben ‘triple junction’, where the focus of regional thermal doming  
558 and erosion was situated (Underhill and Partington, 1993; Coward et al., 2003). In particular, an  
559 overall Early-Middle Jurassic tectonic uplift has been highlighted by the burial history modeling of  
560 Well 15/6-1 (Fig. 7c; Patruno and Reid, 2018). Furthermore, the Devonian-Carboniferous succession  
561 between Fault 6 and Anticline A in Figure 7a underwent an initial Variscan tilting and a successive Mid  
562 Cimmerian uplifting-related tilting, which had an increasingly greater magnitude towards the proto-  
563 Viking Graben. As a consequence, these reflectors are now characterized by a greater overall easterly  
564 tilt (ca. 83 ms/km) than the overlying Permo-Triassic over the same area (ca. 35 ms/km), which was  
565 only affected by the Mid Cimmerian tilting.

566 Minor Early Alpine compression events are highlighted by the gentle anticlinal folding of the  
567 entire Carboniferous-Top Cretaceous succession over inverted Permo-Triassic extensional basins,  
568 with lower Paleocene strata progressively onlapping against the antiformal culmination (e.g., Fig. 7, 8  
569 and 12). These compressional events are probably Late Cretaceous in age, as highlighted by Chalk  
570 strata becoming anomalously thin towards the antiformal culmination, which corresponds to the  
571 Permo-Triassic hangingwall depocentres (Figs. 7a-8). The inversion of the Devonian extensional  
572 master-fault on the Kraken High (Figs. 10 and 12) highlights a slightly posterior, Late Paleocene  
573 compressional event.

574 The Permo-Triassic and Late Jurassic rifting events left behind a number of syn-depositional  
575 fault-driven intra-platform tectonic depocentres, such as several half-grabens on the Piper Shelf (Figs.  
576 7a, 7d and 9) and the Crawford-Skipper Basin (Figs. 8-9 and 12; Patruno and Reid, 2017). The mini-  
577 basins on the Piper Shelf were mostly filled with Rotliegend sediments (e.g., the Fault 6 half-graben in  
578 Fig. 7a), suggesting a main Permian-age for the post-Variscan rift development over this area, with  
579 minor Triassic and Jurassic reactivations. Both Permian and Triassic faults are present on the  
580 Crawford-Skipper Basin: they share a mean north-northeast orientation which is parallel to the border  
581 faults of the nearby Viking Graben (Fig. 9), but show negligible Late Jurassic reactivation, suggesting  
582 that in the Jurassic the entire extensional strain had been transferred to the incipient Viking Graben  
583 border faults (Figs. 9 and 12).

584

585

#### 586 *Structural reactivation and inversion patterns in the NA*

587 Following the Variscan Orogeny, the basement of the NA underwent repeated episodes of  
588 extension during the Late Paleozoic-Mesozoic times. Our subsurface interpretation suggest that,  
589 presumably starting from the Late Paleozoic and Triassic, in the study area a prominent extensional  
590 basin developed and was infilled by at least 5 km of syn-tectonic sediments (Figs. 16-17). Comparable  
591 extensional basins were also reconstructed further east in the Montagna dei Fiori area and in the  
592 Central Adriatic (Fig. 18). The subsequent Jurassic-Cretaceous extensional event was less severe and  
593 achieved an overall reduced amount of down-throw (Fig. 17). The shallower and high-frequency  
594 setting of Jurassic normal faults with respect to previous structures suggest that the thick Triassic  
595 evaporitic interval acted as decollement level during the extension, influencing fault vertical growth  
596 and transversal spacing.

597 The pre-orogenic configuration of basement and Triassic decollement strongly controlled the  
598 style of compressive structures during the Apennines inversion tectonics. The low-wavelength folds  
599 are commonly related to minor thrusts propagated from shallow detachments and following short-cut  
600 trajectories with respect to the pre-existing Jurassic normal faults. Conversely, the large-wavelength  
601 anticlines forming the prominent mountain fronts and delimited by regional thrusts (e.g., the Sibillini  
602 Mts thrust) correspond to main thick skinned structures emanating from basement (Figs. 18 and 19).  
603 Fieldwork and seismic interpretation typically indicate thrusts cross-cutting through hanging- and  
604 foot-wall ramps; these geometric relationships imply a reduced shortening amount with respect to  
605 previous thin-skinned reconstructions (e.g., Bally et al., 1986).

606 Normal fault networks were widely observed in several foreland basins all over the world (e.g.,  
607 Sinclair, 1997) and have also been described in the NA/UMAR foredeep basins. Syn-orogenic normal  
608 faults developed in a foreland tectonics context before the onset of contractional deformation and  
609 generated structural highs near-parallel to the flexure axis and to the subsequent compressive  
610 structures, therefore controlling the thickness, dispersal and facies distribution of the syn-tectonic  
611 foredeep deposits (Tavarnelli et al., 1998; Tavarnelli and Peacock, 1999; Scisciani et al., 2000a; 2001;  
612 2002; Mazzoli et al., 2002; Calamita et al., 2003). Several of these normal faults frequently reactivated

613 pre-existing extensional structures, including Jurassic and Cretaceous pre-orogenic faults (Calamita et  
614 al., 2011), as observed in similar settings where foreland down-warping resulted in the reactivation of  
615 inherited passive-margin structures (Frankowicz and McClay, 2010; Langhi et al., 2011; Saqab and  
616 Bourget, 2015).

617 In general the strong subsidence recorded in foredeep basins is triggered by the flexure of the  
618 foreland plate due to the load exerted by the adjacent growing orogenic wedge (Cross, 1986). The  
619 foreland flexure is locally accommodated by pre-orogenic extension affecting the shallow brittle crust  
620 (“flexural extension” - Turcotte and Schubert, 1982; Doglioni, 1995). The syn-orogenic normal faults in  
621 the Apennines were also classically interpreted in term of flexural bending extension (e.g., Boccaletti  
622 et al., 1990); however, the normal faults within the UMAR and in adjacent NA sectors show distinctive  
623 architectural characteristics that differ with respect to those of typical flexural bending settings (Fig.  
624 19). In the NA, Miocene normal faults are commonly foreland-dipping and are located in the inner  
625 edges of foredeep basins (e.g., in the eastern sector of the Sibillini Mts). In the proposed  
626 reconstruction (Fig. 19), the Late Miocene UMAR is interpreted as an embryonic large wavelength  
627 (about 40 km in width) uplift developed in proximity of the advancing Apennines thrust front. This  
628 suggests that during the Late Miocene the Adriatic foreland underwent foreland flexure accompanied  
629 by normal faulting, prior to large-wavelength (about 40 km) uplift, with reactivation at shallow levels  
630 of the pre-existing normal faults. The large-scale uplifted “peripheral bulge” almost corresponds to  
631 the whole UMAR, suggesting a large-scale basin inversion, with embryonic vertical extrusion by  
632 positive inversion of the Late Paleozoic-Mesozoic extensional basin at depth, possibly promoted by  
633 mechanical weakening of the NA foreland lithosphere due to flexural normal faulting.

634  
635 *The controlling factor of multi-phase reactivations and inversions*

636 Although the ESP and the NA underwent different tectonic evolutions within distinct settings,  
637 they both show evidence of cyclic reactivation of faults and structural grains, with alternating  
638 extension and compression (Fig. 20). Therefore, these areas are expected to be characterized by some  
639 of the geological elements that, in past studies, have been suggested to promote this sort of recurring  
640 reactivations, at scales ranging from a single fault plane to an entire basin or chain, as predicted by  
641 the Wilson Cycle concept. The main reported factors include: (1) nature and composition of  
642 sedimentary cover and crust, (2) thermal conditions, (3) crustal thickness, (4) amount/rate and  
643 direction of deformation, (5) frequency, orientation and mechanical/petrophysical characteristics of  
644 fractures and shear zones, (6) fluid occurrence and relative pressure, and (7) amount/rate of  
645 sedimentation/erosion (Sibson, 1985; Williams et al., 1989; Butler et al., 1997; Turner and Williams,  
646 2004; Morley et al., 2008; Buitter et al., 2009; Bonini et al., 2012; Lafosse et al., 2016).

647 Both analysed areas rest onto a relatively attenuated continental lithosphere (Zanella et al.,  
648 2003; Artemieva, 2007; Molinari and Morelli, 2011). In particular, in the far undeformed Adriatic  
649 foreland, where crustal thickness was preserved by the Cenozoic contractional and extensional  
650 tectonics, the Moho is relatively shallow (about 30-35 km in depth) (Finetti et al., 2005; Miller and  
651 Piana Agostinetti, 2012). Under present-day onshore Scotland and Greenland Caledonian core

652 complexes, the Moho is also at relatively shallow depths (c. 50 km - Snyder, 1991) for a fully collisional  
653 orogen. The thickness of the crust in the NS was probably reduced to 30-40 km at the end of the  
654 Devonian extensional collapse (Schlindwein and Jokat, 1999) and is currently 10-30 km, which are  
655 typical values for rift basins (Zanella et al., 2003).

656 Elevated geo-thermal gradient and inherited basement grain are “classical” drivers for long-  
657 term lithosphere weakening, consequently favouring the cyclical reactivation of the former rifted  
658 structural grain during the compressional and extensional collapse parts of a Wilson Cycle  
659 (Krabbendam, 2001).

660 Previous numerical modelling studies have demonstrated that a short time-interval between  
661 rifting-related crustal thinning and the subsequent compression prevents the basin and the  
662 underlying mantle from cooling, favouring positive basin inversion (Burov and Diament, 1995; Buiter  
663 et al., 2009). This however is in direct contrast to our Apennines case study, where the post-rift phase  
664 lasted 140-190 Myr.

665 In our interpretation, instead, the mechanical weakening of the foreland lithosphere due to pre-  
666 inversion flexural normal faulting, tectono-magmatic phases and frequently reactivation of inherited  
667 discontinuities, accompanied by possible crustal hydration, is the key to explain the observed  
668 polyphase basin inversions in the two study areas.

669 In relatively old and cold basins, numerical modelling indicates that small amounts of strain  
670 softening are required to promote basin inversion by reactivation of inherited fault zones. In  
671 particular, the weakening mechanism of shear zones or the cyclic re-utilization of pre-existing  
672 discontinuities are thought to be long-lived driving processes (e.g., Butler et al., 1995; Imber et al.,  
673 1997; Hatcher, 2001; Thomson and Underhill, 1993; Holdsworth et al., 2001; Scisciani, 2009). Shear  
674 zone weakening is enhanced by high fluid pressures, clay-scale gouge and phyllosilicate-rich foliated  
675 fault rocks (e.g., Collettini et al., 2009). Several of these key-elements have been clearly documented  
676 in several reactivated faults in both the NA and the NS, as further explained below.

677 The main positive inversion stages affecting the NS/ESP foreland were preceded by relevant  
678 tectono-magmatic phases (Fig. 2) during the Carboniferous to Lower Permian and middle Jurassic,  
679 associated to the development of large wavelength erosional unconformities. The NS Mid Cimmerian  
680 Unconformity, in particular, causes Aalenian to upper Triassic interval to be missing in wells even in  
681 relative structural depocentres (e.g., the Piper Shelf) (Fig. 7; Patruno and Reid, 2017), and is  
682 associated with the extrusion of the Rattray Series and the Forties Igneous Province (Ziegler, 1992;  
683 Underhill and Partington, 1993; 1994). This widespread erosion is the result of the impingement of a  
684 broad-based (>1250 km diameter) transient plume head at the base of the lithosphere (“Mid North  
685 Sea Doming” event, *sensu* Underhill and Partington, 1993). Analogously, in the NA Adriatic foreland, a  
686 Palaeogene regional uplift and extensive erosion is associated with the near-complete absence of  
687 Paleogene sediments in wellbores, and Miocene deposits unconformably locally resting onto Lower  
688 Cretaceous carbonates (Rusciadelli et al., 2003; Satolli et al., 2014). This regional uplift was also  
689 concomitant with an extensive Paleogene anorogenic intra-plate magmatism that affected the

690 Adriatic foreland, associated to intrusive and effusive ultra-mafic products sourced by the mantle (Bell  
691 et al., 2013).

692 The overall reduction of the mechanical resistance of the rocks in the study areas was thus likely  
693 favored by: (a) the magmatic-related increase in heat-flow and geothermal fluids; and (b) the  
694 diagenetic processes associated with the development of several long-lasting, erosional and  
695 compound erosional surfaces. Stress localization subsequently took place within the thermally-  
696 weakened portions of the crust and multi-phase reactivations of pre-existing lineaments ensued  
697 (Kusznir and Park, 1987).

698 In relation to this, it is interesting noting the very quick transition in the Viking Graben from  
699 high-magnitude Aalenian uplift to Bajocian-Bathonian proto-rifting and Callovian-Berriasian main rift  
700 (Patruno, 2017). Also, the locus of maximum Aalenian uplift quickly became the 'triple junction'  
701 between the axes of the three main Late Jurassic rift systems of the NS (the Viking Graben, Central  
702 Graben and Moray Firth).

703 In addition, the existence of foreland units affected by syn-orogenic normal faults has several  
704 implications on fluid circulation and mechanical characteristics of the foreland plate. Pre-orogenic  
705 formations in the foreland are commonly overlain by a veneer of hemipelagic shales and marls which  
706 predates the deposition of thick coarse grained turbidites, acting as a fluid barrier (Ricci Lucchi, 1986).  
707 However, when this confining layer is offset and breached by syn-orogenic normal faults, the deep  
708 reservoir becomes hydraulically interconnected to the shallow one. Consequently, deep and light  
709 fluids leak-off (hydrocarbons, Co<sub>2</sub> and hot water) while cold and dense saltwater may intrude into the  
710 deep carbonate reservoir recharging or enhancing the deep circulation. Analogously, in uplifted  
711 forelands the direct exposure of eroded and in places karstified carbonates promotes the meteoric  
712 water infiltration along the fracture network into the crust and recharge the ground-water  
713 circulations (Mindszenty et al., 1995; Allen et al., 2001; O'Brien et al., 1999). In the NA foreland, an  
714 increase in salinity of migrating fluids caused diffuse dolomitization of carbonates along Jurassic  
715 normal faults reactivated during Miocene syn-orogenic foreland tectonics (Ronchi et al., 2003).  
716 Further evidence of ascending hydrocarbon-charged fluids through a pathway composed of syn-  
717 orogenic fractures and faults network (Scisciani et al., 2000a) in the Late Miocene NA foreland is  
718 testified by the occurrence of cold-seep carbonate build-ups, authigenic patches and carbonate  
719 breccias (Iadanza et al., 2013).

720 Analogously, in the Norwegian Northern NS, reverse fault slippage and gas leakage along  
721 sections of previously sealing reservoir-bounding faults occurred in recent times due to a combination  
722 of increase in compressional stress associated with postglacial rebound and locally elevated pore  
723 pressure due to the local presence of natural gas in fault footwalls (Wiprut and Zoback, 2000; 2002). It  
724 is arguable that similar mechanisms acted on the ESP, where several Alpine-age reverse-fault  
725 reactivations have been identified (e.g., Figs. 4d and 7) and where there are multiple evidence of  
726 hydrocarbon seepage (Richardson et al., 2005; Patruno and Reid, 2016; 2017) and possible fluid  
727 leakage (Patruno et al., in press).

728           Moreover, the infiltration of aqueous fluids may lead to the formation of clay minerals, often  
729 leading to important changes in mechanical behaviour of the fault zones, such as local anisotropy  
730 enhancement and the bulk shear strength reduction, and increased fluid pressures during shearing  
731 (Warr and Cox, 2001).

732

733

734

### **Summary and Conclusions**

735           The Caledonian-Variscan orogens in Northern-Central Europe and in the Apennines range of  
736 Italy are classical examples of thrust belts developed at the expense of former passive margins that  
737 underwent multiple events of extension and compression. Both settings represent key regions to  
738 study the effects of how a complete Wilson Cycle is achieved and preserved in the geological record.

739           In the present work, we have selected two study areas set in the above-mentioned regions,  
740 where field structural data and subsurface data allow the recognition of at least one  
741 “classical/complete” Wilson Cycle along with several “foreland/incomplete” Wilson Cycles, with long-  
742 term preservation of structural grain and polyphase reactivation of pre-existing structures. These two  
743 study areas are the offshore East Shetland Platform (ESP) in the UK North Sea and the onshore  
744 Northern Apennines (NA) of Italy. Regional geology, structural field evidence and subsurface data (2D  
745 and 3D seismic reflection and well-logs) have been here integrated with the aim to reconstruct the  
746 tectonic evolution and the common features that were significant in controlling the stress localisation  
747 along inherited zones of weakness that suffered repeated reactivation.

748           In the ESP, the relatively shallow Palaeozoic-Tertiary sedimentary cover, combined with a  
749 remarkable penetration depth of recently acquired 3D broadband seismic reflection data revealed  
750 several events of compression and extension that have been taking place since the Caledonian  
751 Orogeny. We interpret multiple reactivation of the Caledonian basement structures during both  
752 negative (e.g., the Devonian post-collision collapse, Permian-Triassic and Middle-Late Jurassic rifting  
753 events) and positive inversion tectonics (e.g., from far-field Variscan and Alpine orogenic phases).

754           Similarly in the NA, due to exceptional outcrop exposures and availability of abundant  
755 subsurface data (e.g., exploration wells and seismic profiles), we have been able to recognize  
756 repeated rifting and mountain building processes. This area underwent: i) compression during the  
757 Variscan Orogeny; ii) extension during the Late Paleozoic-Early Mesozoic rifting and Jurassic Alpine  
758 Tethys ocean opening; iii) Apenninic compression in Cenozoic times; and iv) late/post-orogenic  
759 extension in the Miocene to Recent.

760           The outcomes of this study indicate that inherited normal faults related to pre-orogenic rifting  
761 phases promoted multiple, deep-rooted, basement-involved positive basin inversion, with different  
762 amounts and rates of vertical extrusion of previous wedge-shaped graben. In turn, normal faults  
763 produced by negative inversion and post-orogenic extensional collapse were also strongly influenced  
764 by the location of precursor compressional discontinuities (e.g., thrust ramps). In the NA this has

765 resulted in distinct patterns and segmentation of the recent post-orogenic normal faults that are  
766 responsible for the present-day seismicity.

767 In the two study areas, pre-inversion thermal softening and fault weakening of the foreland  
768 lithosphere, particularly if accompanied by possible crustal hydration and tectono-magmatic phases,  
769 are suggested to represent the main controlling factors that promote cyclical structural reactivations,  
770 during both full Wilson Cycles and far-field foreland inversions.

771 This study, moreover, illustrates how the structural signature of a complete Wilson Cycle is best  
772 preserved in foreland domains flanking orogenic systems and produced at the expenses of pre-  
773 orogenic rifted margins. In these settings, earlier lineaments are not completely obscured by later  
774 deformations, but are still legible in the structural record, thus enabling us to investigate the role,  
775 degree and intensity of structural inheritance phenomena. Foreland domains may, therefore, be  
776 regarded as ideal settings to study the factors controlling crustal reactivation processes during both  
777 positive and negative inversion histories.

778

779

780

781

## 782 **Acknowledgements**

783 The authors gratefully acknowledge PGS for the permission to publish the seismic section in  
784 Figure 11, from the 3D GeoStreamer NS dataset (BBK and NVG surveys). We thank Stuart Archer and  
785 Thomas Phillips for their thorough and helpful comments, which led to a much improved paper. This  
786 work was supported by the Chieti-Pescara University funds (V. Scisciani).

787



788

789 **Figure captions**

790 **Figure 1:** Location map of the study area including (a) the East Shetland Platform in the UK offshore and (b) the Northern  
791 Apennines of Italy.

792 **Figure 2:** Synoptic scheme showing the main tectonic, stratigraphic and magmatic events that occurred in the East  
793 Shetland Platform and Northern Apennines (pre-mid Permian evolution derived from Sardinia). The ESP and NA were  
794 subject to two Proterozoic-Paleozoic plate cycles, albeit not completely overlapping and with different chronological  
795 duration, namely the *Iapetus-Caledonian Cycle* and the *Rheic-Variscan Cycle* (see the text). Following the Variscan  
796 Orogeny, the NA underwent a further complete plate cycle whereas the NS have been subject to at least two incomplete  
797 Meso-Cenozoic intra-plate extension-compression cycles in an intra-plate setting.

798 **Figure 3:** Paleogeographic reconstructions during the Ordovician (a), Late Carboniferous (b), Late Jurassic (c) Paleocene (d)  
799 and Early Oligocene (e); compiled from different authors (Decourt et al., 2000; Stamply and Borel, 2002; Coward et al.,  
800 2003; Scisciani and Montefalcone, 2006; Nance et al., 2010;). The figures illustrate the plate configuration during the  
801 Iapetus-Caledonian (a), Rheic-Variscan (b) and Alpine-Apennines (c-d-e) plate cycles (see the text for the discussion).

802 **Figure 4:** (A) Central and Northern North Sea location map, showing the East Shetland Platform and the Greater East  
803 Shetland Platform (sensu Patruno and Reid, 2016) with location of the PGS seismic surveys. (B) East Shetland Platform  
804 location map, including the position of the main hydrocarbon fields, the wells with the Devonian interval, and the  
805 relationships between the Devonian Orcadian Basin and the Late Jurassic platform tectonic elements (modified after  
806 Patruno & Reid, 2017). The position of the seismic lines discussed in the present work, as well as the PGS 3D MultiClient  
807 GeoStreamer surveys, is shown. (C) Onshore outcrop and offshore Permian subcrop map of the East Shetland Platform,  
808 West of Shetlands and Moray Firth areas (modified after Patruno et al., in press). The main tectonic lineaments, the  
809 igneous intrusions and the extent of the Zechstein-age halokinetic salt are also shown (A, B and C modified after Patruno,  
810 2017). (D) Sketch map of basement units in the northern North Sea and surrounding areas (modified from Lundmark et  
811 al., 2014); the Dalradian basement of the ESP is delimited to the ENE by the Walls Boundary Fault, corresponding to the  
812 offshore prosecution of the Great Glen Fault, and to the SE by the continuation offshore of the Iapetus oceanic units with  
813 an interposed volcanic arc basement (e.g., Utsira High and East Shetland Basin Basement).

814 **Figure 5:** Structural sketch map of Central and Northern Apennines; upper left inset for location.

815 **Figure 6:** West-to-east oriented well correlation panel spanning the southern margins of the East Shetland Platform, from  
816 the Halibut Horst, through the Piper Shelf and the Fladen Ground Spur (UKCS Quadrants 14, 15 and 16) to the western  
817 edge of the South Viking Graben. Modified after Patruno et al. (in press).

818 **Figure 7:** Figure showing the complex multi-phase inversion tectonics in the southern East Shetland Platform (UKCS  
819 Quadrants 15-16), near the transition between the Platform and the Witch Ground Graben (ca. 36 km further south) and  
820 the South Viking Graben (right-hand side in section A). This figure includes the following parts: (A) Interpreted seismic  
821 cross-section (PGS GeoStreamer® MC3D-Q15-2014 3D seismic survey), along a similar transect as the correlation panel in  
822 Figure 6; (B) Close-up of the interpretation of Section A (C) total subsidence curve below present-day sea level and  
823 tectonic subsidence rate graphs from Well 15/6-1 (backstripping method of Allen and Allen, 2005); (D) TWT thickness map  
824 of the Permian to Carboniferous interval. LC = Late Cretaceous; EC = Early Cretaceous; LJ = Late Jurassic; MJ = Middle  
825 Jurassic (post-Aalenian); Tr = Triassic (mostly Early Triassic); Z = Zechstein Group (latest Permian); Ro = Rotliegend Group  
826 (Late Permian); C = Carboniferous. This figure has been modified after Reid and Patruno (2015), Patruno and Reid (2018)  
827 and Patruno et al. (in press).

828 **Figure 8:** Regional N-S seismic reflection line straddling the western edge of the East Shetland Platform, parallel to the  
829 Viking Graben. The Kraken High and the Fladen Ground Spur are two prominent Variscan structural highs, where a thin  
830 Chalk/Jurassic veneer is the only stratigraphic unit that separates a thick Devonian and Tertiary successions. Between  
831 these highs, the Crawford-Skipper Basin (sensu Patruno and Reid, 2017) is an area hosting a much more complete  
832 Carboniferous-Cretaceous succession. Figure modified after Patruno and Reid (2017) and Patruno et al. (in press).

833 **Figure 9:** Map showing 633 different faults on the East Shetland Platform area constrained by 3D seismic coverage. The  
834 faults have been mapped in 3D and classified according to their kinematic and main age of activity. The predominance of  
835 N-striking faults parallel to the Viking Graben and overall E-striking faults parallel to the Witch Ground Graben, despite the  
836 wide variation in activity age, suggests long-term structural inheritance. Figure modified after Patruno (2017). For a full  
837 statistical appraisal of these structures see Patruno et al. (in press).

838 **Figure 10:** Northwest-southeast trending seismic line across the Paleocene Kraken Oil field, highlighting an expanded  
839 Devonian succession in the hangingwall of a likely lower Devonian masterfault, successively subject to a partial  
840 Palaeogene-age inversion, leading to the formation of a fault-related anticline in the Paleocene section (i.e., the structural  
841 closure of the Kraken Field itself). Figure modified after Patruno and Reid (2017) and Patruno et al. (in press).

842 **Figure 11:** Overall northwest-to-southeast arbitrary line to the north of the Kraken Field, displaying again the Devonian  
843 syncline (Units 1 and 2) within the ESP associated with the partly inverted masterfault shown in Figure 10. Below the  
844 Devonian reflectors there are opaque seismic-stratigraphic units (Units 3 and 4), characterized by no visible reflector,  
845 followed by another unit with high-amplitude reflectors (Units 5 and 7), highlighting both compressional (south-eastern  
846 sector) and extensional deep-seated structures. Unit 3: inferred granitic intrusion. Also see Patruno et al. (2017) for  
847 further details.

848 **Figure 12:** Schematic reconstruction of the structural and stratigraphic evolution of the regional N-S line (Fig. 8). These  
849 cartoons were reconstructed based on: stratal geometries; inferred depositional thickness trends (seismic and wells);  
850 backstripping analyses; facies variations in the wells. Also see Patruno and Reid (2017) for further details.

851 **Fig. 13:** Simplified geological and structural map of the south-eastern sector of the Northern Apennines (modified from  
852 Scisciani et al., 2014) transected by the arc-shaped Umbria-Marche Apennine Ridge (UMAR); upper left inset for location.  
853 Dotted and continuous lines mark the location of the seismic reflection profile (A-A') of Fig. 16 and geological cross-section  
854 (B-B') of Fig. 17, respectively.

855 **Fig. 14** (a) Structural map of the Igno Mt. area (location in Fig. 13 - modified from Scisciani et al., 2014); (b) Geological  
856 cross-section (trace in (a)), and restored template across the Igno Mt.-Valnerina thrust system.

857 **Fig. 15:** (a) Simplified geological map of the Sibillini Mts thrust eroded and exposed along the Fiastrone Valley; (b)  
858 exposure of the overturned thrust-related anticline in the hangingwall block of the Sibillini Mts thrust along the northern  
859 flank of the Fiastrone Valley; (c) geological cross-section showing the overturned anticline and the ramp trajectory of the  
860 thrust fault across the Lower Jurassic strata (CM: Calcare Massiccio Fm.) and the steeply dipping forelimb in the  
861 hangingwall block; and (d) restored template showing the shortcut trajectory of the future Sibillini Mountains thrust with  
862 respect to the pre-thrusting normal faults.

863 **Fig. 16:** Geological interpretation of a regional seismic reflection profile across the UMAR; trace location in Figs. 5 and 13.

864 **Fig. 17:** Balanced crustal geological cross-section (a) across the UMAR reconstructed by integrating the results of surface  
865 geology and seismic interpretation (trace in Figs. 5 and 13). The restored template (b) illustrates the geometry of the late  
866 Paleozoic-Triassic extensional basin that was inverted and extruded during Miocene.

867 **Fig. 18:** Regional geological cross-section (a) and simplified restoration (b) across the Northern Apennines from the Umbria  
868 Valley to the Plio-Quaternary Adriatic basin (trace in Fig. 5). The transect derives from the present study (C-D segment)  
869 and previous reconstructions (E-F-G segment - modified from Scisciani and Montefalcone, 2006; Scisciani, 2009; Pace et  
870 al., 2015).

871 **Fig. 19:** a) Sketch map illustrating the reconstructed distribution of thickness and facies of late Tortonian-Messinian pre-  
872 gypsum deposits. b) Schematic cross-section showing the embryonic growth of the UMAR that was interposed between  
873 the thrust front of the Apennines chain and depocentre of the Messinian Laga Basin.

874 **Fig. 20:** Examples of fault reactivation in positive and negative inversion tectonic setting in the ESP and NA: a) positive  
875 reactivation during the Alpine foreland tectonics (late Cretaceous-Paleocene) of a Devonian and Triassic normal fault  
876 flanking to the west the Crawford Spur in the ESP; b) Pliocene-Quaternary positive reactivation of a Triassic-Early Jurassic

877 normal fault in the Adriatic basin in front of the Northern Apennines (seismic line location in Fig. 19 - modified from Pace  
878 et al., 2015); c) positive inversion of a synsedimentary Devonian normal fault (note the divergent Du syn-rift wedge in the  
879 hangingwall of the NW-dipping extensional fault) in the ESP (modified from Platt and Cartwright, 1998); the south-  
880 eastward thinning of the basal Devonian unit (Dl) towards the inverted fault is also consistent with the negative  
881 reactivation of an early reverse fault; d) portion of the seismic line of Fig. 16 showing the negative inversion of a Neogene  
882 thrust fault by the Quaternary SW-dipping normal faults (Colfiorito Basin boundary faults). Normal faults = tick black lines  
883 with black arrow; thrust and reverse faults = red lines with red arrow; double arrow (black and red arrow labelled with "i")  
884 = inverted faults; Tb = Top basement; Dl = Devonian lower unit; Du = Devonian upper unit; Do = onlap surface.

885

887 **References**

888

- 889 Abramovitz, T., and Thybo, H. (2000). Seismic images of Caledonian lithosphere-scale collision structures in the  
890 southeastern North Sea along Mona Lisa Profile 2. *Tectonophysics*, 317, 27-54.
- 891 Alberti, M., Decandia, F.A., and Tavarnelli, E. (1996). Modes of propagation of the compressional deformation in the  
892 Umbria–Marche Apennines. *Memorie della Società Geologica Italiana*, 51, 71–82.
- 893 Alberts, M.A., and Underhill, J.R. (1991). The effect of Tertiary structuration on Permian gas prospectivity, Cleaver Bank  
894 area, southern North Sea, UK In: Spencer, A.M. (Ed.) *Generation, Accumulation, and Production of Europe's*  
895 *Hydrocarbons*. Special Publication, EAPG, Oxford University Press, Oxford, pp. 161-173.
- 896 Allen, P.A., Burgess, P.M., Galewsky, J., and Sinclair, H.D. (2001). Flexural-eustatic numerical model for drowning of the  
897 Eocene perialpine carbonate ramp and implications for Alpine geodynamics. *Geological Society of America Bulletin*,  
898 113(8), 1052-1066.
- 899 Artemieva, I. M. (2007), Dynamic topography of the East European craton: Shedding light upon lithospheric structure,  
900 composition and mantle dynamics, *Global Planet. Change*, 58(1), 411–434.
- 901 Bally, A., Burbi, W., Cooper, J. C. and Ghelardoni, L. (1986). Balanced sections and seismic reflection profiles across the  
902 Central Apennines. *Mem. Soc. Geol. It.*, 107, 109-130.
- 903 Barba, S., and Basili, R. (2000). Analysis of seismological and geological observations for moderate-size earthquakes: the  
904 Colfiorito fault system (central Apennines, Italy). *Geophysical Journal International*, 141, 241-252.
- 905 Bartholomew, I.D., Peters, J.M. and Powell, C.M. (1993). Regional structural evolution of the North Sea: oblique slip and  
906 the reactivation of basement lineaments. In: Parker, J.R. (Ed.), *Petroleum Geology of Northwest Europe: Proceedings of*  
907 *the 4th Conference*, The Geological Society, London, 1109-1122.
- 908 Bassett, M.G. (2003). Sub-Devonian geology. In: Evans, D., Graham, D., Armour, A., Bathurst, P. (editors and coordinators).  
909 *The Millennium Atlas: petroleum geology of the central and northern North Sea*. The Geological Society of London,  
910 London, 61-63.
- 911 Bell, K., Lavecchia, G. and Rosatelli, G. (2013). Cenozoic Italian magmatism isotope constraints for possible plume-related  
912 activity. *J. South Am. Earth Sci.*, 41, 2240.
- 913 BGS 250k Marine Bedrock Map. Available online at: <http://www.maremap.ac.uk/view/search/searchMaps.html?> and  
914 <http://www.bgs.ac.uk/products/offshore/DigRock250.html> [accessed on 15/3/2017]
- 915 Bluck, B.J., (2001). Caledonian and related events in Scotland. *Transactions of the Royal Society of Edinburgh: Earth*  
916 *Sciences*, 91, 375-404.
- 917 Boccaletti, M., Calamita, F., Deiana, G., Gelati, R., Massari, F., Moratti, G., and Ricci Lucchi, F. (1990). Migrating foredeep-  
918 thrust belt system in the northern Apennines and southern Alps. *Palaeogr. Palaeoclimatol. Palaeoecol.*, 77, 3–14.
- 919 Bonini, M., Sani, F., and Antonielli, B. (2012). Basin inversion and contractional reactivation of inherited normal faults: A  
920 review based on previous and new experimental models. *Tectonophysics*, 522–523, 55–88.
- 921 Bortolotti, V., and Principi, G. (2005). Tethyan ophiolites and Pangea break-up. *The Island Arc*, 14, 442–470.
- 922 Bradley, D.C., and Kidd, W.S.F. (1991). Flexural extension of the upper continental crust in collisional foredeeps. *Geol. Soc.*  
923 *Am. Bull.*, 103 (11), 1416–1438.
- 924 Buchanan, J.G. and Buchanan, P.G. (1995). Basin Inversion. *Geological Society Special Publication*, 88, pp. 596.
- 925 Buitter, S.J.H., Pfiffner, O.A. and Beaumont, C. (2009). Inversion of extensional sedimentary basins: A numerical evaluation  
926 of the localisation of shortening, *Earth and Planetary Science Letters*, 288, 492-504, doi: 10.1016/j.epsl.2009.10.011
- 927 Burov, B., and Diament, M. (1995). The effective elastic thickness ( $T_e$ ) of continental lithosphere: what does it really  
928 mean? *Journal of Geophysical Research: Solid Earth* 100 (B3), 3905–27.
- 929 Butler, C.A., Holdsworth, R.E. and Strachan, R.A. (1995). Evidence for Caledonian sinistral strike-slip motion and associated  
930 fault zone weakening, Outer Hebrides Fault Zone, NW Scotland. *Journal of the Geological Society, London*, 152, 743–  
931 746.
- 932 Butler, M. (1998). The geological history of the Wessex basin: a review of new information from oil exploration. In:  
933 Underhill, IR. (Ed.) *Development and Evolution of the Wessex Basin*. Geological Society of London Special Publication  
934 133, 67-86.
- 935 Butler, R.W.H., Holdsworth, R. E., and Lloyd, G. E. (1997). The role of basement reactivation in continental deformation.  
936 *Journal of the Geological Society of London*, 154, 69–72.

937 Butler, R.W.H., and Mazzoli, S. (2006). Styles of continental contraction: A review and introduction, in S. Mazzoli, and R. W.  
938 H. Butler (eds), *Styles of continental contraction: Geological Society of America*, 1–10.

939 Butler, R. W. H., Tavarnelli, E. and Grasso, M. (2006). Structural inheritance in mountain belts: an Alpine-Apennine  
940 perspective. *Journal of Structural Geology*, 28, 1893–908.

941 Calamita, F., Pierantoni, P.P., and Zamputi, M. (1993). Il sovrascorrimento di M. Cavallo-M. Primo tra il F. Chieti e il F.  
942 Potenza (Appennino Umbro-Marchigiano): carta geologica e analisi strutturale. Scale 1:25000, 1 sheet. *Boll. Soc. Geol.*  
943 *It.*, 112, 825–835.

944 Calamita, F., Coltorti, M., Piccinini, D., Pierantoni, P.P., Pizzi, A., Ripepe, M., Scisciani, V., and Turco, E. (2000). Quaternary  
945 faults and seismicity in the Umbria-Marche Apennines (Central Italy): evidence from the 1997 Colfiorito earthquake.  
946 *Journal of Geodynamics*, 29, 245-264.

947 Calamita, F., Paltrinieri, W., Pelorosso, M., Scisciani, V., and Tavarnelli, E. (2003). Inherited Mesozoic architecture of the  
948 Adria continental palaeomargin in the neogene central Apennines orogenic system, Italy. *Boll. Soc. Geol. Ital.*, 122,  
949 307–318.

950 Calamita, F., Patruno, S., Pomposo, G., and Tavarnelli, E. (2007). Geometry and kinematics of the thrust-related anticlines  
951 from the central outer Apennines: the role of the Jurassic normal faults ('Geometria e cinematica delle anticlinali  
952 dell'Appennino centrale esterno: il ruolo delle faglie dirette giurassiche'). *Rendiconti Società Geologica Italiana*, 4, 167-  
953 192.

954 Calamita, F., Satolli, S., Scisciani, V., Esestime, P., and Pace, P. (2011). Contrasting styles of fault reactivation in curved  
955 orogenic belts: examples from the Central Apennines (Italy). *Geol. Soc. Am. Bull.* 123, 1097–1111.  
956 <http://dx.doi.org/10.1130/B30276.1>.

957 Calamita, F., Pace, P., Satolli, S. (2012). Coexistence of fault-propagation and fault-bend folding in curve-shaped foreland  
958 fold-and-thrust belts: examples from the Northern Apennines (Italy). *Terra Nova*, 24, 396–406.  
959 <http://dx.doi.org/10.1111/j.1365-3121.2012.01079.x>.

960 Carmignani, L., and Kligfield, R. (1990). Crustal extension in the northern Apennines: the transition from compression to  
961 extension in the Alpi Apuane core complex. *Tectonics*, 9, 1275–1303. <http://dx.doi.org/10.1029/TC009i006p01275>.

962 Carmignani, L., Carosi, R., Di Pisa, A., Gattiglio, M., Musumeci, G., Oggiano, G., and Pertusati, P.C. (1994). The Hercynian  
963 Chain in Sardinia (Italy). *Geodinamica Acta*, 7, 31-47.

964 Castellarin, A., Colacicchi, R., Praturlon, A., and Cantelli, C. (1982). The Jurassic-Lower Pliocene history of the Ancona-Anzio  
965 line (Central Italy). *Mem. Soc. Geol. It.*, 24, 325-336.

966 Chiaraluce, L. Di Stefano, R. Tinti, E. Scognamiglio, L. Michele, M. Casarotti, E. Cattaneo, M. De Gori, P. Chiarabba, C.  
967 Monachesi, G. Lombardi, A. Valoroso, L. Latorre, and D. Marzorati, S. (2017). The 2016 Central Italy Seismic Sequence:  
968 A First Look at the Mainshocks, Aftershocks, and Source Models. *Seismological Research Letters*, 88(3), 757-771. DOI:  
969 10.1785/0220160221

970 Ciarapica, G., and Passeri, L. (2002). The paleogeographic duplicity of the Apennines. *Boll. Soc. Geol. It.*, Vol. Spec. 1, 67-75.

971 Ciarapica, G., and Passeri, L. (2005). Late Triassic and Early Jurassic sedimentary evolution of the Northern Apennines: an  
972 overview. *Boll. Soc. Geol. It.*, 124, 189-201.

973 Collettini, C., Niemeijer, A.R., Viti, C., and Marone, C. (2009). Fault zone fabric and fault weakness. *Nature*, 462, 907-910.

974 Cooper, M.A. and Williams, G.D. (1989). Inversion Tectonics. *Geological Society of London Special Publication*, 44, pp. 356.

975 Corfield, S.M., Gawthorpe, R.L., Gage, M., Fraser, A.J., and Besley, A., (1996). Inversion tectonics of the Variscan foreland  
976 of the British Isles. *Journal of the Geological Society of London*, 153, 17-32.

977 Coward M. P. (1994) – Inversion tectonics. In: Hancock, P. L., ed., *Continental Deformation: Oxford, Pergamon*, p. 289-304.

978 Coward, M.P., (1990). Caledonian framework. In: Brooks, J., and Hardman, R.F.P. (Eds.), *Tectonic Events responsible for*  
979 *Britain's Oil and Gas reserves. Special Publication, Geological Society, London.*

980 Coward, M.P., Enfield, M.A., and Fischer, M.W. (1989). Devonian basins of Northern Scotland: Evidence of inversion  
981 related to late Caledonide-Variscide tectonics. In: Copper, M.A., Williams, G.W. (Eds.), *Inversion Tectonics. Special*  
982 *Publication of the Geological Society of London*, 44, 275-307.

983 Coward, M.P., Dewey, J., Hempton, M., and Holroyd, J. (2003). Tectonic evolution. In: Evans, D., Graham, D., Armour, A.,  
984 Bathurst, P. (editors and coordinators). *The Millennium Atlas: petroleum geology of the central and northern North*  
985 *Sea. The Geological Society of London, London*, 17-33.

986 Cross, T. A. (1986). Tectonic controls of foreland basin subsidence and Laramide style deformation, western United States.  
987 In: Allen, P.A. and Homewood, P. (Eds), *Foreland Basins, International Association of Sedimentologists, Special*  
988 *Publication*, 8, 15–39.

989 D'Agostino, N., Jackson, J. A., Dramis, F., and Funicello, R. (2001). Interactions between mantle upwelling, drainage  
990 evolution and active normal faulting: an example from the central Apennines (Italy). *Geophys. J. Int.*, 147, 475–497.

991 Dalziel, I.W.D., Dalla Salda, L.H., and Gahagan, L.M. (1994). Paleozoic Laurentia-Gondwana interaction and the origin of the  
992 Appalachian-Andean Mountain systems. *Geol. Soc. Amer. Bull.*, 106, 243-252.

993 Davies, R.J., O'Donnell, D., Bentham, P.N., Gibson, J.P.C., Curry, M.R., Dunay, R.E. and Maynard, J.R. (1999). The origin and  
994 genesis of major Jurassic unconformities within the triple junction area of the North Sea, UK. In: Fleet, A.J., and Boldy,  
995 S.A.R. (Eds.), *Petroleum Geology of Northwestern Europe: Proceedings of the 5th Conference*, The Geological Society,  
996 London, 117-131.

997 Deiana, G., and Piali, G. (1994). The structural provinces of the Umbro-Marchean Apennines. *Mem. Soc. Geol. It.*, 48, 473-  
998 484.

999 Decourt, J., Ricou, L.E. and Vrielynck, B. (1993). *Atlas Tethys Palaeoenvironmental Maps*. Gauthier-Villars, Paris, 307 pp.,  
1000 14 maps, 1 plate.

1001 Dercourt, J., Gaetani, M., Vrielynck, B., Barrier, E., Biju-Duval, B., Brunet, M.F., Cadet, J.P., Crasquin, S. and Sandulescu, M.  
1002 (2000). *Atlas Peri-Tethys Paleogeographical maps: CCGM/CGMW*, Paris, maps 6, 7, 9, 10, 11, 12, 13, 16, 17, 18, 19, 22,  
1003 23, 24.

1004 Dewey, J.F., Helman, M.L., Turco, E., Hutton, D.W.H., and Knott, S.D. (1989). Kinematics of the western Mediterranean. In:  
1005 Coward, M.P., Dietrich, D., Park, R.G. (Eds.), *Alpine Tectonics*, *Geol. Soc. Lond. Spec. Publ.*, 45, 265–283.

1006 Doglioni, C. (1995). Geological remarks on the relationships between extension and convergent geodynamic settings.  
1007 *Tectonophysics*, 252 (1), 253–267.

1008 Doglioni, C., and Flores, G. (1997). Italy. In: Moores and Fairbridge (Eds), *Encyclopedia of European and Asian Regional  
1009 Geology*. Chapman and Hall, 414-435.

1010 Emergeo Working Group (2016). The 24 August 2016 Amatrice Earthquake: Coseismic Effects, doi: 10.5281/zenodo.61568.

1011 Færseth, R.B., and Ravnås, R. (1998) Evolution of the Oseberg Fault-Block in the context of the northern North Sea  
1012 structural framework. *Marine and Petroleum Geology*, 15, 467-490.

1013 Fantoni, R., and Franciosi, R. (2010). Mesozoic extension and Cenozoic compression in Po Plain and Adriatic foreland. In F.  
1014 P. Sassi (Ed.) *Nature and geodynamics of the lithostere in northern Adriatic* (10.1007/s12210-010-0102-4). *Rend. Fis.  
1015 Acc. Lincei*, Vol. 21(1), 181–196.

1016 Fazlikhani, H., Fossen, H., Gawthorpe, R.L., Faleide, J.I., and Bell, R.E., (2017). Basement structure and its influence on the  
1017 structural configuration of the northern North Sea rift. *Tectonics*, 36, 1151-1177. doi: 10.1002/2017TC004514.

1018 Fettes D.J., Macdonald, R., Fitton, J.G., Stephenson, D., and Cooper, M.R., (2011). Geochemical evolution of Dalradian  
1019 metavolcanic rocks: implications for the break-up of the Rodinia supercontinent. *Journal of the Geological Society*, 168,  
1020 1133-1146.

1021 Finetti, I.R. and Del Ben, A. (2005). Crustal tectono-stratigraphy of the Ionian Sea from integrated new CROP seismic data.  
1022 In: Finetti, I.R. (Ed.). *CROP Project: Deep Seismic Exploration of the Central Mediterranean and Italy*, Atlas in  
1023 *Geosciences 1*. Elsevier, Chapter 19, 447-470.

1024 Finetti, I.R., Del Ben, A., Forlin, E., Pipan, M., Prizzon, A., Calamita, F., Crescenti, U., Rusciadelli, G., Scisciani, V., (2005).  
1025 Crustal geological section across Central Italy from Corsica to the Adriatic sea based on geological and CROP seismic  
1026 data. In: Finetti, I.R. (Ed.), *CROP Project: Deep Seismic Exploration of the Central Mediterranean and Italy*, Atlas in  
1027 *Geosciences 1*. Elsevier, 159–196.

1028 Franceschelli, M., Puxeddu, M., and Cruciani, G. (2005) - Variscan Metamorphism in Sardinia, Italy: review and discussion.  
1029 *J. Virtual Explorer*, 19, paper 2.

1030 Frankowicz, E., and McClay, K. R. (2010). Extensional fault segmentation and linkages, Bonaparte Basin, outer North West  
1031 Shelf, Australia. *AAPG Bulletin*, 94, 977-1010.

1032 Fraser, A.J., and Gawthorpe, R.L. (1990). Tectono-stratigraphic development and hydrocarbon habitat of the Carboniferous  
1033 in Northern England. In: Hardman, R.P.F. and Brooks, J. (eds) *Tectonic Events Responsible for Britain's Oil and Gas  
1034 Reserves*. Special Publication Geological Society of London, 55, 49-86.

1035 Fraser, S., Robinson, A., Johnson, H., Underhill, A., and Kadolsky, D., (2003). Upper Jurassic. In: Evans, D., Graham, C.,  
1036 Armour, A., Bathurst, P. (Eds.), *The Millennium Atlas: petroleum geology of the central and northern North Sea*. The  
1037 Geological Society of London, London, UK, 157-189.

1038 Freer, G., Hurst, A., Middleton, P. (1996). Upper Jurassic sandstone reservoir quality and distribution on the Fladen Ground  
1039 Spur. In: Hurst, A., et al. (Eds.), *Geology of the Humber Group: Central Graben and Moray Firth*, UKCS. Geological  
1040 Society Special Publication, 114, 235-249. Geological Society, London.

1041 Galli, P., Galadini, F., and Pantosti, D. (2008). Twenty years of paleoseismology in Italy. *Earth-Science Rev.*, 88 (1,2), 89-117.  
1042 <http://dx.doi.org/10.1016/j.earscirev.2008.01.001>.

1043 Giacomini, F., Bomparola, R.M., Ghezzi, C., and Guldbransen, H. (2006). The geodynamic evolution of the Southern  
1044 European Variscides: constraints from the U/Pb geochronology and geochemistry of the lower Paleozoic magmatic-  
1045 sedimentary sequences of Sardinia (Italy). *Contrib. Mineral. Petrol.*, 152, 19-42.

1046 Glennie, K.W., and Underhill, J.R. (1998). Origin, development and evolution of structural styles. In: Glennie, K.W. (Ed.)  
1047 *Petroleum Geology of the North Sea: Basic Concepts and Recent Advances*, Fourth Edition, 42-84. Blackwell Science.

1048 Glennie, K.W., Higham, J., and Stemmerik, L. (2003). Chapter 8: Permian. In: Evans, D., Graham, C., Armour, A., and  
1049 Bathurst, P. (Eds.), *The Millennium Atlas: petroleum geology of the central and northern North Sea*. The Geological  
1050 Society of London, 91-103.

1051 Harding, T.P. (1985). Seismic characteristics and identification of negative flowers structures, positive flowers structures,  
1052 and positive structural inversion. *AAPG Bulletin*, 69, 582-600.

1053 Hatcher, R.D. (2001), Rheological partitioning during multiple reactivation of the Palaeozoic Brevard fault zone, Southern  
1054 Appalachians, USA. In Holdsworth, R.E., et al. (Eds), *The nature and tectonic significance of fault zone weakening*:  
1055 Geological Society [London] Special Publication, 186, 257-271.

1056 Hay, S., Jones, C.M., Barker, F., and He, Z. (2005). Exploration of Unproven Plays: Mid North Sea High. PGL Report,  
1057 Aberdeen (U.K.), 213 pp.

1058 Hendrie, D.B., Kusznir, N.J., and Hunter, R.H. (2003). Jurassic extension estimates for the North Sea 'triple junction' from  
1059 flexural backstripping: implications for decompression melting models. *Earth and Planetary Science Letters*, 116, 113-  
1060 127.

1061 Hillis, R.R, Thomson, K., and Underhill, J.R. (1994). Quantification of Tertiary erosion in the Inner Moray Firth by sonic  
1062 velocity data from the Chalk and Kimmeridge Clay. *Mar. Petro Geol.* 11, 283-93.

1063 Holdsworth, R. R., Stewart, M., Imber, J., and Strachan, R. A. (2001). The structure and rheological evolution of reactivated  
1064 continental fault zones: a review and case study. In: Miller, J. A., Holdsworth, R. E., Buick, I. S., and Handy, M. R. (eds)  
1065 *Continental Reactivation and Reworking*. Geological Society, London, Special Publications 184, 115-137.

1066 Husmo, T., Hamar, G., Høiland, O., Johannessen, E.P., Rømulund, A., Spencer, A., and Titterton, R., (2003). Lower and  
1067 Middle Jurassic. In: Evans, D., Graham, C., Armour, A., Bathurst, P. (Eds.), *The Millennium Atlas: petroleum geology of  
1068 the central and northern North Sea*. The Geological Society of London, London, UK, 129-155.

1069 Kusznir, N.J., and Park, R.G. (1987). The extensional strength of the continental lithosphere: its dependence on continental  
1070 gradient, and crustal composition and thickness. In: M. P. Coward, J. F. Dewey, and P. L. Hancock, (Eds.), *Continental  
1071 Extension Tectonics*, Geological Society of London Special Publication, 28, 35-52.

1072 Iadanza, A., Sampalmieri, G., Cipollari, P., Mola, M., and Cosentino, D., (2013). The brecciated limestones of the Maiella  
1073 Basin (Italy): rheological implications of hydrocarboncharged fluid migration in the Messinian Mediterranean Basin.  
1074 *Palaeogeogr. Palaeoclimatol. Palaeoecol.* 390, 130-147.

1075 Imber, J., Holdsworth, R. E., Butler, C. A., and Lloyd, G. E. (1997). Fault-zone weakening processes along the reactivated  
1076 Outer Hebrides Fault Zone, Scotland. *Journal of the Geological Society, London*, 154, 105-109.

1077 Johnson, R.J., and Dingwall, R.G. (1981). The Caledonides: their influence on the stratigraphy of the Northwest European  
1078 Shelf. In: Illing, L.V. and Hobson, G.P. (Eds) *Petroleum Geology of the Continental Shelf of North-West Europe*. Heyden,  
1079 London, pp. 88-97.

1080 Jones, E., Jones, R., Ebdon, C., Ewen, D., Milner, P., Plunkett, J., Hudson, G., and Slater, P. (2003). Eocene. In: Evans, D.,  
1081 Graham, C., Armour, A. and Bathurst, P. (Eds): *The Millennium Atlas: Petroleum Geology of the Central and Northern  
1082 North Sea*. The Geological Society (London), 261-277.

1083 Korme, T., Acocella, V. and Abebe, B. (2004). The role of pre-existing structures in the origin, propagation and architecture  
1084 of the faults in the Main Ethiopian Rift. *Gondwana Research*, 7(2), 467-479.

1085 Kozur, H. (1991). The evolution of the Meliata-Hallstatt ocean and its significance for the early evolution of the Eastern  
1086 Alps and western Carpathians. In: Channell, J.E.T., Winterer, E.L., Jansa, L.F. (Eds.), *Paleogeography and  
1087 Paleocyanography of Tethys*. *Palaeogeogr. Palaeoclimatol. Palaeoecol.*, 87, 109-135.

1088 Krabbendam, M. (2001). When the Wilson cycle breaks down: How orogens can produce strong lithosphere and inhibit  
1089 their future reworking. In Miller, J.A., et al., (Eds.), *Continental reactivation and reworking: Geological Society of  
1090 London Special Publication*, 184, 57-75. doi: 10.1144/GSL.SP.2001.184.01.04.

1091 Kusznir, N.J., and Park, R.G. (1987). The extensional strength of the continental lithosphere: its dependence on geothermal  
1092 gradient, and crustal composition and thickness. In: Coward, M.P., Dewey, J.F., and Hancock, P.L. (Eds.), *Continental  
1093 Extensional Tectonics*. *Geol. Soc. Spec. Publ.*, 28, 35-52.

1094 Lafosse, M., Boutoux, A., Bellahsen, N., and Le Pourhiet, L. (2016). Role of tectonic burial and temperature on the inversion  
1095 of inherited extensional basins during collision. *Geological Magazine*, 153(5-6), 811-826.  
1096 doi:10.1017/S0016756816000510

1097 Langhi, L., Ciftci, N. B., and Borel, G. D. (2011). Impact of lithospheric flexure on the evolution of shallow faults in the Timor  
1098 foreland system. *Marine Geology*, 284, 40–54.

1099 Leveridge, B., and Hartley, A.J. (2006). The Variscan Orogeny: the development and deformation of  
1100 Devonian/Carboniferous basins in SW England and South Wales. In: Brenchley, P.J.; Rawson, P.F., (Eds.), *The geology of*  
1101 *England and Wales*. London, Geological Society of London, 225-255.

1102 Lundmark, A. M., Sæther, T. and Sørli, R. (2014). Ordovician to Silurian magmatism on the Utsira High, North Sea:  
1103 implications for correlations between the onshore and offshore Caledonides. In: Corfu, F., Gasser, D. & Chew, D. M.  
1104 (eds) 2014. *New Perspectives on the Caledonides of Scandinavia and Related Areas*, The Geological Society, Special  
1105 Publications, London, 390, 513-523.

1106 Mac Niocaill, C., van der Pluijm, B.A., Van der Voo, R. (1997). Ordovician paleogeography and the evolution of the Iapetus  
1107 ocean. *Geology*; 25(2), 159–162.

1108 Macdonald, R., and Fettes, D.J. (2007). The tectonomagmatic evolution of Scotland. *Transactions of the Royal Society of*  
1109 *Edinburgh. Earth Sciences*, 97, 213-295.

1110 Malinverno, A., and Ryan, W.B.F. (1986). Extension in the Tyrrhenian Sea and shortening in the Apennines as result of arc  
1111 migration driven by sinking of the lithosphere. *Tectonics*, 5, 227–245. <http://dx.doi.org/10.1029/TC005i002p00227>.

1112 Marshall, J.E.A. and Hewett, A.J. (2003). Chapter 6: Devonian. In: Evans, D., Graham, C., Armour, A., Bathurst, P. (eds.), *The*  
1113 *Millennium Atlas: petroleum geology of the central and northern North Sea*. The Geological Society of London, London,  
1114 UK, 65-81.

1115 Mazzoli, S., Deiana, G., Galdenzi, S., and Cello, G. (2002). Miocene fault-controlled sedimentation and thrust propagation  
1116 in the previously faulted external zones of the Umbria-Marche Apennines, Italy. In: Bertotti, G., Schulmann, K., and  
1117 Cloetingh, S.A.P.L., (Eds.) *Continental Collision and the Tectono-sedimentary Evolution of Forelands: Stephan Mueller*  
1118 *Special Publication Series*, 195–209.

1119 Mazzoli, S., Pierantoni, P.P., Borraccini, F., Paltrinieri, W., and Deiana, G. (2005). Geometry, segmentation pattern and  
1120 displacement variations along a major Apennine thrust zone, central Italy. *Journal of Structural Geology*, 27, 1940-  
1121 1953, doi:10.1016/j.jsg.2005.06.002.

1122 McClay, K.R., Norton, M.G., Coney, P., Davis, G.H. (1986). Collapse of the Caledonide Orogen and the Old Red Sandstone.  
1123 *Nature*, London, 525, 147-149.

1124 McKerrow, W.S., Mac Niocaill, C., and Dewey, J.F. (2000a). The Caledonian Orogeny redefined. *Journal of the Geological*  
1125 *Society*, London, 157, 1149-1154.

1126 McKerrow, W.S., Mac Niocaill, C., Ahlberg, P.E., Clayton, G., Cleal, C. J. and Eagar, R.M.C. (2000b). The Late Palaeozoic  
1127 relations between Gondwana and Laurussia. *Geological Society, London, Special Publications* 2000, 179, 9-20.

1128 Mendum, J.R. (2012). Late Caledonian (Scandian) and Proto-Variscan (Acadian) orogenic events in Scotland. *Journal of the*  
1129 *Open University Geological Society*, 33 (1), 37-51.

1130 Miller, M. S., and Piana Agostinetti, N. (2012). Insights into the evolution of the Italian lithospheric structure from S  
1131 receiver function analysis, *Earth Planet. Sci. Lett.*, 345, 49–59, doi:10.1016/j.epsl.2012.06.028.

1132 Mindszenty, A., D'Argenio, B., and Aiello, G. (1995). Lithospheric bulges recorded by regional unconformities. The case of  
1133 Mesozoic-tertiary Apulia. *Tectonophysics*, 252, 137-161.

1134 Mirabella, F., Barchi, M., Lupattelli, A., Stucchi, E. and Ciaccio, M.G. (2008). Insights on the seismogenic layer thickness  
1135 from the upper crust structure of the Umbria-Marche Apennines (central Italy). *Tectonics*, 27, TC1010,  
1136 doi:10.1029/2007TC002134.

1137 Molinari, I., and Morelli, A. (2011). EPcrust: A reference crustal model for the European Plate, *Geophys. J. Int.*, 185, 352–  
1138 364, doi:10.1111/j.1365-246X.2011.04940.x.

1139 Morley, C.K., Tingay, M., Hillis, R., and King, R. (2008). Relationship between structural style, overpressures, and modern  
1140 stress, Baram Delta Province, northwest Borneo. *Journal of Geophysical Research*, 113, B09410.  
1141 doi:10.1029/2007JB005324.

1142 Mudge, D.C., and Copestake, P. (1992). Lower Palaeogene stratigraphy of the northern North Sea. *Marine and Petroleum*  
1143 *Geology*, 9, 287-301.

1144 Nance, R.D., Gutiérrez-Alonso, G., Keppie, J.D., Linnemann, U., Murphy, J.B., Quesada, C., Strachan, R.A., and Woodcock,  
1145 N. H. (2010). Evolution of the Rheic ocean. *Gondwana Research*, 17(2), 194–222.



1146 Nance, R.D., Guitierrez-Alonso, G., Keppie, J.D., Linnemann, U., Murphy, J.B., Quesada, C., Strachan, R.A., and Woodcock,  
1147 N.H. (2012). A brief history of the Rheic Ocean. *Geoscience Frontiers*, 3(2), 125-135.

1148 Nøttvedt, A., Berge, A. M., Dawers, N. H., Færseth, R. B., Häger, K. O., Mangerud, G., and Puigdefabregas, C. (2000). Syn-  
1149 rift evolution and resulting play models in the Snorre-H area, northern North Sea. In: Nøttvedt, A., et al., eds.,  
1150 Dynamics of the Norwegian Margin: Geological Society, London, Special Publications, 167, 179-218.

1151 O'Brien, G. W., Lisk, M., Duddy, I. R., Hamilton, J., Woods P., and Cowley, R. (1999). Plate convergence, foreland  
1152 development and fault reactivation: primary controls on brine migration, thermal histories and trap breach in the  
1153 Timor Sea, Australia. *Marine and Petroleum Geology*, 16, 533-560.

1154 Pace, P., Scisciani, V., and Calamita, F. (2011). Styles of plio-quadernary positive inversion tectonics in the Central-Southern  
1155 Apennines and in the Adriatic Foreland, *Rend. Online Soc. Geol. Ital.*, 15, 92–95.

1156 Pace, P., Scisciani, V., Calamita, F., Butler, R. W. H., Iacopini, D., and Esestime, P. (2015). Inversion structures in a foreland  
1157 domain: Seismic examples from the Italian Adriatic Sea. *Interpretation*, 3(4). <http://dx.doi.org/10.1190/INT-2015-0013.1>.

1158

1159 Patacca, E., and Scandone, P. (1989). Post-Tortonian mountain building in the Apennines. The role of the passive sinking of  
1160 a relic lithospheric slab. In: Boriani A., Bonafede M., Piccardo G.B. and Vai G.B. (Eds.), *The Lithosphere in Italy.*  
1161 *Advances in Earth Science Research. Atti Convegni Lincei*, 80, 157-176.

1162 Patruno, S. (2017). A new look at the geology and prospectivity of a North Sea frontier area with modern seismic: the East  
1163 Shetland Platform. 79th EAGE Conference and Exhibition, Paris, 12-15 June 2017, extended abstract and oral  
1164 presentation. Extended abstract available online at:  
1165 <http://www.earthdoc.org/publication/publicationdetails/?publication=88346>

1166 Patruno, S. and Reid, W., (2016). An introduction to the plays of the East Shetland Platform and Mid North Sea High (UK  
1167 29th Frontier Licensing Round). *GeoExpro*, June 2016.

1168 Patruno, S. and Reid, W., (2017). New plays on the Greater East Shetland Platform (UKCS Quadrants 3, 8-9, 14-16) – part  
1169 2: Newly reported Permo-Triassic intra-platform basins and their influence on the Devonian-Paleogene prospectivity of  
1170 the area. *First Break* (peer-reviewed 'Technical Article' sections), 35, 59-69.

1171 Patruno, S. and Lampart, V. (2018). Newly-observed post-Variscan extensional mini-basins: the key to the prospectivity  
1172 of the under-explored platform areas of the North Sea? Extended abstract presented at the 80th EAGE Conference and  
1173 Exhibition 2018, 11–14 June 2018, Copenhagen, Denmark. Doi: 10.3997/2214-4609.201801040  
1174 <http://www.earthdoc.org/publication/publicationdetails/?publication=92429>

1175 Patruno, S. and Reid, W. (2018). Complex multiphase inversion tectonics in the southern East Shetland Platform, offshore  
1176 United Kingdom. In: MISRA, A.A. and MUKHERJEE, S. (eds) *Atlas of Structural Geological Interpretation from Seismic*  
1177 *Images*. Wiley-Blackwell, Oxford, 73–76. ISBN: 978-1-119-15832-5, Wiley-Blackwell.

1178 Patruno, S., Hampson, G.J., and Jackson, C. A-L. (2015a). Quantitative characterisation of deltaic and subaqueous  
1179 clinoforms. *Earth-Science Reviews*, 142, 79-119.

1180 Patruno, S., Hampson, G.J., Jackson, C. A-L., and Dreyer, T., (2015b). Clinoform geometry, geomorphology, facies character  
1181 and stratigraphic architecture of ancient sand-prone subaqueous delta: Upper Jurassic Sognefjord Formation, Troll  
1182 Field, Offshore Norway. *Sedimentology*, 62(1), 350-388.

1183 Patruno, S., Hampson, G.J., Jackson, C. A-L., and Whipp P.S. (2015c). Quantitative progradation dynamics and stratigraphic  
1184 architecture of ancient shallow-marine clinoform sets: a new method and its application to the Upper Jurassic  
1185 Sognefjord Formation, Troll Field, offshore Norway. *Basin Research*, DOI: 10.1111/bre.12081.  
1186 <http://onlinelibrary.wiley.com/doi/10.1111/bre.12081/abstract>

1187 Patruno, S., Triantaphyllou, M.V., Erba, E., Dimiza, M.D., Bottini, C., and Kaminski, M.A., (2015d). The Barremian and  
1188 Aptian stepwise development of the 'Oceanic Anoxic Event 1a' (OAE 1a) crisis: integrated benthic and planktic high-  
1189 resolution palaeoecology along the Gorgo a Cerbara stratotype section (Umbria-Marche Basin, Italy). *Palaeogeography,*  
1190 *Palaeocology, Palaeoecology*, 424, 147-182.

1191 Patruno, S., Reid, W., Berndt, C., Feuilleaubeis, L. (in press). Polyphase tectonic inversion and its role in controlling  
1192 hydrocarbon prospectivity in the Greater East Shetland Platform and Mid North Sea High, offshore UK. In: A.A.  
1193 Monaghan, J.R. Underhill, A.J. Hewett, J.E.A. Marshall (Eds.), *Palaeozoic Plays of NW Europe*, vol. 471, The Geological  
1194 Society, Special Publications, London, United Kingdom (2018) (May 4) <https://doi.org/10.1144/SP471.9>  
1195 <http://sp.lyellcollection.org/content/early/2018/05/03/SP471.9> (in press)

1196 Pegrum, R.M., and Spencer, A.M. (1990). Hydrocarbon plays in the northern North Sea. In: Brooks, J. (Ed.), *Classic*  
1197 *Petroleum Provinces*. Geological Society Special Publication, 50, 441-470.

1198 Peryt, T.M., Geluk, M., Mathiesen, A., Paul, A. and Smith, K. (2010). Chapter 8: Zechstein. In: Doornebal, H., Stevenson, A.  
1199 (Editors). *Petroleum Geological Atlas of the Southern Permian Basin Area*, 123-147. EAGE Publications b.v. (Houten),  
1200 342 pp.

1201 Pizzi, A., and Galadini, F. (2009). Pre-existing cross-structures and active fault segmentation in the northern-central  
1202 Apennines (Italy). *Tectonophysics* 476, 1, 304–319.

1203 Pizzi, A., and Scisciani, V. (2000). Methods for determining the Pleistocene–Holocene component of displacement on  
1204 active faults reactivating pre-Quaternary structures: examples from the Central Apennines (Italy). *J. Geodyn.*, 29, 445–  
1205 457. [http://dx.doi.org/10.1016/S0264-3707\(99\)00053-8](http://dx.doi.org/10.1016/S0264-3707(99)00053-8).

1206 Platt, N.H. (1995). Structure and tectonics of the northern North Sea: new insights from deep penetration regional seismic  
1207 data. In: Lambiase, J.J. (Ed.), *Hydrocarbon habitat in rift basins*. Geological Society of London Special Publication, 80,  
1208 103-113.

1209 Platt, N.H., and Cartwright, J.A. (1998). Structure of the East Shetland Platform, northern North Sea. *Petroleum*  
1210 *Geoscience*, 4, 353-362.

1211 Reid, W., and Patruno, S. (2015). The East Shetland Platform: unlocking the platform potential. With significant  
1212 advancements in seismic acquisition technology, it is time to re-visit the East Shetland Platform. *GeoExpro*, November  
1213 2015, 12(6), 41-46.

1214 Ricci Lucchi, F. (1986). The Oligocene to Recent foreland basins of the northern Apennines: in Allen, P.A., and Homewood,  
1215 P. (Eds.), *Foreland Basins: International Association of Sedimentologists Special Publication*, 8, 105-139.

1216 Richardson, N.J., Allen, M.R., and Underhill, J.R. (2005). Role of Cenozoic fault reactivation in controlling pre-rift plays, and  
1217 the recognition of Zechstein Group evaporite-carbonate lateral facies transitions in the East Orkney and Dutch Bank  
1218 basins, East Shetland Platform, UK North Sea. In: Doré, A.G., and Vining, B.A. (Eds.). *Petroleum Geology: North-West*  
1219 *Europe and Global Perspectives – Proceedings of the 6th Petroleum Geology Conference*, 337-348. Published by the  
1220 Geological Society, London.

1221 Ring, U. (1994) The influence of preexisting structure on the evolution of the Cenozoic Malawi rift (east African rift  
1222 system). *Tectonics*, 12, 313-326.

1223 Romão, J., Coke, C., Dias, R., and Ribeiro, A. (2005). Transient inversion during the opening stage of the Wilson Cycle  
1224 “Sardic phase” in the Iberian Variscides. *GeodinamicaActa*, 18(2), 15-29.

1225 Ronchi P., Casaglia F., and Ceriani, A. (2003). The multiphase dolomitization of the Liassic Calcare Massiccio and Corniola  
1226 successions (Montagna dei Fiori, Northern Apennines, Italy). *Boll. Soc. Geol. It.*, 122(2), 157-172.

1227 Rossi, P., Oggiano, G., and Cocherie, A. (2009). A restored section of the “southern Variscan realm” across the Corsica–  
1228 Sardinia microcontinent. *Comptes Rendus Geoscience*, 341(2-3), 224–238. doi: 10.1016/j. crte.2008.12.005

1229 Rusciadelli G., Viandante, M.G., Calamita, F., and Cook, A.C. (2003) - Burial-exhumation history of the central Apennines  
1230 (Italy), from the foreland to the chain building: thermochronological and geological data. *Terra Nova*, 17(6), 560-572.

1231 Saqab, M.M., and Bourget, J. (2015). Structural style in a young flexure-induced oblique extensional system, north-western  
1232 Bonaparte Basin, Australia. *Journal of Structural Geology*, 77, 239-259.

1233 Satolli, S., Pace, P., Viandante, M. G., and Calamita, F. (2014). Lateral variations in tectonic style across cross-strike  
1234 discontinuities: an example from the Central Apennines belt (Italy). *International Journal of Earth Sciences*, 103, 2301–  
1235 13.

1236 Scheck, M., Thybo, H., Lassen, A., Abramovitz, T., and Laigle, M. (2002). Basement structure in the southern North Sea,  
1237 offshore Denmark, based on seismic interpretation. Geological Society, London, Special Publications 2002, 201, 311-  
1238 326.

1239 Schlindwein, V., and Jokat, W. (1999). Structure and evolution of the continental crust of northern east Greenland from  
1240 integrated geophysical studies. *Journal of Geophysical Research*, 104, NO. B7, 15,227-15,245.

1241 Scisciani, V., Calamita, F., Bigi, S., De Girolamo, C., and Paltrinieri, W. (2000a). The influence of syn-orogenic normal faults  
1242 on Pliocene thrust system development: the Maiella structure (Central Apennines, Italy). *Mem. Soc. Geol. It.*, 55, 193–  
1243 204.

1244 Scisciani, V., Rusciadelli, G., and Calamita, F. (2000b). Faglie normali nell'evoluzione tortoniano-messiniana dei bacini  
1245 sinorogenici dell'Appennino centrale esterno. *Boll. Soc. Geol. It.*, 119, 715–732.

1246 Scisciani, V., Calamita, F., Tavarnelli, E., Rusciadelli, G., Ori, G.G. and Paltrinieri, W. (2001). Foreland-dipping normal faults  
1247 in the inner edges of syn-orogenic basins: a case from the Central Apennines, Italy. *Tectonophysics*, 330, 211-224.

1248 Scisciani, V., Tavarnelli, E., and Calamita, F., (2002). The interaction of extensional and contractional deformations in the  
1249 outer zones of the Central Apennines, Italy. *Journal of Structural Geology*, 24, 1647–1658.  
1250 [http://dx.doi.org/10.1016/S0191-8141\(01\)00164-X](http://dx.doi.org/10.1016/S0191-8141(01)00164-X).

- 1251 Scisciani, V. (2009). Styles of positive inversion tectonics in the Central Apennines and in the Adriatic foreland: Implications  
1252 for the evolution of the Apennine chain (Italy). *Journal of Structural Geology*, 31, 1276–94.
- 1253 Scisciani V., and Montefalcone, R. (2005). Evoluzione neogenico-quadernaria del fronte della catena centro-appenninica:  
1254 vincoli dal bilanciamento sequenziale di una sezione geologica regionale. *Boll. Soc. Geol. It.*, 124, 579-599.
- 1255 Scisciani, V., and Montefalcone, R. (2006). Coexistence of thin- and thick-skinned tectonics: an example from the Central  
1256 Apennines, Italy. In: Mazzoli, S., and Butler, R.W.H. (Eds.), *Styles of Continental Contraction*. *Geol. Soc. Am., Special  
1257 Paper 414*, 33–54. [http://dx.doi.org/10.1130/2006.2414\(03\)](http://dx.doi.org/10.1130/2006.2414(03)).
- 1258 Scisciani, V., and Calamita, F. (2009). Active intraplate deformation within Adria: Examples from the Adriatic region.  
1259 *Tectonophysics*, 476, 57-72. doi.org/10.1016/j.tecto.2008.10.030.
- 1260 Scisciani, V., Agostini, S. Calamita, F. Cilli, A. Giori, I. Pace, P., and Paltrinieri, W. (2010). The influence of pre-existing  
1261 extensional structures on the Neogene evolution of the Northern Apennines foreland fold-and-thrust belt. *Rend.  
1262 Online Soc. Geol. Ital.*, 10, 125–128.
- 1263 Scisciani, V., Agostini, S. Calamita, Pace, P., F. Cilli, A. Giori, I., and Paltrinieri, W. (2014). Positive inversion tectonics in  
1264 foreland fold-and-thrust belts: a reappraisal of the Umbria-Marche Northern Apennines (Central Italy) by integrating  
1265 geological and geophysical data. *Tectonophysics*, 637, 218–237.
- 1266 Scisciani, V., and Esestima, P. (2017). The Triassic Evaporites in the Evolution of the Adriatic Basin. In: Soto, J.I., Flinch, J.F,  
1267 and Tari, G. (Eds). *Permo-Triassic Salt Provinces of Europe, North Africa and the Atlantic Margins: Tectonics and  
1268 Hydrocarbon Potential*, Elsevier, Chapter 23, 499-516.
- 1269 Scotese, C.R., and Mckerrow, W.S. (1990). Revised world map and introduction. In: W.S. McKerrrow and C.R. Scotese (Eds.).  
1270 *Paleozoic Paleogeography and Biogeography*. *Geol Soc. London Memoirs*, 51, 1-21.
- 1271 Seranne, M. (1992). Devonian extensional tectonics versus Carboniferous inversion in the northern Orcadian basin.  
1272 *Journal of the Geological Society*, 149, 27-37.
- 1273 Serpelloni, E., Anzidei, M., Baldi, P., Casula, G. , and Galvani, A. (2005). Crustal velocity and strain-rate fields in Italy and  
1274 surrounding regions: New results from the analysis of permanent and non-permanent GPS networks, *Geophys.  
1275 J. Int.*, 161, 3, 861–880.
- 1276 Sibson, R.H. (1977). Fault rocks and fault mechanisms. *Journal of the Geological Society (London)*, 133, 191-213.
- 1277 Sibson, R.H. (1985). A note on fault reactivation. *Journal of Structural Geology*, 7, 751–754.
- 1278 Sinclair, H. (1997). Tectonostratigraphic model for underfilled peripheral foreland basins: an Alpine perspective. *Geol. Soc.  
1279 Am. Bull.* 109, 324-346.
- 1280 Snyder, D.B. (1991) Reflections from a Relic Moho in Scotland?, in *Continental Lithosphere: Deep Seismic Reflections* (Eds.  
1281 R. Meissner, L. Brown, H.-J. Dürbaum, W. Franke, K. Fuchs and F. Seifert), American Geophysical Union, Washington, D.  
1282 C. doi: 10.1029/GD022p0307
- 1283 Stampfli, G.M., and Borel, G.D. (2002). A plate tectonic model for the Paleozoic and Mesozoic constrained by dynamic  
1284 plate boundaries and restored synthetic oceanic isochrons. *Earth and Planetary Science Letters*, 196(1-2), 17-33.
- 1285 Steel, R.J. (1993) Triassic-Jurassic megasequence stratigraphy in the Northern North Sea: rift to post-rift evolution. In:  
1286 *Petroleum Geology of North-West Europe: Proceedings of the 4th Conference* (Ed J.R. Parker), 299-315. Geological  
1287 Society of London, London.
- 1288 Stemmerik, L., Ineson, J.R. and Mitchell, J.G., (2000). Stratigraphy of the Rotliegend Group in the Danish part of the  
1289 Northern Permian Basin, North Sea. *Journal of the Geological Society, London*, 157, 1127-1136.
- 1290 Stephenson, and Gould, (1995). *British Regional Geology: the Grampian Highlands* (4th edition). London: HMSO for the  
1291 British Geological Survey.
- 1292 Stephenson, D., Bevins, R.E., Millward, D., Highton, A.J., Parsons, I., Stone, P., and Wadsworth, W.J. (1999). Caledonian  
1293 Igneous Rocks of Great Britain. *Geological Conservation Review Series*, No. 17, Joint Nature Conservation Committee,  
1294 Peterborough, 648 pp.
- 1295 Stephenson, D. Mendum, J.R., Fettes, Douglas J., Leslie, and Graham, A. (2013). The Dalradian rocks of Scotland: an  
1296 introduction. *Proceedings of the Geologists' Association*, 124 (1-2), 3-82. 10.1016/j.pgeola.2012.06.002
- 1297 Strachan, R. A., (2000). Late Neoproterozoic to Cambrian accretionary history of Eastern Avalonia and Armorica on the  
1298 active margin of Gondwana. In: Woodcock, N. H.; Strachan, R. A. *Geological History of Britain and Ireland*. Blackwell,  
1299 127–139.
- 1300 Strachan, R.A., Smith, M., Harris, A.L. and Fettes, D.J. (2002). The Northern Highland and Grampian terranes. In: Trewin, N.  
1301 (ed) *Geology of Scotland* (4th edition). Geological Society, London, 81-147.

1302 Tavarnelli, E., Decandia, F.A. and Alberti, M. (1998). The transition from extension to compression in the Messinian Laga  
1303 Basin and its significance in the evolution of the Apennine belt-foredeep-foreland system. *Ann. Tectonicae*, 12, 10 133-  
1304 144.

1305 Tavarnelli, E., and Peacock, D.C.P. (1999). From extension to contraction in syn-orogenic foredeep basins: the Contessa  
1306 section, Umbria-Marche Apennines, Italy. *Terra Nova*, 11, 55-60.

1307 Thomson, K., and Underhill, J.R. (1993). Controls on the development and evolution of structural styles in the Inner Moray  
1308 Firth Basin. In: Parker, J.R. (Ed.), *Petroleum Geology of Northwest Europe: Proceedings of the 4th Conference*, The  
1309 Geological Society, London, 1167-1178.

1310 Toghiani, (2002). *The geology of Britain: an introduction*. Airlife Publishing, 192 pp.

1311 Trench, A., and Torsvik, T.H., 1992. The closure of the Iapetus Ocean and Tornquist Sea: new palaeomagnetic constraints.  
1312 *Journal of the Geological Society*, 149, 867-870.

1313 Turcotte, D., and Schubert, G. (1982). *Geodynamics*. Wiley, New York.

1314 Turner, J.P., Williams, G.A., (2004). Sedimentary basin inversion and intra-plate shortening. *Earth-Science Reviews*, 65,  
1315 277–304.

1316 Turner, C., Cronin, B., Hoth, S., Jones, M., Knaust, D., Reid, W., Patruno, S., Riley, L., (2018). The South Viking Graben:  
1317 Overview of Upper Jurassic rift geometry, biostratigraphy and extent of Brae Play submarine fan systems. In: Colin B.,  
1318 Turner, C.C., and Bryan, T. (Eds), *Rift-related coarse-grained submarine fan reservoirs; the Brae Play, South Viking*  
1319 *Graben, North Sea: American Association of Petroleum Geologists (AAPG) Memoir 115*, p. -.

1320 Underhill, J.R. (1991). Implications of Mesozoic-Recent basin development in the western Inner Moray Firth, UK. *Mar.*  
1321 *Petro Geol.* 8, 359-369.

1322 Underhill, J.R., and Partington, M.A. (1993). Jurassic thermal doming and deflation in the North Sea: implication of the  
1323 sequence stratigraphic evidence. In: Parker, J.R. (Ed.), *Petroleum Geology of Northwest Europe: Proceedings of the 4th*  
1324 *Conference*, The Geological Society, London, United Kingdom, 337-346.

1325 Underhill, J.R. and Partington, M.A. (1994). Use of maximum flooding surfaces in determining a regional control on the  
1326 Intra-Aalenian Mid Cimmerian sequence boundary: implications of North Sea basin development and Exxon's Sea-Level  
1327 Chart. In: Posamentier, H.W., and Wiemer, P.J. (Eds.) *Recent Advances in Siliciclastic Sequence Stratigraphy*. Memoir  
1328 No. 58, AAPG, Tulsa, OK, 49-84.

1329 Unida, S., and Patruno, S. (2016). The palynostratigraphy of the upper Maiolica, Selli Level and the lower Marne a Fucoidi  
1330 units in the proposed Barremian/Aptian (Lower Cretaceous) GSSP stratotype at Gorgo a Cerbara, Umbria-Marche  
1331 Basin, Italy. *Palynology*, 40(2), 230-246.

1332 Vai, G.B. (2001). Basement and early (pre-Alpine) history. In: Vai, G.B., and Martini, I.P. (Eds.). *Anatomy of an Orogen: the*  
1333 *Apennines and Adjacent Mediterranean Basins*, Kluwer Academic Publishers, 121-150.

1334 Vauchez, A., Barruol, G., and Tommas, A. (1997). Why do continents break-up parallel to ancient orogenic belts?. *Terra*  
1335 *Nova*, 9, 62–66.

1336 von Raumer, J.F., and Stampfli, G.M. (2008). The birth of the Rheic Ocean — Early Palaeozoic subsidence patterns and  
1337 subsequent tectonic plate scenarios. *Tectonophysics*, 461(1), 9-20.

1338 Warr, L.N., and Cox, S.C. (2001). Clay mineral transformations and weakening mechanisms along the Alpine Fault, New  
1339 Zealand. *Geological Society, London, Special Publications*, 186, 85–101.

1340 Williams, G.D., Powell, C.M., and Cooper, M.A. (1989). Geometry and kinematics of Inversion Tectonics. In: Cooper, M.A.,  
1341 Williams, G.D. (Eds.), *Inversion Tectonics*. Geological Society of London, Special Publication, 44, 3-15.

1342 Wilson, J.T. (1966). Did the Atlantic close and then re-open?. *Nature*, 211, 676–681.

1343 Wilson, R.W., Holdsworth, R.E., Wild, L.E., McCaffrey, K.J.W., England, R.W., Imber, J., and Strachan, R.A. (2010).  
1344 Basement-influenced rifting and basin development: a reappraisal of post-Caledonian faulting patterns from the North  
1345 Coast Transfer Zone, Scotland. In: Law, R.D., Butler, R.W.H., Holdsworth, R.E., Krabbendam, M., Strachan, R.A. (Eds.),  
1346 *Continental Tectonics and Mountain building: the legacy of Peach and Horne*. Geological Society, London, Special  
1347 *Publications*, 335, 795-826.

1348 Wiprut, D., and Zoback, M.D. (2000). Fault reactivation and fluid flow along a previously dormant normal fault in the  
1349 northern North Sea. *Geology*, 28(7), 595–598.

1350 Wiprut, D., and Zoback, M.D. (2002). Fault reactivation, leakage potential, and hydrocarbon column heights in the  
1351 northern North Sea. *Norwegian Petroleum Society Special Publications*, 11, 203-219.

1352 Zanella, E., and Coward, M.P. (2003). Structural framework. In: Evans, D., Graham, D., Armour, A., Bathurst, P. (editors and  
1353 coordinators). *The Millennium Atlas: petroleum geology of the central and northern North Sea*. The Geological Society  
1354 of London, London, 45-59.

- 1355 Zarella, E., Coward, M.P., and McGrandle, A. (2003). Crustal structure. In: Evans, D., Graham, D., Armour, A., Bathurst, P.  
1356 (editors and coordinators). The Millennium Atlas: petroleum geology of the central and northern North Sea. The  
1357 Geological Society of London, London, 17-33.
- 1358 Ziegler, P.A. (1988). Laurussia – The Old Red Continent. Devonian of the World: Proceedings of the 2nd International  
1359 Symposium on the Devonian System – Memoir 14, Volume I: Regional Syntheses, 15-48.
- 1360 Ziegler, P.A. (1990). Geological Atlas of Western and Central Europe (2nd Edition). Shell Internationale Petroleum  
1361 Maatschappij B.V., The Hague.
- 1362 Ziegler, P.A. (1992). North Sea rift system. Tectonophysics, 208, 55-75.
- 1363 Ziegler, P.A. (2012). Evolution of Laurussia: A Study in Late Palaeozoic Plate Tectonics. Springer Science Business Media, 6  
1364 Dec 2012, 100 pp.
- 1365 Ziegler, P.A., Schumacher, M.E., Dèzes, P., van Wees, J.D., and Cloetingh, S. (2004). Post-Variscan evolution of the  
1366 lithosphere in the Rhine Graben area; constraints from subsidence modelling. In: Wilson, M., Neumann, E.R., Davies,  
1367 G.R., Timmerman, M.J., Heeremans, M. and Larsen, B.T. (Eds): Permo-Carboniferous magmatism and rifting in Europe.  
1368 Geological Society Special Publication (London), 223, 289-317.
- 1369 Ziegler, P.A., Schumacher, M., Cloetingh, S., and Van Wees, J.-D. (2006). Post-Orogenic evolution of the Variscan  
1370 lithosphere in the area of the European rift system. In: Gee, D.G. and Stephenson, R.A. (Eds): European Lithosphere  
1371 Dynamics. Geological Society Memoir (London), 32, 97-112.



Fig. 1

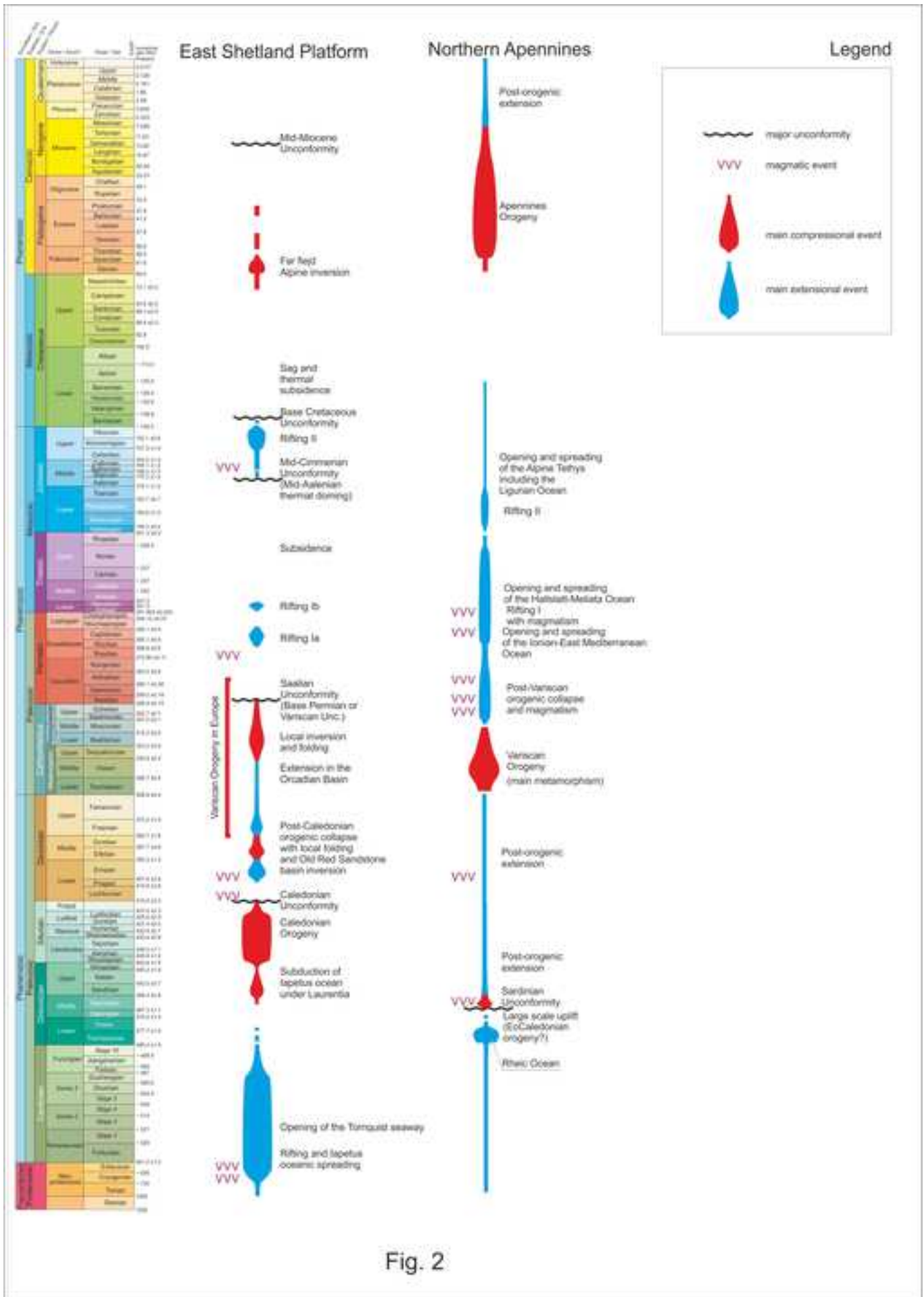


Fig. 2



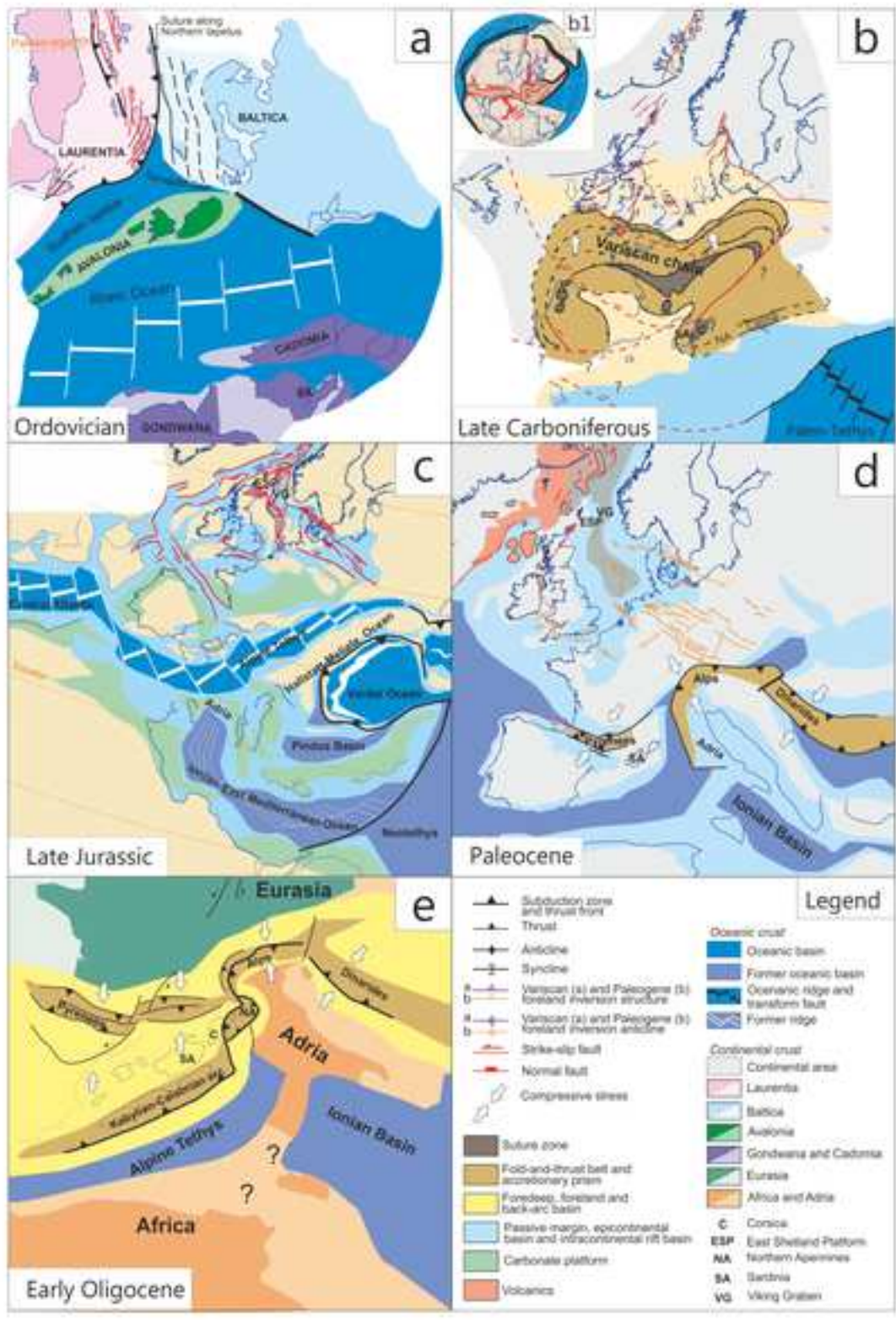


Fig. 3



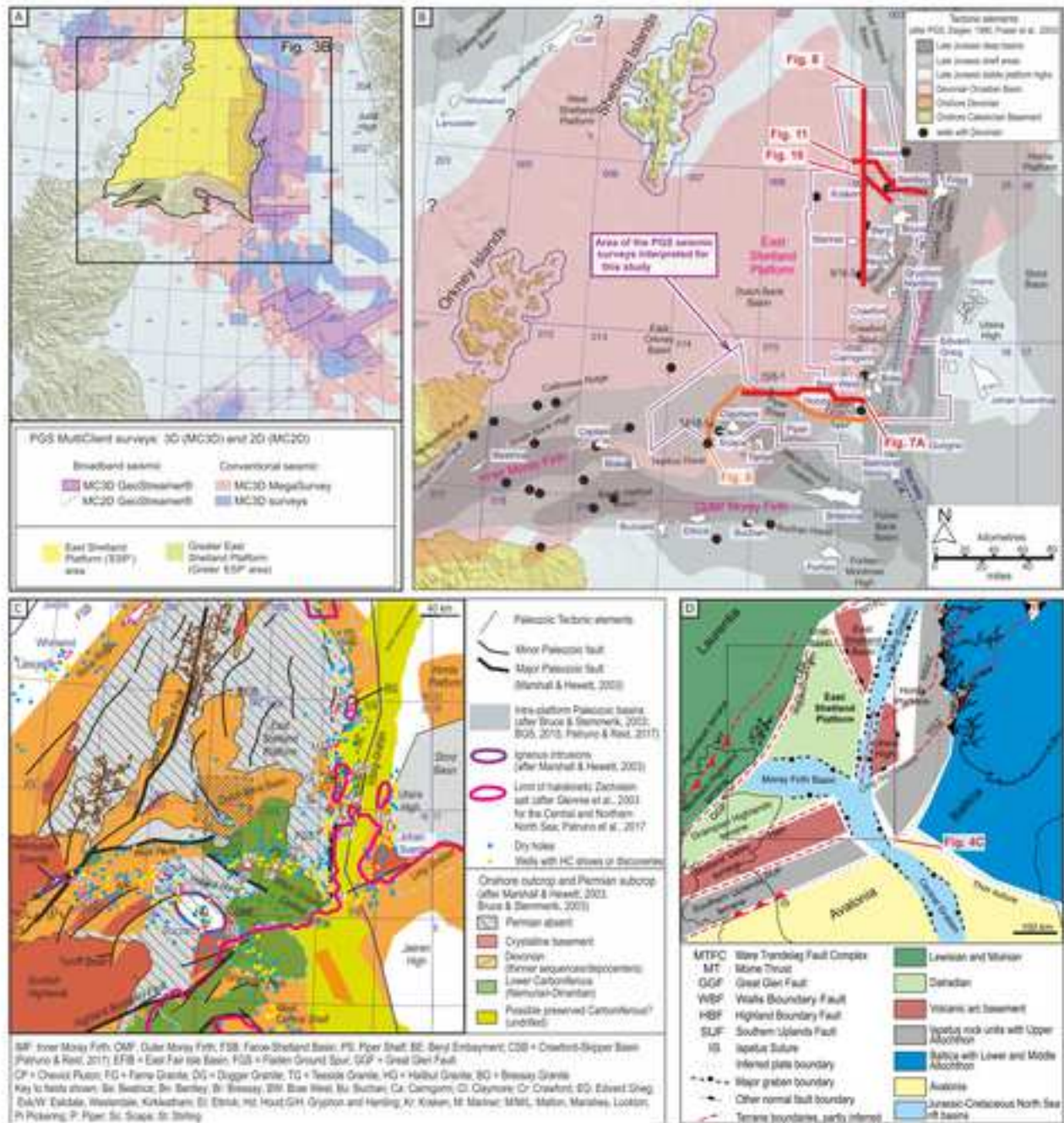


Fig. 4

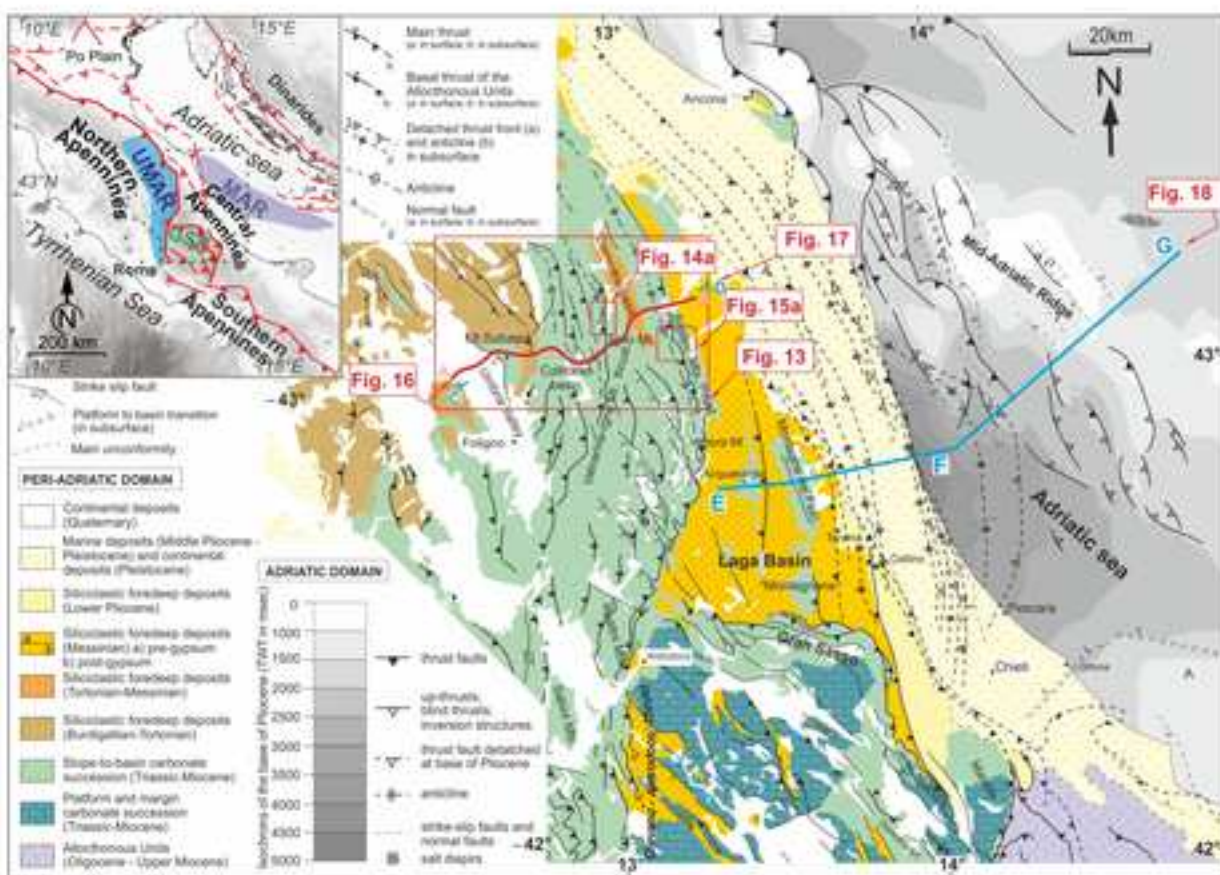
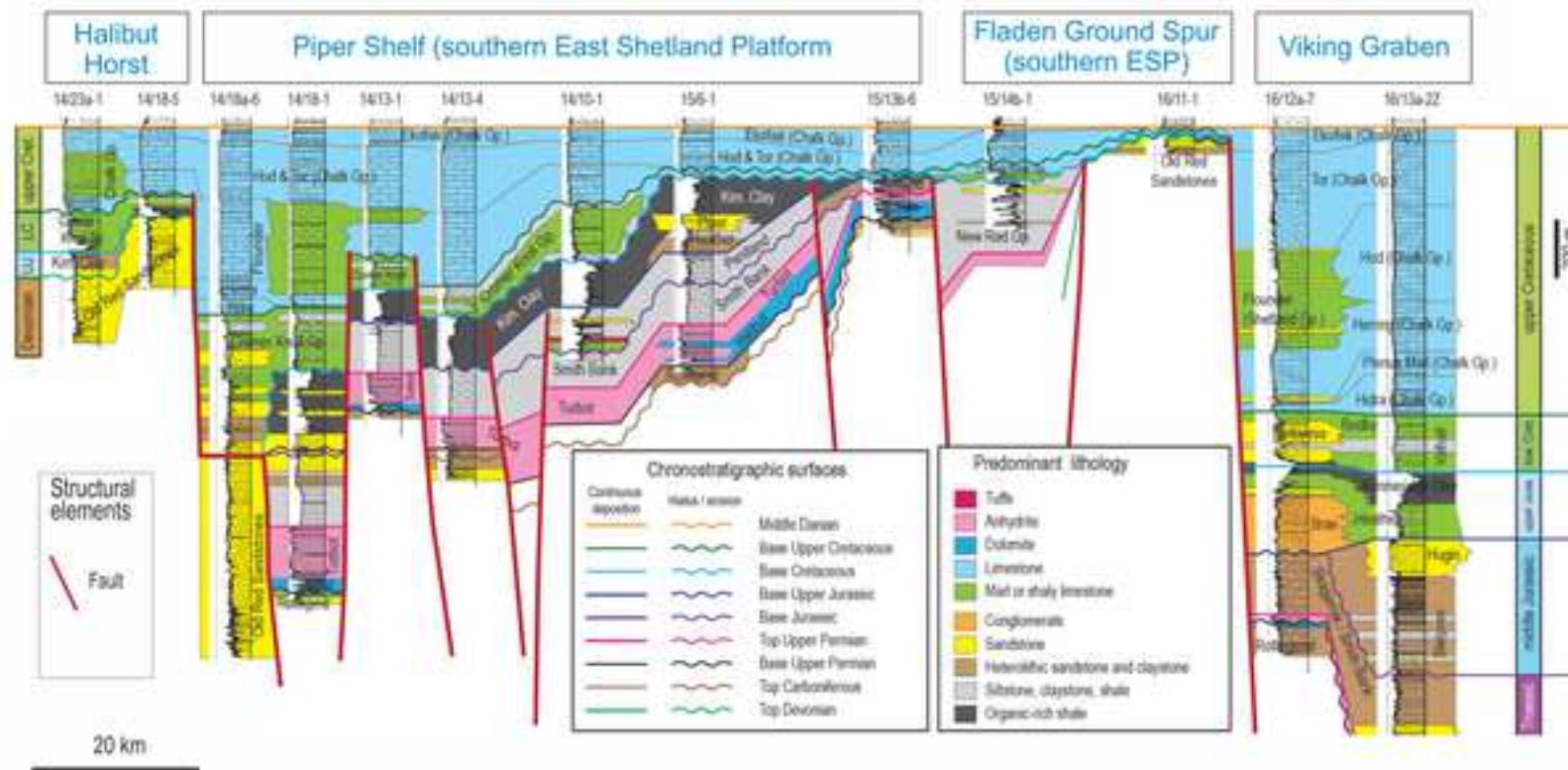


Fig. 5



Fig. 6



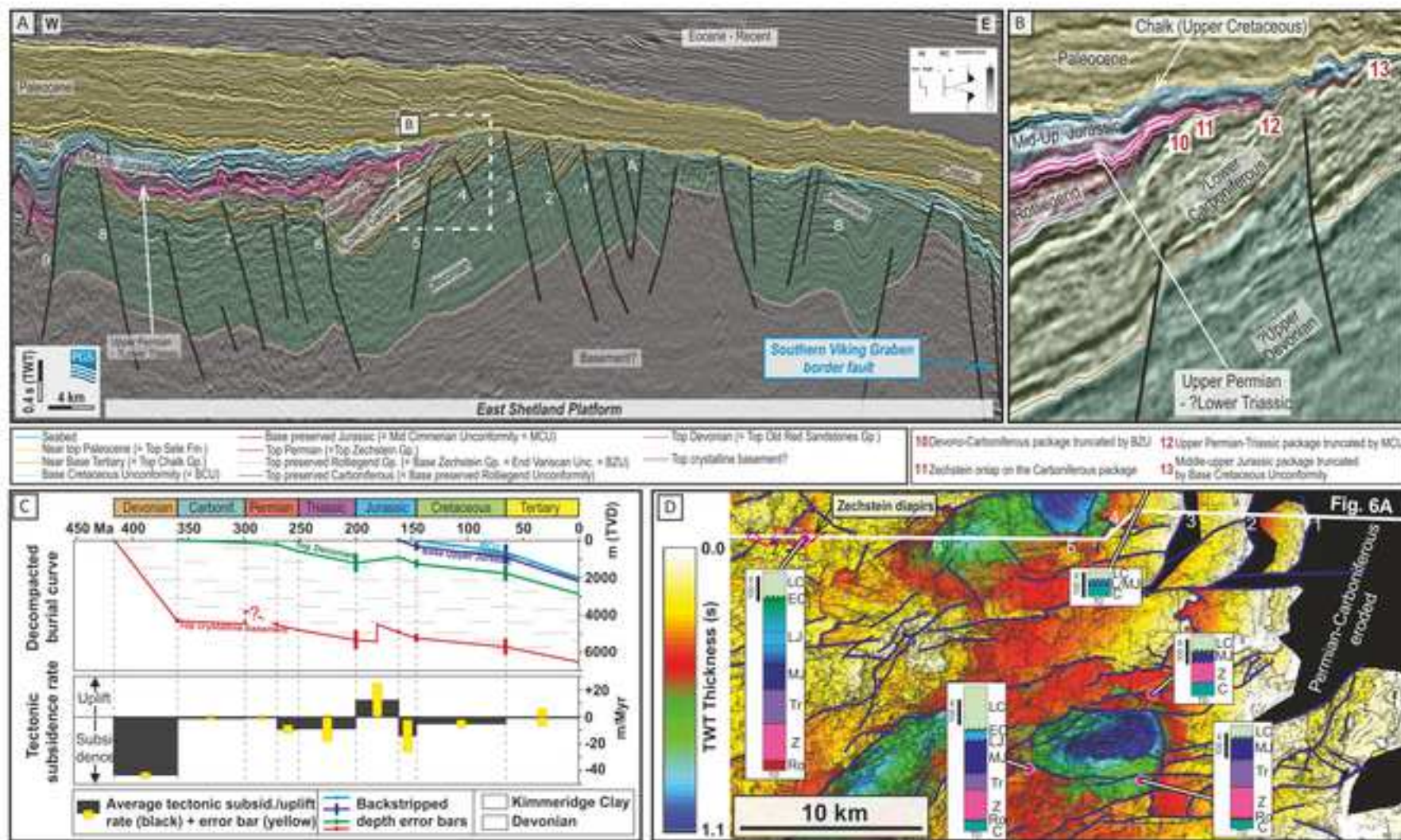


Fig. 7



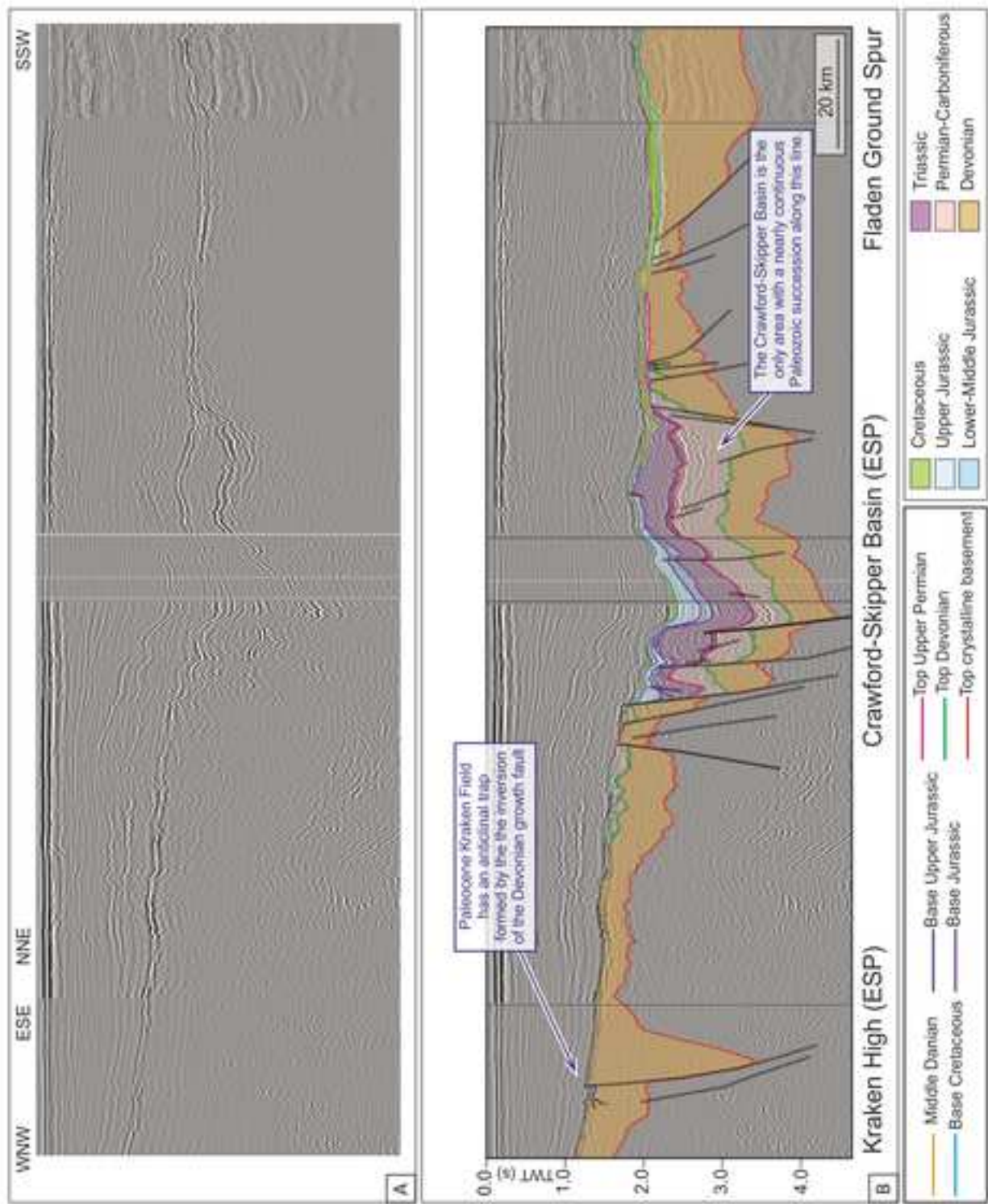


Fig. 8

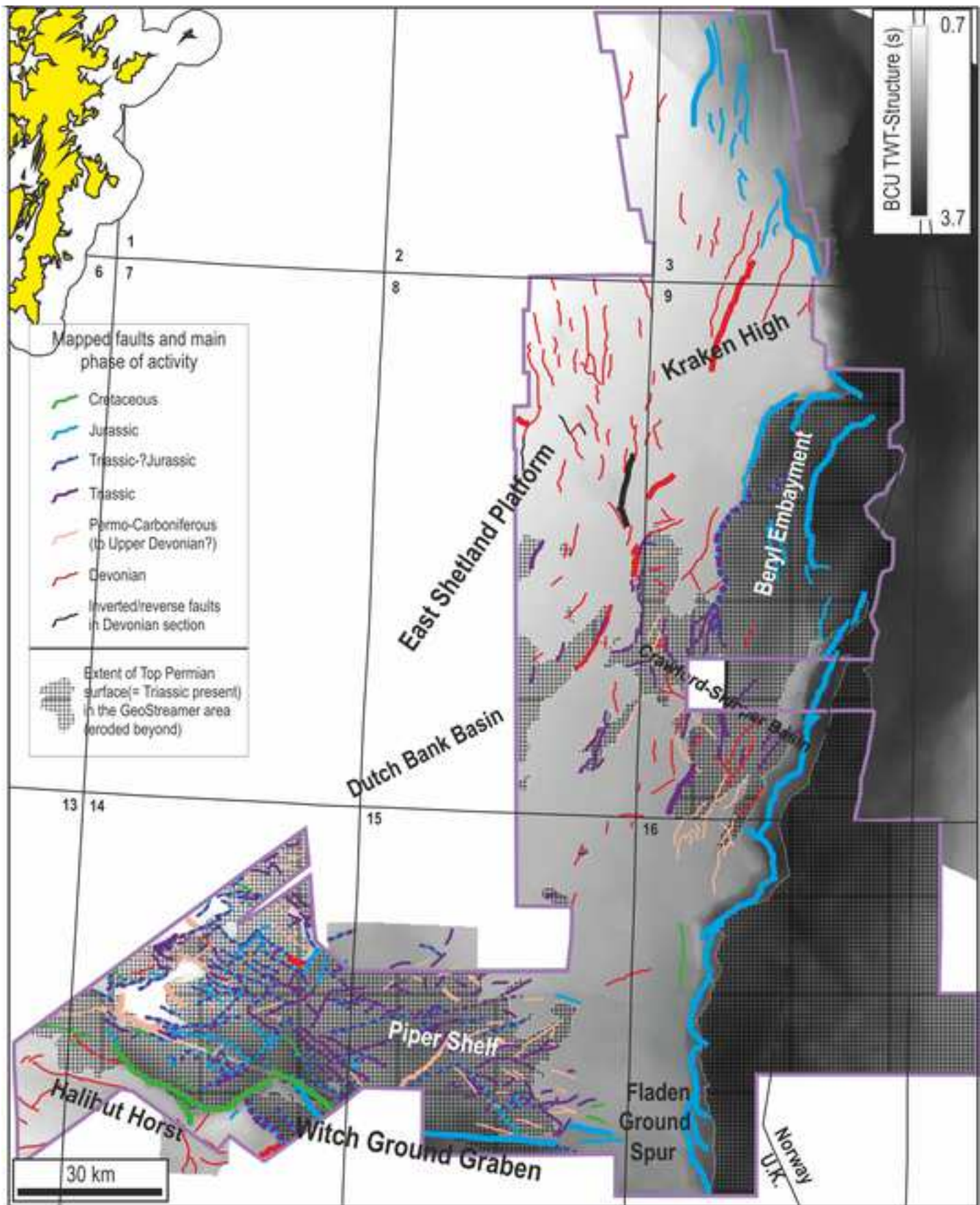


Fig. 9

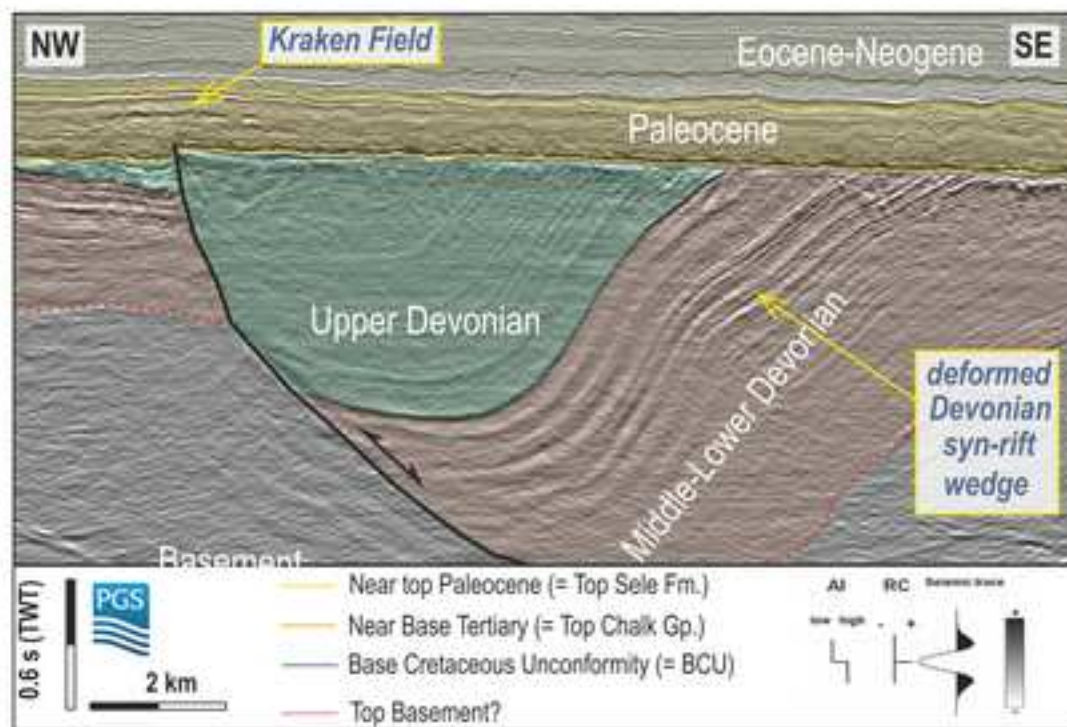


Fig. 10



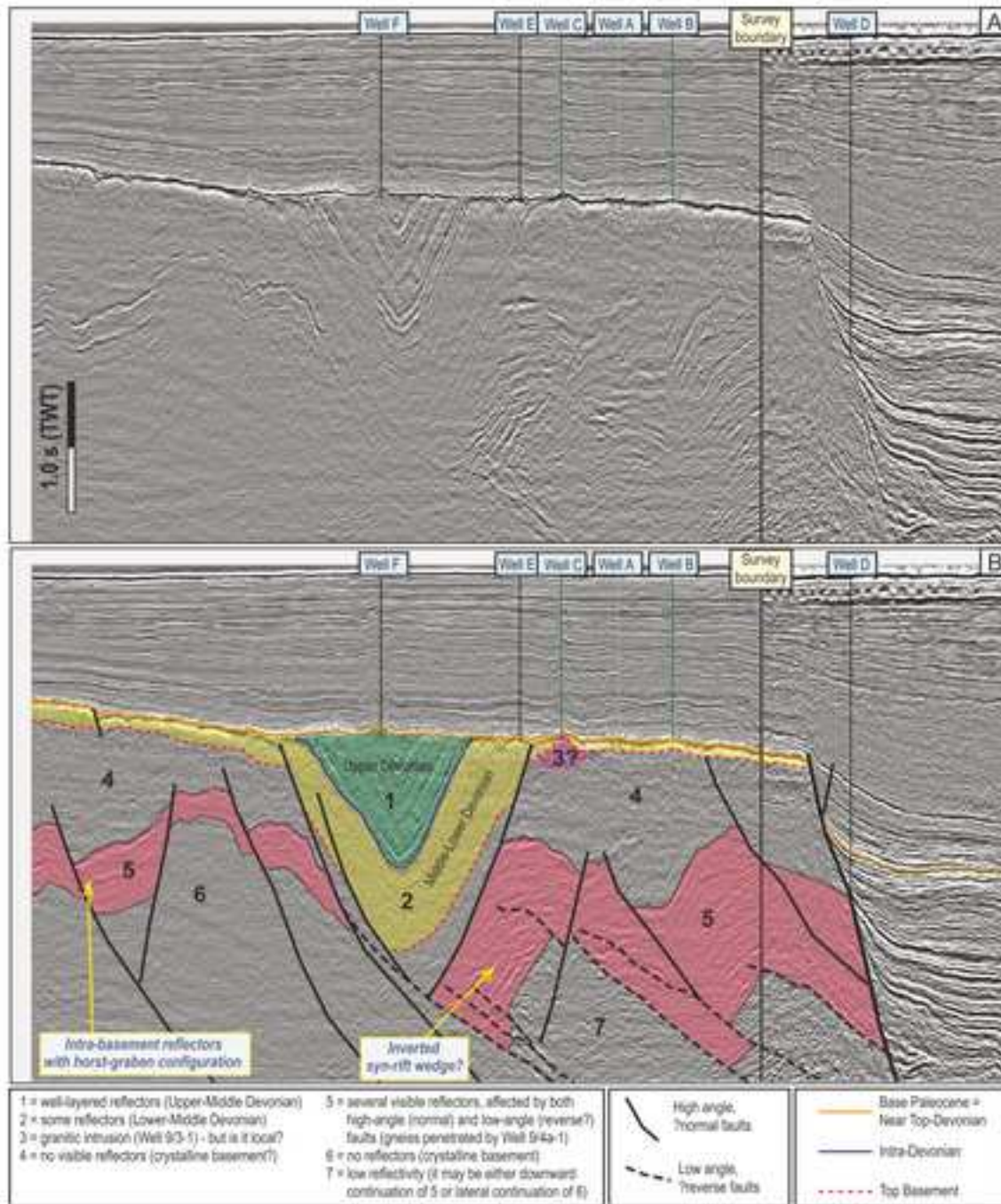


Fig. 11



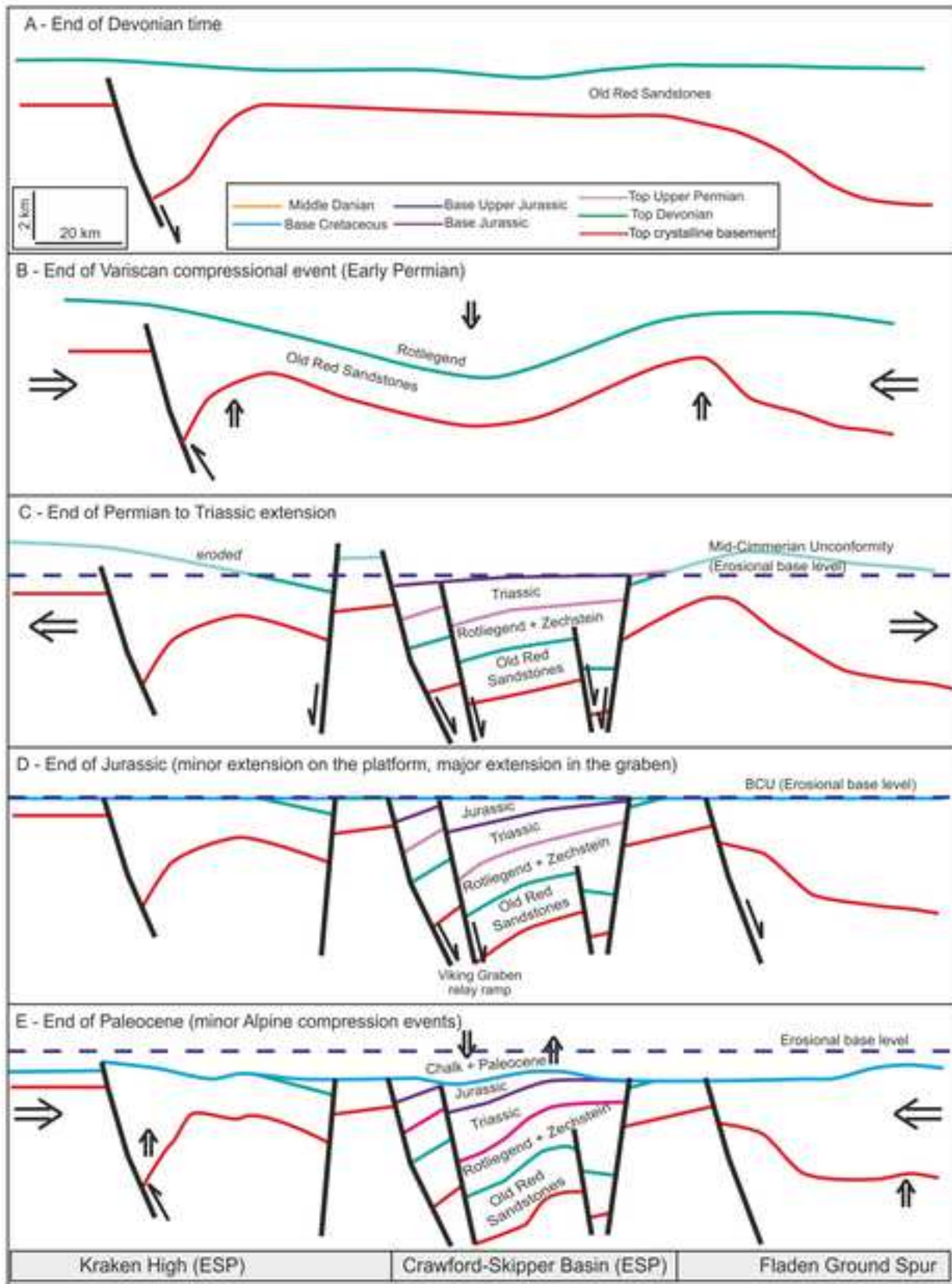


Fig. 12

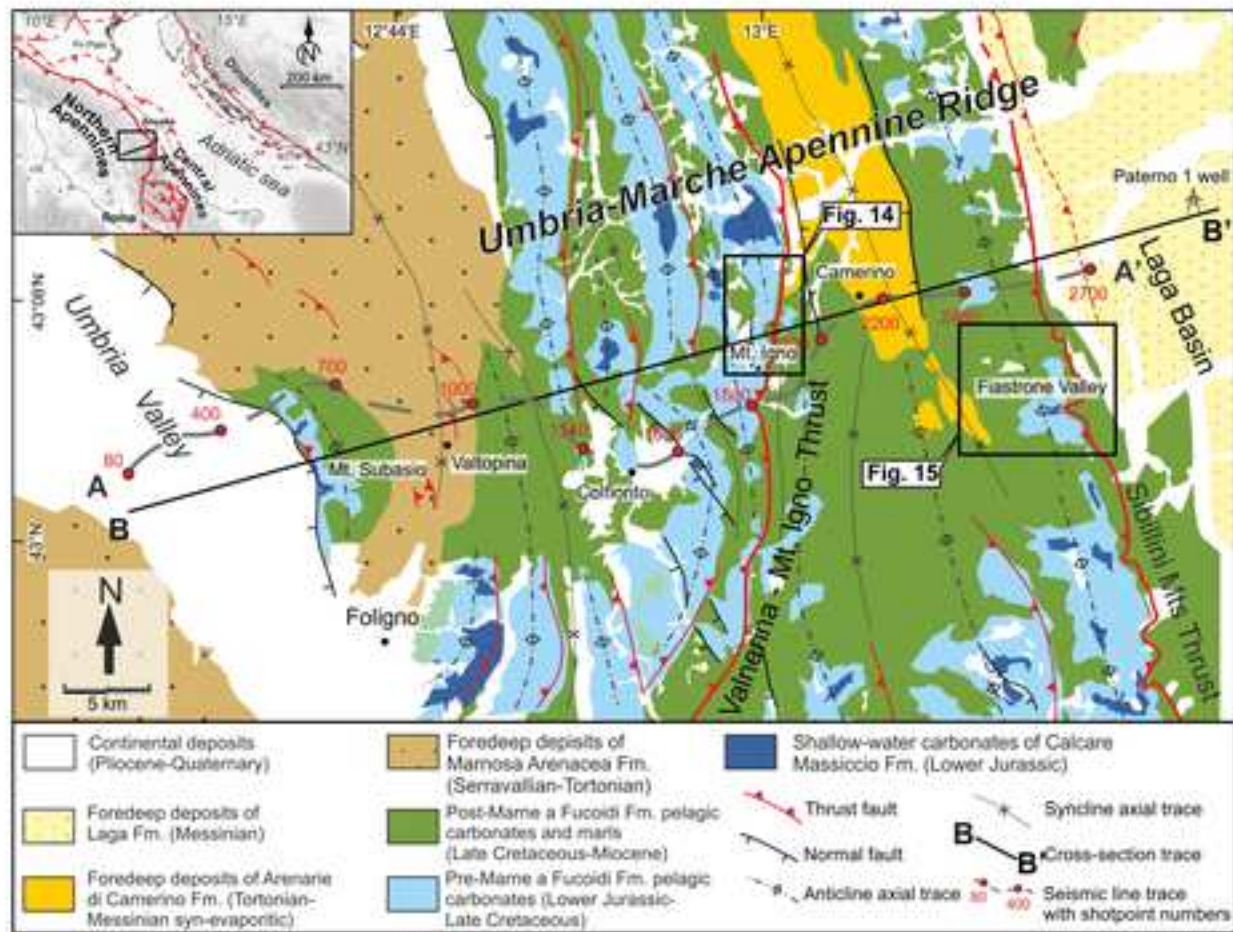


Fig. 13

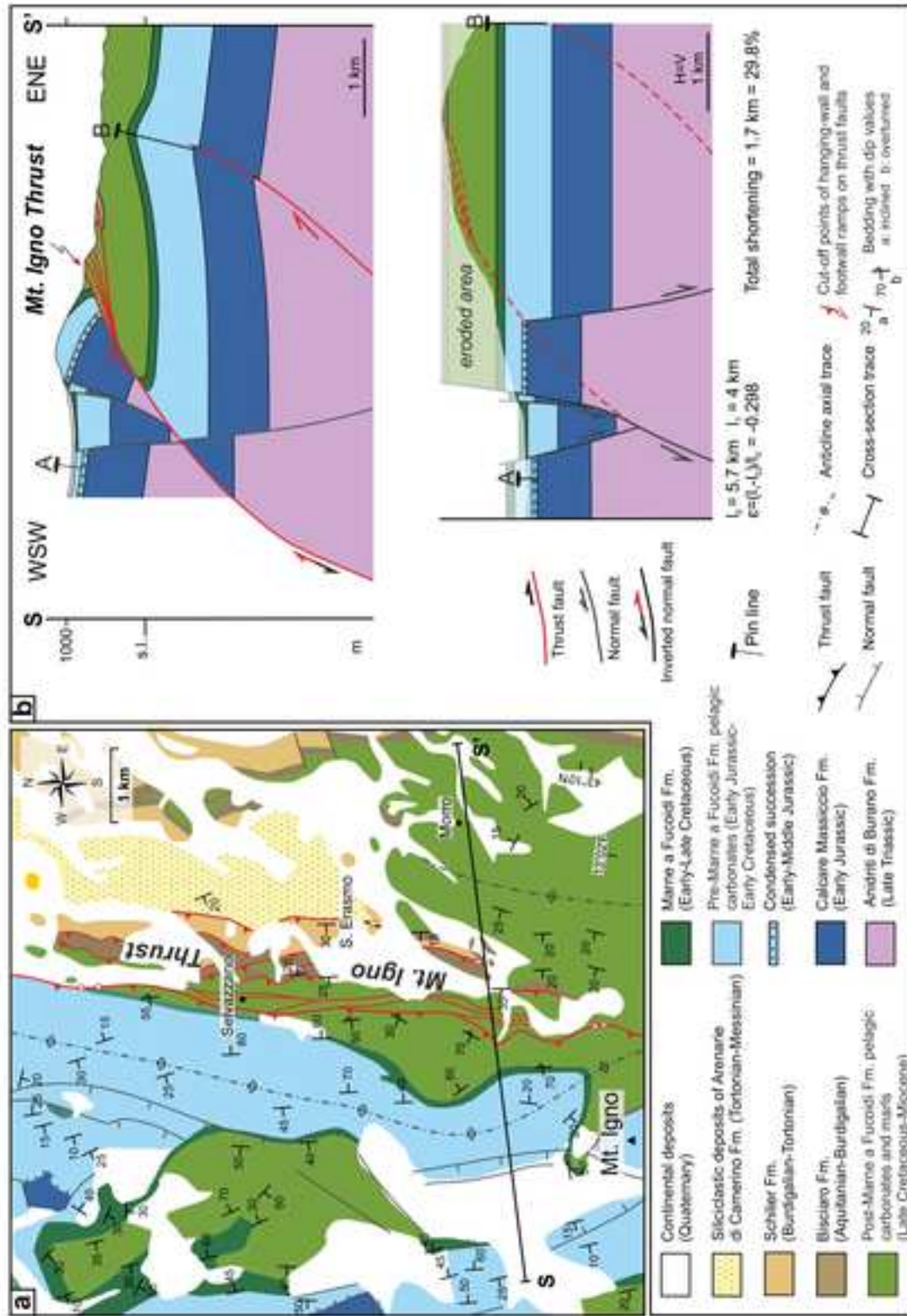


Fig. 14



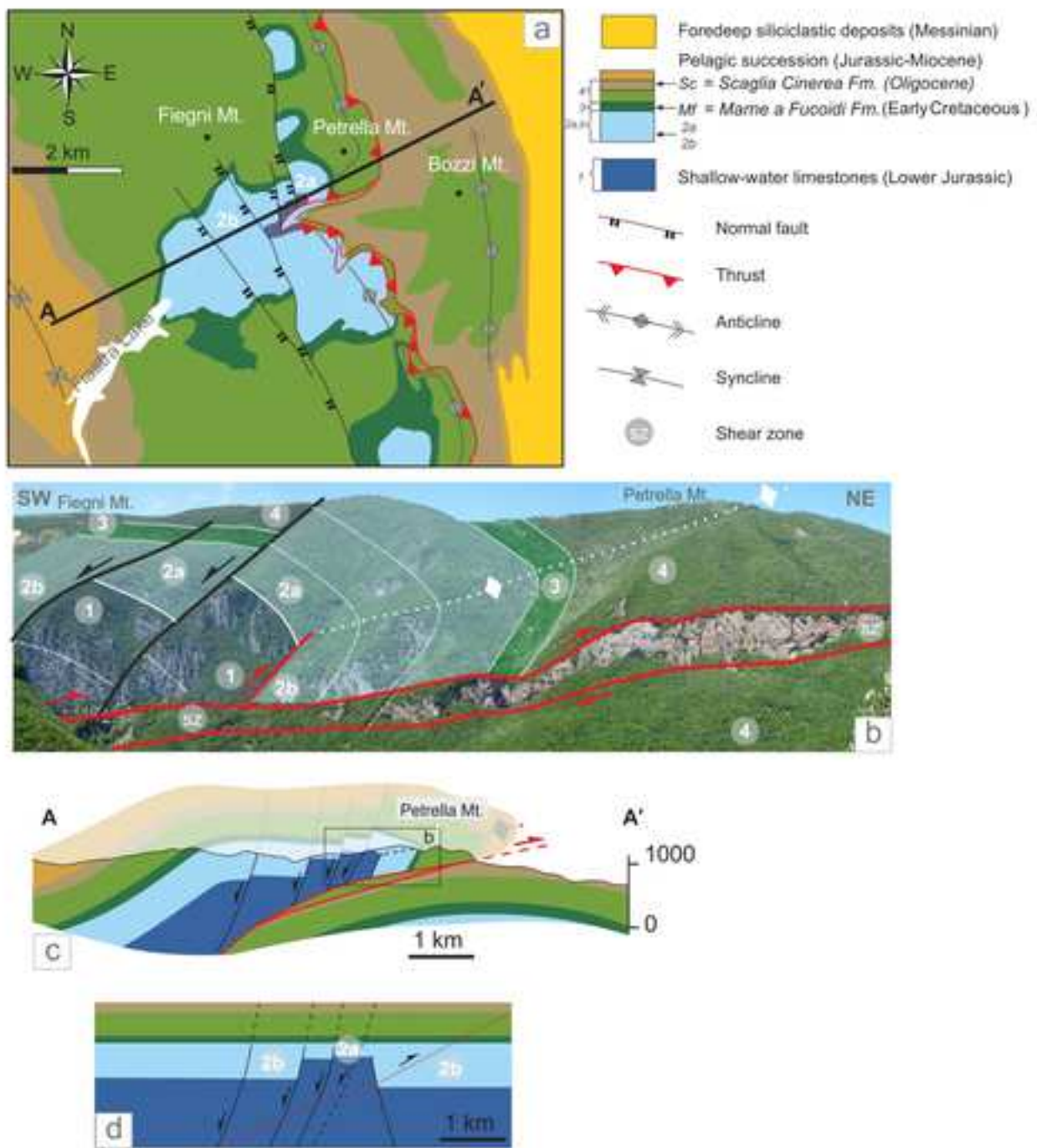
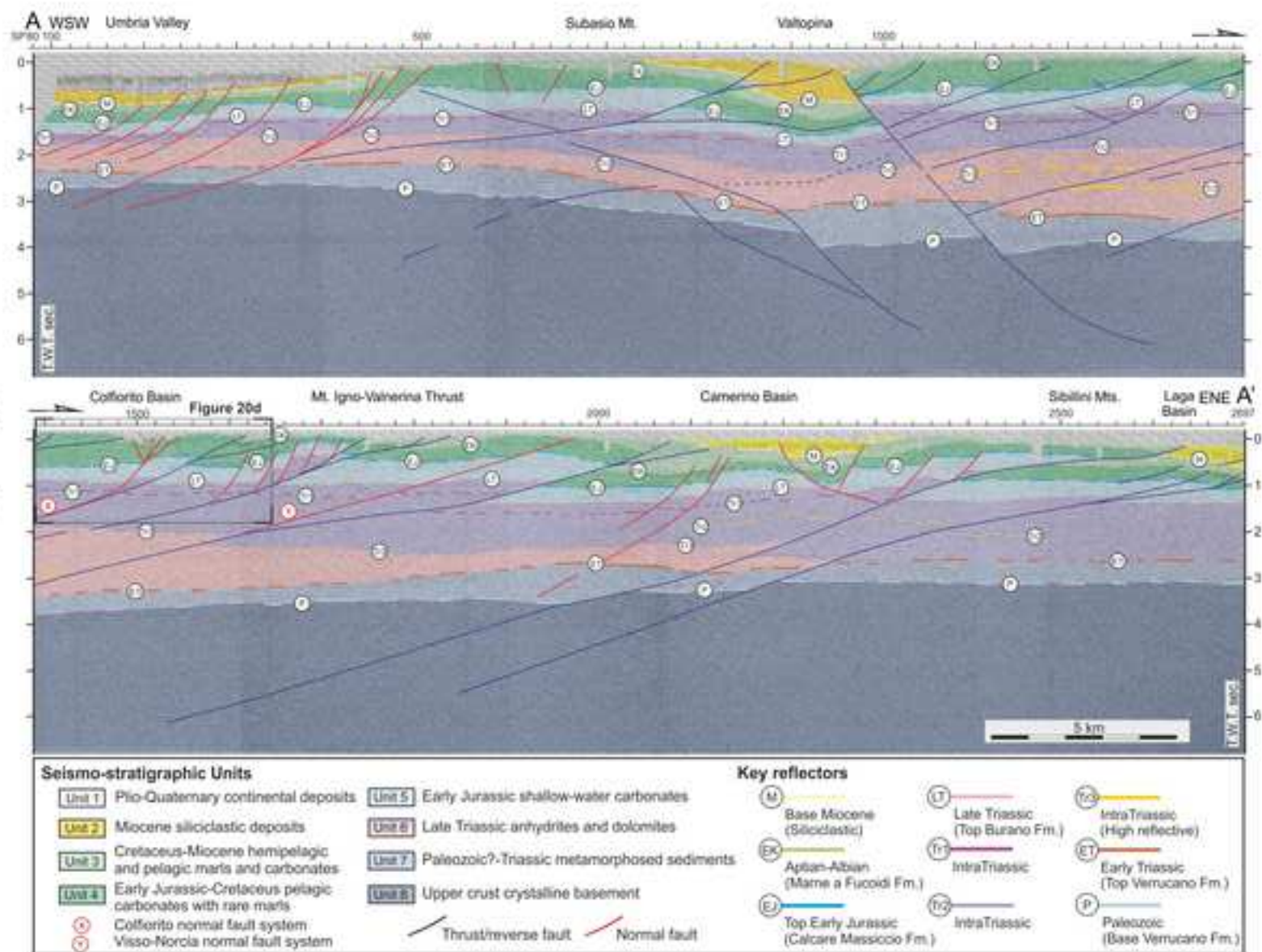


Fig. 15

Fig. 16



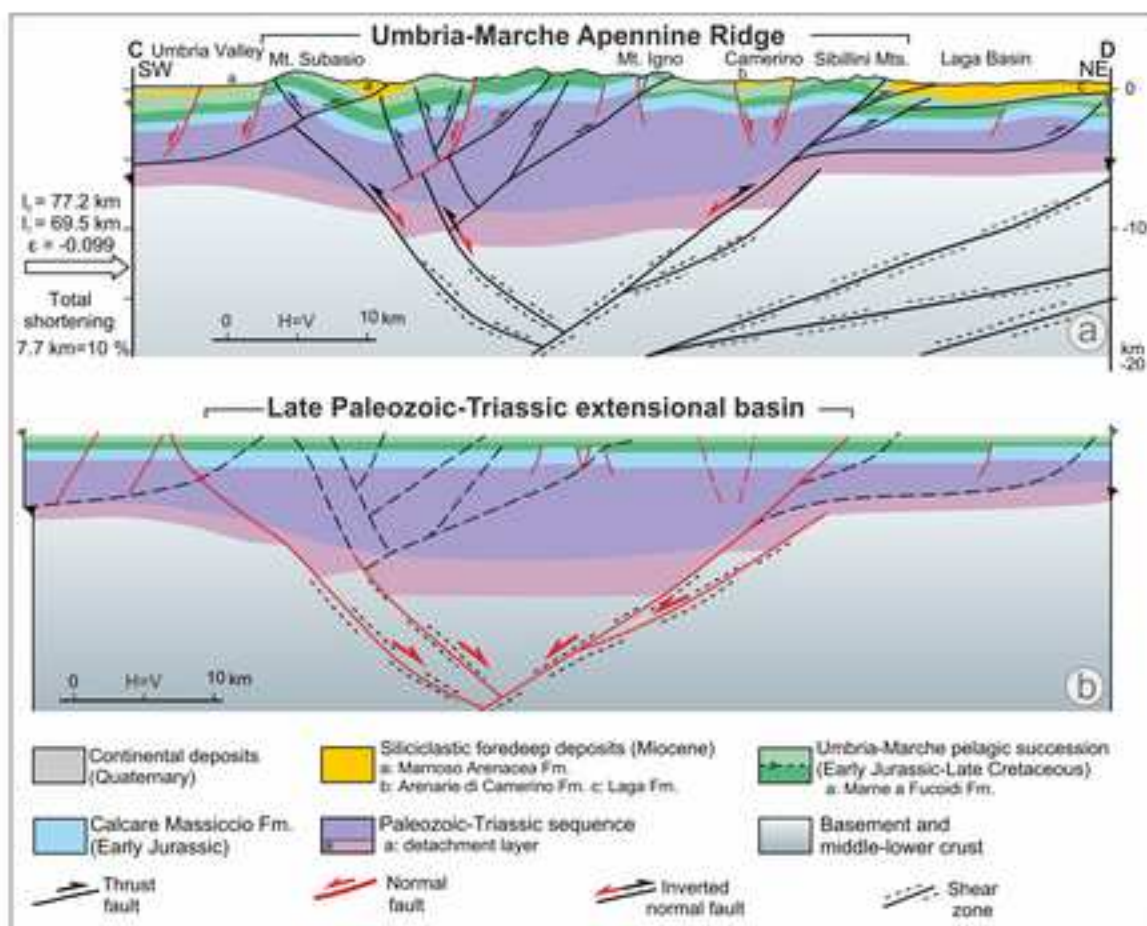


Fig. 17

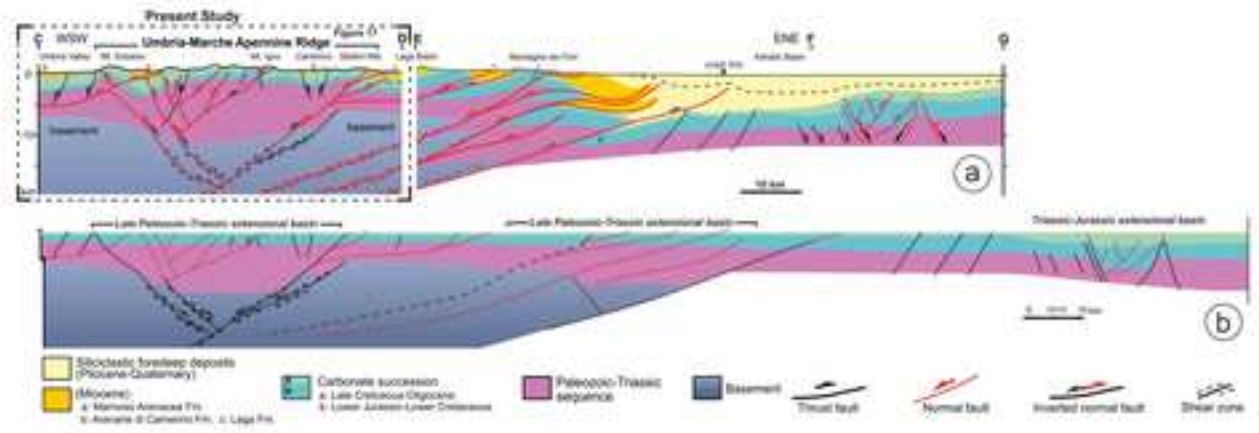


Fig. 18



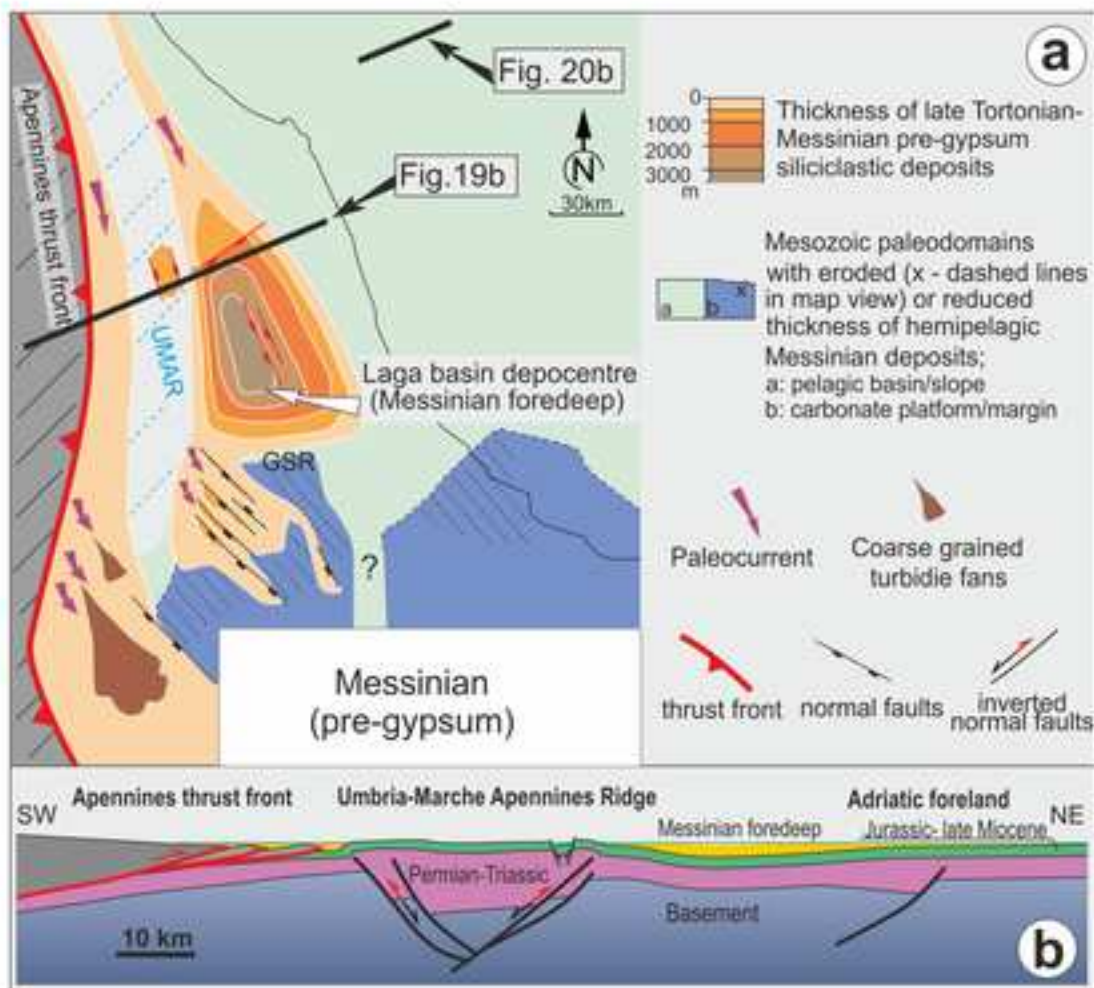


Fig. 19



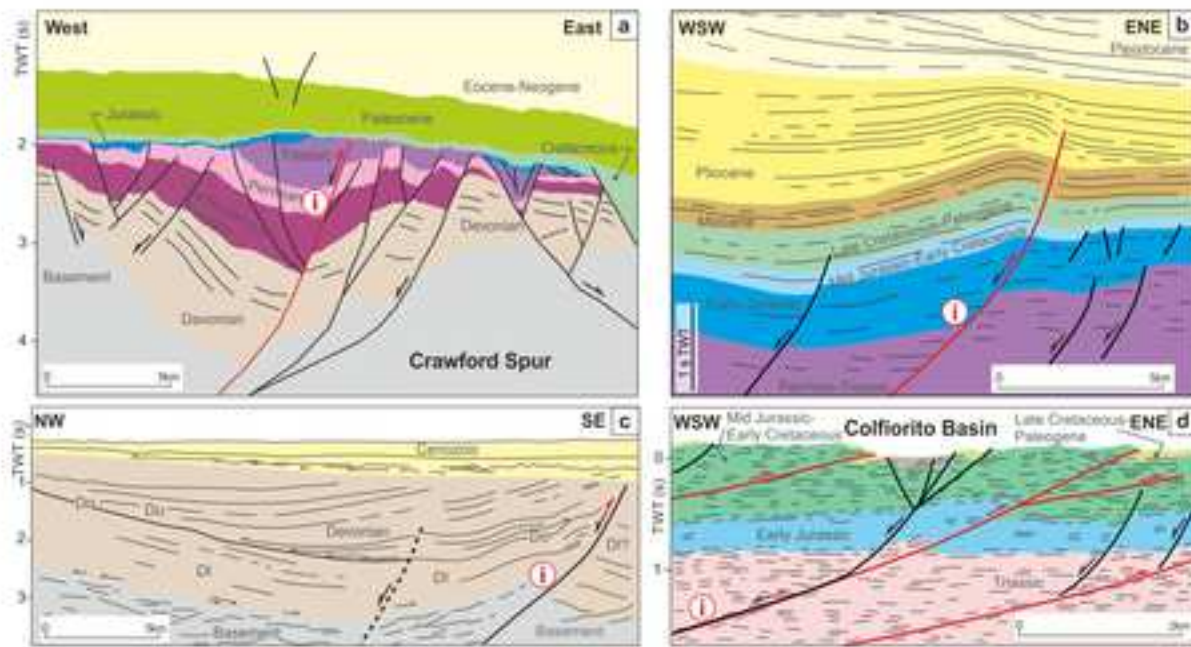


Fig. 20